

TEMPORAL AND SPATIAL CONTROL OF RNA STABILITY IN THE EARLY
EMBRYO OF *DROSOPHILA MELANOGASTER*

Thesis by

Arash Bashirullah

In Partial Fulfillment of the Requirements
for the Degree of
Doctor of Philosophy

California Institute of Technology

Pasadena, California

1999

(Submitted May 10, 1999)

Acknowledgements

First and foremost, I would like to thank my advisor, Howard Lipshitz. In the past six years Howard has been an inspiring and supportive mentor. He has also been a trusted friend, and has allowed me to feel like an intellectual colleague and a "partner-in-crime" in the venture of science. I will sorely miss the daily interactions with him that have made my days as a graduate student so gratifying. Thank you Howard, for your patience, guidance and encouragement.

Countless other people have shaped my scientific and personal development during graduate school. My committee members, Elliot Meyerowitz, Paul Sternberg, Barbara Wold, and Kai Zinn have supported me over the years. C.-c. Hui, Sean Egan and Rod McInnes have been generous with much needed advice and encouragement. Many graduate students, postdocs, and technicians have shared their expertise and insights despite the demands of their own work. I especially want to thank all my lab-mates, past and present, for making graduate school rewarding and fun.

Finally, my heartfelt gratitude goes to my family and friends for their steadfast support and patience.

Abstract

Early embryogenesis in metazoa is controlled by maternally synthesized products. Among these products, the mature egg is loaded with transcripts representing approximately two thirds of the genome. A subset of this maternal RNA pool is degraded prior to the transition to zygotic control of development. This transfer of control of development from maternal to zygotic products is referred to as the midblastula transition (or MBT). It is believed that the degradation of maternal transcripts is required to terminate maternal control of development and to allow zygotic control of development to begin.

Until now this process of maternal transcript degradation and the subsequent timing of the MBT has been poorly understood. I have demonstrated that in the early embryo there are two independent RNA degradation pathways, either of which is sufficient for transcript elimination. However, only the concerted action of both pathways leads to elimination of transcripts with the correct timing, at the MBT. The first pathway is maternally encoded, is triggered by egg activation, and is targeted to specific classes of mRNAs through *cis*-acting elements in the 3' untranslated region (UTR). The second pathway is activated 2 hr after fertilization and functions together with the maternal pathway to ensure that transcripts are degraded by the MBT. In addition, some transcripts fail to degrade at select subcellular locations adding an element of spatial control to RNA degradation. The spatial control of RNA degradation is achieved by protecting, or masking, transcripts from the degradation machinery. The RNA degradation and protection events are regulated by distinct *cis*-elements in the 3' untranslated region (UTR). These results provide the first systematic dissection of this highly conserved process in development and demonstrate that RNA degradation is a novel mechanism used for both temporal and spatial control of development.

Table of Contents

Acknowledgements	ii
Abstract	iii
Table of Contents	iv
Chapter 1: RNA localization in development	1
Chapter 2: Joint action of two RNA degradation pathways controls the timing of maternal transcript elimination at the midblastula transition in <i>Drosophila melanogaster</i>	62
Appendix 1: Mammalian NUMB is an evolutionarily conserved signaling adapter protein that specifies cell fate	74
Appendix 2: Fringe boundaries coincide with Notch-dependent patterning centers in mammals and alter Notch-dependent development in <i>Drosophila</i>	87

Chapter 1

RNA localization in development

With permission, from the *Annual Review of Biochemistry*,
Volume 67, copyright 1998, by Annual Reviews
www.AnnualReviews.org

RNA LOCALIZATION IN DEVELOPMENT

Arash Bashirullah,^{1,3} Ramona L. Cooperstock,^{1,2} and
Howard D. Lipshitz^{1,2}

¹Program in Developmental Biology, Research Institute, The Hospital for Sick Children, Toronto, Canada M5G 1X8; ²Department of Molecular & Medical Genetics, University of Toronto, Toronto, Canada; ³Division of Biology, California Institute of Technology, Pasadena, California; e-mail: lipshitz@sickkids.on.ca

KEY WORDS: *Drosophila*, *Xenopus*, *Saccharomyces*, oocyte, embryo, RNA-binding protein, cytoskeleton, microtubules, microfilaments, 3'-untranslated region (3'-UTR)

ABSTRACT

Cytoplasmic RNA localization is an evolutionarily ancient mechanism for producing cellular asymmetries. This review considers RNA localization in the context of animal development. Both mRNAs and non-protein-coding RNAs are localized in *Drosophila*, *Xenopus*, ascidian, zebrafish, and echinoderm oocytes and embryos, as well as in a variety of developing and differentiated polarized cells from yeast to mammals. Mechanisms used to transport and anchor RNAs in the cytoplasm include vectorial transport out of the nucleus, directed cytoplasmic transport in association with the cytoskeleton, and local entrapment at particular cytoplasmic sites. The majority of localized RNAs are targeted to particular cytoplasmic regions by *cis*-acting RNA elements; in mRNAs these are almost always in the 3'-untranslated region (UTR). A variety of *trans*-acting factors—many of them RNA-binding proteins—function in localization. Developmental functions of RNA localization have been defined in *Xenopus*, *Drosophila*, and *Saccharomyces cerevisiae*. In *Drosophila*, localized RNAs program the antero-posterior and dorso-ventral axes of the oocyte and embryo. In *Xenopus*, localized RNAs may function in mesoderm induction as well as in dorso-ventral axis specification. Localized RNAs also program asymmetric cell fates during *Drosophila* neurogenesis and yeast budding.

CONTENTS

INTRODUCTION	336
PATTERNS OF RNA LOCALIZATION	342
<i>Drosophila</i> Oocytes and Early Embryos	342
<i>Xenopus</i> Oocytes	348
<i>Ascidian</i> Oocytes	352
<i>Echinoderm</i> Oocytes	353
<i>Zebrafish</i> Embryos	353
Polarized Somatic Cells	353
MECHANISMS OF RNA LOCALIZATION	355
Nucleo-Cytoplasmic Transport	355
Transport from One Cell Type into Another	355
Transport Out of Mitochondria	356
Generalized Degradation with Localized Protection	356
Directed Cytoplasmic Transport of RNA	357
Entrapment/Anchoring of RNA at the Site of Localization	362
RNA Transport/Anchoring Particles	363
CIS-ACTING ELEMENTS THAT TARGET RNAs FOR LOCALIZATION	364
Mapping of Cis-Acting Elements in Localized RNAs	364
Cis-Acting Sequences for Localization Map to the 3'-Untranslated Region of mRNAs	365
Cis-Acting Sequences for Localization Map Within Non-Protein-Coding RNAs	367
Alternative Splicing Can Generate Localized vs Unlocalized RNA Isoforms	367
Discrete Localization Elements	368
Repeated/Redundant Localization Elements	369
Dispersed/Nonredundant Localization Elements	370
Additive Function of Localization Elements	371
Elements That Function in Translational Control During or After Localization	371
Primary, Secondary, Tertiary, and Quaternary Structures	372
TRANS-ACTING FACTORS INVOLVED IN RNA LOCALIZATION AND TRANSLATIONAL CONTROL OF LOCALIZED RNAs	373
Identification of Trans-Acting Factors	373
Factors That Interact Directly with Defined RNA Elements	374
Other Factors That Function in RNA Localization	377
Summary	382
DEVELOPMENTAL FUNCTIONS OF RNA LOCALIZATION	383
Specification of the Anterior-Posterior and Dorsal-Ventral Axes of the <i>Drosophila</i> Oocyte	383
Specification of Anterior Cell Fates in the <i>Drosophila</i> Embryo	384
Specification of Abdominal Cell Fates in the <i>Drosophila</i> Embryo	385
Assembly of Polar Granules and Specification of Germ Cells in the <i>Drosophila</i> Embryo	386
Signaling of Dorso-Ventral Axis and Mesoderm Induction in the <i>Xenopus</i> Embryo	386
Specification of Cell Fates During Asymmetric Cell Divisions	387
EVOLUTIONARY CONSIDERATIONS	388

INTRODUCTION

Since the early days of experimental embryology it has been suggested that the asymmetric distribution of substances in the egg cytoplasm might confer particular fates to cells that receive that cytoplasm (reviewed in 1). However, it is only in the past 13 years that specific maternally synthesized, asymmetrically distributed RNA and protein molecules have been identified in oocytes and

early embryos of *Xenopus*, *Drosophila*, ascidians, zebrafish, and echinoderms. This review focuses largely on RNAs that are localized to specific cytoplasmic regions in eggs and early embryos. It addresses both the mechanisms of cytoplasmic RNA localization and the developmental functions of this localization. Some consideration is also given to RNA localization later in development, in differentiating or differentiated cells. However, since both the mechanisms and the functions of this later localization are not well understood, the emphasis here is on RNA localization in oocytes.

This review considers only RNAs that are asymmetrically distributed in the cytoplasm. Examples of RNAs that are localized to and within the nucleus—even to specific chromosomes or regions of chromosomes (2–4)—are covered elsewhere. The first maternally synthesized cytoplasmically localized RNAs were identified in *Xenopus* in a molecular screen for RNAs enriched in either the vegetal (*Vg* RNAs) or animal (*An* RNAs) hemisphere of the *Xenopus* oocyte (5). Shortly thereafter, an RNA was discovered that is localized to the anterior pole of the *Drosophila* oocyte and early embryo (6). This RNA is encoded by the *bicoid* maternal effect locus (7), which plays a crucial role in specifying cell fates in the anterior half of the early *Drosophila* embryo (8). The facile combination of genetics and molecular biology in *Drosophila* led to *bicoid* becoming the first case in which it was demonstrated that RNA localization per se was important for normal development. Delocalization of *bicoid* RNA led to defects in anterior cell fate specification (7). Over 75 cytoplasmically localized RNAs have now been identified, and many of these are localized in eggs, early embryos, or differentiating cells (Table 1).

To date, it has been possible to address both the mechanisms and the developmental functions of RNA localization almost exclusively in *Drosophila* and *Xenopus*. The large size of the *Xenopus* oocyte has allowed mapping of sequences necessary and sufficient for RNA localization through injection of in vitro synthesized transcripts engineered to contain an exogenous reporter sequence and part or all of the localized RNA. Further, in some cases inactivation, delocalization, or degradation of specific RNAs has been induced through microinjection of antisense RNA or DNA. The ability to manipulate *Xenopus* oocytes and to apply various cytoskeleton-destabilizing drugs or other inhibitors has demonstrated the importance of the cytoskeleton in RNA localization.

Drosophila oocytes and early embryos are also large and have also been used for drug and inhibitor studies. In contrast to *Xenopus*, however, the ability to generate transgenic lines that express reporter-tagged transcripts during oogenesis has obviated the need for micronjection studies, although some of these have been conducted. Finally, the ability to obtain mutations in the endogenous gene that encodes the localized RNA or in factors that function in trans in its localization or in its translational regulation, has facilitated analyses of the

Table 1 Localized RNAs

Species	Transcript name	Protein product	Localization pattern	Cell	Reference
Ascidians	<i>Actin</i>	Cytoskeletal component	Myoplasm and ectoplasm	Oocyte	249
	<i>PCNA</i>	Auxiliary protein of DNA polymerase	Ectoplasm	Oocyte	100
	<i>Ribosomal protein L5</i>	Ribosomal component	Myoplasm	Oocyte	102
	<i>YC RNA</i>	Noncoding RNA	Myoplasm	Oocyte	101
<i>Drosophila</i>	<i>Add-hts</i>	Cytoskeletal component	Anterior	Oocyte and embryo	16, 17
	<i>Bicaudal-C</i>	Signal transduction/ RNA-binding protein	Anterior	Oocyte	18
	<i>Bicaudal-D</i>	Cytoskeleton interacting protein (?)	Anterior	Oocyte	19
	<i>bicoid</i>	Transcription factor	Anterior	Oocyte and embryo	7, 32
	<i>crumbs</i>	Transmembrane protein	Apical	Cellular blastoderm	67
	<i>Cyclin B</i>	Cell cycle regulator	Posterior and perinuclear	Oocyte and embryo	59, 62
	<i>egalitarian</i>	Novel	Anterior	Oocyte	20
	<i>even-skipped</i>	Transcription factor	Apical	Cellular blastoderm	69
	<i>fushi tarazu</i>	Transcription factor	Apical	Cellular blastoderm	64
	<i>germ cell-less</i>	Nuclear pore associated protein	Posterior	Oocyte and embryo	57, 239
	<i>gurken</i>	Secreted growth factor	Anterior-dorsal	Oocyte	21
	<i>hairy</i>	Transcription factor	Apical	Cellular blastoderm	65
	<i>Hsp83</i>	Molecular chaperone	Posterior	Embryo	63
	<i>inscuteable</i>	Novel	Apical	Neuroblast	127
	<i>K10</i>	Novel	Anterior	Oocyte	22
<i>mtlrRNA</i>	Noncoding RNA	Posterior	Oocyte and embryo	61, 134	

(Continued)

Table 1 (Continued)

Species	Transcript name	Protein product	Localization pattern	Cell	Reference
	<i>nanos</i>	RNA binding protein	Posterior	Oocyte and embryo	28, 43
	<i>orb</i>	RNA binding protein	Posterior	Oocyte and embryo	23
	<i>oskar</i>	Novel	Posterior	Oocyte and embryo	24, 25
	<i>Pgc</i>	Noncoding RNA	Posterior	Oocyte and embryo	26
	<i>prospero</i>	Transcription factor	Apical/basal	Neuroblast	127
	<i>pumilio</i>	RNA binding protein	Posterior	Embryo	250
	<i>runt</i>	Transcription factor	Apical	Cellular blastoderm	66
	<i>sevenless</i>	Transmembrane receptor	Apical	Eye imaginal Epithelial cells	126
	<i>tudor</i>	Novel	Posterior	Oocyte	27
	<i>wingless</i>	Secreted ligand	Apical	Cellular blastoderm	68
	<i>yemanuclein-α</i>	Transcription factor	Anterior	Oocyte	251
Echinoderms	<i>SpCOUP-TF</i>	Hormone receptor	Lateral to animal-vegetal axis	Oocyte	103
Mammals	<i>β-actin</i>	Cytoskeletal component	Specialized periphery	Fibroblasts, myoblasts, and epithelial cells	123–125
	<i>Arc</i>	Cytoskeletal component	Somatodendritic	Neurons	104
	<i>BC-1</i>	Noncoding RNA	Somatodendritic and axonal	Neurons	107, 111
	<i>BC-200</i>	Noncoding RNA	Somatodendritic	Neurons	108
	<i>CaMKIIα</i>	Signalling component	Somatodendritic	Neurons	109
	<i>F1/GAP43</i>	PKC substrate	Somatodendritic	Neurons	104
	<i>InsP3 receptor</i>	Integral membrane receptor	Somatodendritic	Neurons	110

(Continued)

Table 1 (Continued)

Species	Transcript name	Protein product	Localization pattern	Cell	Reference
	<i>MAP2</i>	Cytoskeletal component	Somatodendritic	Neurons	106
	<i>MBP</i>	Membrane protein	Myelinating membrane	Oligodendrocyte and Schwann cells	120
	<i>Myosin heavy chain</i>	Cytoskeletal component	Peripheral	Muscle	252
	<i>OMP/odorant receptors</i>	Integral membrane receptor	Axonal	Neurons	118, 119
	<i>Oxytocin</i>	Neuropeptide	Axonal	Neurons	115
	<i>Prodynorphin</i>	Neuropeptide	Axonal	Neurons	116, 117
	<i>RC3</i>	PKC substrate	Somatodendritic	Neurons	104
	<i>tau</i>	Cytoskeletal component	Axon hillock	Neurons	112
	<i>Tropomyosin-5</i>	Cytoskeletal component	Pre-axonal pole	Neurons	113
	<i>V-ATPase subunits</i>	Membrane protein	Specialized membrane	Osteoclasts	122
	<i>Vassopressin</i>	Neuropeptide	Axonal	Neurons	253
Xenopus	<i>Actin</i>	Cytoskeletal component	Periplasmic	Oocyte	254
	<i>An1 (a and b)</i>	Cytoplasmic protein (ubiquitin-like)	Animal	Oocyte	5, 81
	<i>An2</i>	mt ATPase subunit	Animal	Oocyte	5, 82
	<i>An3</i>	RNA binding protein	Animal	Oocyte	5
	<i>An4 (a and b)</i>	Novel	Animal	Oocyte	83
	<i>βTrCP</i>	Signaling molecule	Animal	Oocyte	83
	<i>βTrCP-2</i>	Signaling molecule	Vegetal	Oocyte	83
	<i>βTrCP-3</i>	Signaling molecule	Vegetal	Oocyte	83
	<i>B6</i>	NR ^a	Vegetal	Oocyte	70
	<i>B7</i>	NR	Vegetal	Oocyte	70
	<i>B9</i>	NR	Vegetal	Oocyte	70
	<i>B12</i>	NR	Vegetal	Oocyte	70
	<i>C10</i>	NR	Vegetal	Oocyte	70

(Continued)

Table 1 (Continued)

Species	Transcript name	Protein product	Localization pattern	Cell	Reference
	<i>G-proteins</i>	Signaling molecule	Animal	Oocyte	84
	<i>Oct60</i>	Transcription factor	Animal	Oocyte	85
	<i>PKCα</i>	Signaling molecule	Animal	Oocyte	86
	<i>α-tubulin</i>	Cytoskeletal component	Periplasmic	Oocyte	254
	<i>VegT</i> (<i>Antipodean</i>)	Transcription factor	Vegetal	Oocyte	91, 92
	<i>Vgl</i>	Signaling molecule	Vegetal	Oocyte	5
	<i>Xcat-2</i>	RNA-binding protein	Vegetal	Oocyte	78, 79
	<i>Xcat-3</i>	RNA-binding protein	Vegetal	Oocyte	95
	<i>Xcat-4</i>	NR	Vegetal	Oocyte	70
	<i>xl-21</i>	Transcription factor (?)	Animal	Oocyte	87
	<i>Xlan4</i>	P-rich and PEST sequences	Animal	Oocyte	88
	<i>Xlcaax-1</i>	Membrane protein	Animal	Oocyte	89
	<i>Xlsirt</i>	Noncoding RNA	Vegetal	Oocyte	97
	<i>Xwnt-11</i>	Secreted ligand	Vegetal	Oocyte	98
Yeast	<i>ASH1</i>	Transcription factor	Budding site	Mother cell	128, 129
Zebrafish	<i>Vasa</i>	RNA-binding protein	Cleavage plane	Early embryo	209

^aNR, Not reported.

mechanisms of RNA localization, the developmental functions of these RNAs, and of their localization per se.

This review begins with a description of patterns of cytoplasmic RNA localization with an emphasis on *Xenopus* and *Drosophila*. To help explain the patterns and their significance, brief descriptions of the structure and development of *Xenopus* and *Drosophila* oocytes and/or early embryos are included. After considering the patterns of RNA localization, the focus switches to mechanisms. First, the dynamics of RNA localization are considered, including the

role of the cytoskeleton in RNA transport and anchoring. Then specific components of the localization mechanism are dissected; these include *cis*-acting sequences and *trans*-acting factors that function either in localization per se or in control of RNA stability or translation during and after localization. Finally, developmental functions of RNA localization are discussed.

PATTERNS OF RNA LOCALIZATION

All cells are nonhomogeneous since they are compartmentalized into organelles with distinct functions and locations. These inhomogeneities can result in several forms of cellular symmetry and asymmetry. For example, positioning of the nucleus in the center of an otherwise quite homogeneous spherical cell produces spherical symmetry. In such a cell (and there are few if any examples, with the possible exception of some oocytes), certain RNAs might be localized close to the nucleus (perinuclear) while others might be positioned more peripherally. More complex cellular asymmetries result from variations in cell shape and the position of the nucleus and other subcellular organelles. Cells can be radially symmetric or even further polarized in two or three axes. In these cases, RNA localization can occur relative to one, two, or three axes (e.g. to the dorsal anterior pole). Regardless of cell shape or size, RNA distribution patterns are usually based on preexisting asymmetries and can, in turn, lead to the establishment of further asymmetries.

This section describes the dynamics and patterns of subcellular distribution of cytoplasmically localized RNAs. It provides a cellular and developmental context for consideration of the mechanisms and functions of RNA localization in subsequent sections. The emphasis here is on the best understood of the examples listed in Table 1.

Drosophila Oocytes and Early Embryos

STRUCTURE AND DEVELOPMENT OF THE NURSE CELL-OOCYTE COMPLEX
The two bilaterally symmetric *Drosophila* ovaries each consist of about 16 ovarioles. At the anterior tip of the ovariole is the germarium. Here the oogonial stem cells divide asymmetrically producing a stem cell and a committed cell, which is called a cystoblast. Each cystoblast divides four times with incomplete cytokinesis to form 16 cystocyte cells interconnected by cytoplasmic bridges that run through specialized membrane cytoskeletal structures called ring canals. Only 1 of the 16 cystocytes becomes the oocyte, and the remaining 15 become nurse cells. Each 16-cell germarial cyst becomes surrounded by somatically derived follicle cells to form a stage 1 egg chamber. The more posterior part of the ovariole comprises a connected series of progressively older egg chambers ordered such that the youngest is most anterior and the

oldest (stage 14) most posterior relative to the body axis of the female. It takes three days for an egg chamber to produce a mature egg. Except during the final six hours, the nurse cells synthesize large amounts of RNA and protein that are transported into the developing oocyte. Many of these molecules are required during the first two hours of embryonic development prior to the onset of zygotic transcription.

Selection of the oocyte from among the 16 cystocytes is not random. Of the 16 cells, 2 are connected to 4 others and 1 of these always becomes the oocyte (9). A large cytoplasmic structure—called the fusome—containing several cytoskeletal proteins, runs through the ring canals that connect cystocytes and has been implicated in oocyte determination (10–13). The only microtubule organizing center (MTOC) in the 16-cell complex is localized to the pro-oocyte, and microtubule arrays connect all 16 cells through the ring canals (reviewed in 14, 15). Because the MTOC nucleates the minus ends of the microtubules, the microtubule-based cytoskeleton that connects the 16 cells is polarized. This has important consequences for RNA transport from the nurse cells into the oocyte as well as for RNA localization within the oocyte itself.

RNA LOCALIZATION IN STAGE 1–6 EGG CHAMBERS Many RNAs that are later localized within the growing oocyte are first transcribed in all 16 germline cells but accumulate specifically in the pro-oocyte. These include the *Adducin like-huli tai shao* (*Add-hts*) (16, 17), *Bicaudal-C* (18), *Bicaudal-D* (19), *egalitarian* (20), *gurken* (21), *K10* (22), *orb* (23), *oskar* (24, 25), *Polar granule component* (*Pgc*) (26), and *tudor* (27) transcripts. Other RNAs that will later be localized within the oocyte are transcribed at very low levels in the nurse cells at this early stage and so cannot be visualized easily. For example, *nanos* is transcribed at low levels, and oocyte accumulation can be seen only later (28). Additional transcripts, such as *ovarian tumor* (29) and *cytoplasmic tropomyosin II* (*cTmII*) (30), also accumulate in the oocyte at this and later stages but are not localized. Therefore oocyte-specific accumulation is not unique to RNAs that will be localized within the oocyte during later stages of oogenesis but is a property of many RNAs synthesized in the germline of early egg chambers. The fact that many RNAs that accumulate in the early oocyte appear to do so with higher concentrations at the posterior cortex—the site of the only MTOC in the egg chamber (31)—is an early indication of the role of the polarized microtubule network in RNA transport and localization (see below).

The exact stage at which transcription of different localized RNAs commences (or at least the stage at which the transcripts can first be detected) varies. For example, *bicoid* is first transcribed in the nurse cells of stage 5 egg chambers and then accumulates in the oocyte (32), whereas *oskar* (24, 25) and *K10* (22) RNAs already accumulate in the oocyte in the germarium over a day

earlier. Interestingly, the dynamics of accumulation of these RNAs is identical if they are intentionally transcribed at the same time (33). Thus temporal differences in patterns of oocyte accumulation of different RNAs are a consequence of variation in time of transcription and are not indicative of a difference in underlying transport mechanism, which in fact is similar for different RNAs transcribed at distinct stages.

REORGANIZATION OF THE CYTOSKELETON AND RNA LOCALIZATION DURING STAGE 7 The process of nurse cell transcription and oocyte accumulation of RNAs continues through stage 6. During this time oocyte-follicle cell interactions establish anterior-posterior polarity within the oocyte and in the surrounding follicle cells (34, 35). Reciprocal signaling between the follicle cells and the oocyte results in a reorganization of the cytoskeleton such that, by the end of stage 7, the MTOC disappears from the posterior of the oocyte and microtubules become concentrated at the anterior oocyte margin (31, 34, 35). Concomitant with this change in cytoskeletal organization, RNAs that previously accumulated at the posterior of the oocyte localize in a ring-like pattern at the anterior oocyte margin (Figure 1) (e.g. *Bicaudal-C*, *Bicaudal-D*, *bicoid*, *egalitarian*, *gurken*, *K10*, *nanos*, *orb*, *oskar*, and *Pgc*) (18–26). At this stage several proteins are also seen in an anterior ring-like pattern (e.g. *Egalitarian* and *Bicaudal-D*) (20). This redistribution of RNA and protein is likely a consequence of the reorganization of the microtubule network such that the minus ends of microtubules move from the posterior pole to the anterior. Consistent with this, a β -galactosidase fusion to the minus-end-directed microtubule motor, *Nod*, relocates from the posterior pole of the oocyte at stage 6 to a ring around the anterior margin by the end of stage 7 (36). Thus RNAs that are transported into and within the oocyte by minus-end-directed microtubule motors would be expected to accumulate at the anterior rather than the posterior pole. As expected, the transient anterior localization of transcripts (e.g. *Bicaudal-D*, *bicoid*, *K10*, *orb*) is colchicine sensitive (37), and microtubules are required for anterior *Egalitarian* protein localization (20).

Mutations in genes involved in oocyte-follicle cell signaling during stages 6 and 7 cause defects in oocyte polarity (see below) and in the microtubule-based cytoskeleton (e.g. *Delta*, *gurken*, *Notch*, *PKA*) (34, 35, 38, 39). For example, double-anterior oocytes can form in which microtubules have their minus ends at both oocyte poles and their plus ends at its center. Mutations in *homeless* cause a similar disorganization of microtubules (40). Such disorganization results in *bicoid* RNA localization at both poles of the oocyte while *oskar* RNA and plus-end-directed kinesin- β -galactosidase fusion protein localize in the middle (38, 41, 42). These data emphasize that microtubule polarity directs intraoocyte transcript localization.

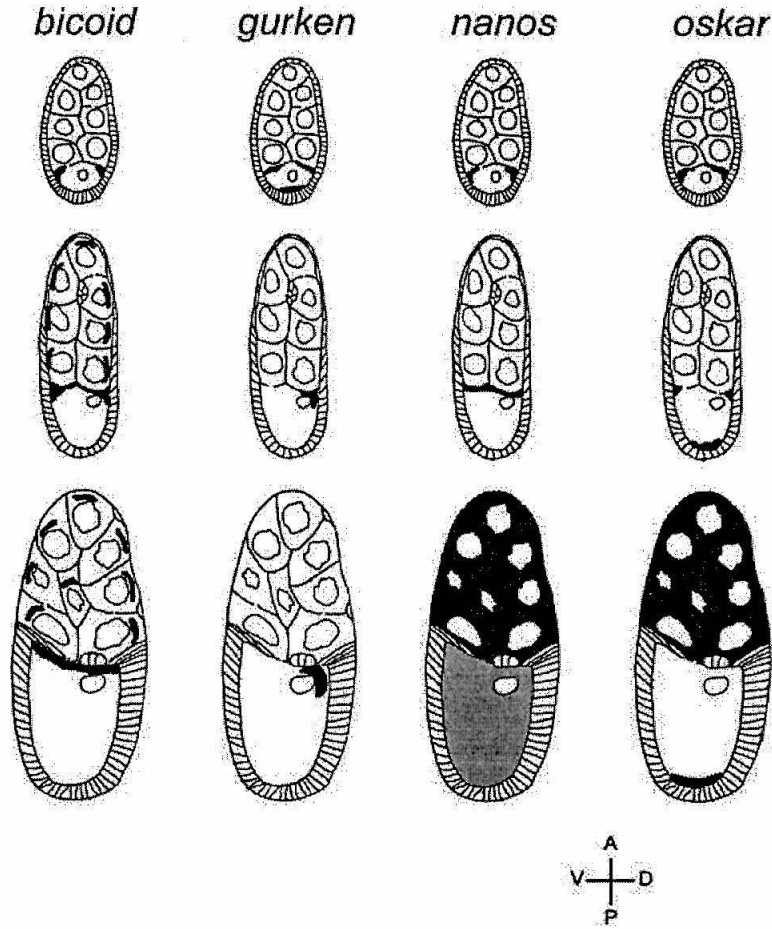


Figure 1 Localization of transcripts during *Drosophila* oogenesis. Transcript distribution patterns are shown in black or gray shading for *bicoid*, *gurken*, *nanos*, and *oskar* RNAs in stage 8 (top row), 9 (middle row), and 10B (bottom row) egg chambers. A, anterior; P, posterior; D, dorsal; V, ventral. Drawings of egg chambers are after King (9).

RNA LOCALIZATION AT STAGES 8–9 Further changes in RNA localization patterns occur at stages 8 and 9. Certain RNAs localize in a general anterior cortical pattern. These include *Bicaudal-C* (18), *Bicaudal-D* (19), *bicoid* (7), *K10* (22), *nanos* (28, 43), *orb* (23), and *Pgc* (26). In contrast, *Add-hts* RNA shifts from a general cortical pattern to an anterior cortical pattern (16, 44, 45; KL Whittaker, D Ding, WW Fisher, HD Lipshitz, manuscript in preparation) whereas *gurken* RNA localizes in a dorso-anterior pattern around the nucleus (21). Others such as *egalitarian* RNA delocalize from the anterior and become

uniformly distributed (20). Still others begin to relocalize to the posterior: *Pgc* RNA spreads posteriorly along the oocyte cortex (26) while *oskar* RNA gradually moves away from the anterior and begins to accumulate at the posterior pole of the oocyte (24, 25).

During this same period a kinesin- β -galactosidase fusion protein localizes to the posterior (41). This observation suggests that, even though it has not been possible to visualize microtubules that traverse antero-posterior axis of the oocyte at this stage (31), they must be present. RNAs that enter the oocyte at this stage or that were previously localized to the anterior of the oocyte in association with minus-end-directed microtubule motors, must dissociate from these motors and associate with plus-end-directed motors in order to be translocated to the posterior pole. One such RNA is *oskar*, which by the end of stage 9, is present only at the posterior pole of the oocyte (24, 25). *oskar* RNA plays a key role in nucleating formation of the polar granules at the posterior pole of the oocyte. The polar granules, which are involved in germ-cell specification (see below), gradually assemble during stages 9–14 of oogenesis (reviewed in 47).

NURSE CELL “DUMPING” AND RNA LOCALIZATION FROM STAGES 10–14 During stages 9 and 10 nurse cells increase synthesis of RNA and protein, dump their contents into the oocyte starting at stage 10B, and degenerate by the end of stage 12. This massive transfer of material is aided by contraction of the actin cortex of nurse cells. “Dumpleless” mutants affect this process as well as ring canal structure. These genes, *chickadee* (encoding a profilin homolog), *singed* (encoding a fascin homolog), and *quail* (encoding a vilin homolog), are involved in F-actin crosslinking, indicating a major role for the actin-based cytoskeleton (48–50). Moreover, these studies demonstrate that the actin-based cytoskeleton is involved in anchoring the nurse cell nuclei so that they do not plug the ring canals during the dumping process. Interestingly, *bicoid* is localized apically in nurse cells during this phase (32). This apical distribution of *bicoid* RNA indicates a preexisting asymmetry within the nurse cells, but whether this transient *bicoid* localization in nurse cells serves any function is unclear. A similar apical nurse cell RNA localization pattern is observed for ectopically expressed *oskar* and *K10* transcripts at this stage (33).

During stage 10B, microtubules rearrange into subcortical parallel arrays in the oocyte, and a microtubule-based process called ooplasmic streaming begins. Capuccino and Spire proteins are required for control of ooplasmic streaming (51, 52). During stages 10B–12 the dumping of large amounts of RNA into the oocyte along with ooplasmic streaming make it difficult to distinguish delocalization of previously localized RNA on the one hand, from a transient stage during which the dumped RNA is becoming localized (i.e. is joining the

previously localized RNA at its intracellular target site) on the other. This is further complicated by the release of many transiently anteriorly localized RNAs, followed by their gradual translocation toward the posterior in some cases, or their complete delocalization in others. As a result, many RNAs appear to be generally distributed in the stage 11 oocyte. These include *Bicaudal-C* (18), *Bicaudal-D* (19), *egalitarian* (20), *nanos* (28), and *orb* (23). Other previously localized transcripts such as *K10* and *gurken* disappear by stage 11 (21, 22).

In contrast, the anterior localization pattern of *bicoid* and *Add-hts* transcripts is maintained throughout these stages (7, 16, 32). Maintenance of this pattern is likely the result of two factors: (a) anteriorly localized RNAs are trapped as they enter the oocyte from the nurse cells (WE Theurkauf, TI Hazelrigg, personal communication) and (b) previously anchored *bicoid* and *Add-hts* RNA is not released from the anterior pole during dumping and so does not have the opportunity to become generally distributed throughout the oocyte (16, 32).

After ooplasmic streaming is completed (stage 12), subcortical microtubules are replaced by randomly oriented short cytoplasmic filaments, and F-actin reorganizes from a dense cortical filament network to an extensive deep cytoplasmic network (31, 54, 55). At this stage, several newly localized RNAs can be seen at the posterior of the oocyte. These include *nanos* (28, 56), *germ cell-less* (57), and probably *orb* (23). In addition, *oskar* and *Pgc* transcripts exhibit a posteriorly enriched pattern (24–26). *bicoid* and *Add-hts* transcripts remain localized at the anterior pole of late oocytes (7, 16, 32).

RNA LOCALIZATION IN EARLY EMBRYOS After egg activation, the cytoskeleton reorganizes once again with actin and tubulin concentrated in the cortex and deeper filamentous networks of microtubules (31, 54, 55). Some longitudinal actin fibers may also be present in the early embryo. The *Drosophila* zygote undergoes 13 synchronous nuclear divisions without cytokinesis, forming a syncytial embryo containing several thousand nuclei that share the same cytoplasm (58). This syncytial state persists until the end of the 14th cell cycle when approximately 6000 nuclei reside at the cortex. Subsequently, invagination of membranes forms individual cells to give the cellular blastoderm. At this point the antero-posterior and dorso-ventral positional fates of the cells are specified.

The two anteriorly localized maternal RNAs—*bicoid* (Figures 1 and 2) and *Add-hts*—persist in early cleavage embryos. *Add-hts* is released and diffuses posteriorly (16), while *bicoid* appears to remain anchored at the anterior cortex (7, 32). By the cellular blastoderm stage both RNAs are gone.

Three RNAs that are posteriorly localized in the oocyte—*oskar*, *nanos* (Figures 1 and 2), and *Pgc*—retain posterior localization in early cleavage stage embryos. By nuclear cycle 6/7 *oskar* RNA is gone (24), whereas *Pgc* and

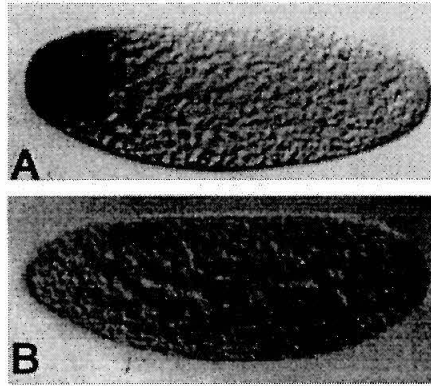


Figure 2 Localized maternal transcripts in early *Drosophila* embryos. A: *bicoid* RNA; B: *nanos* RNA. Images are of whole mount RNA tissue in situ hybridizations to stage 2 embryos using digoxigenin-labeled probes. Anterior is to the left and dorsal toward the top of the page.

nanos RNAs are associated with polar granules and are taken up into pole cells together with these granules (26, 56). Some maternal RNAs do not become posteriorly localized until late in oogenesis or early embryogenesis. Examples are *Cyclin B* (59–62) and *Hsp83* (60, 61, 63) transcripts. By the cellular blastoderm stage, maternal transcripts of *Cyclin B*, *germ cell-less*, *Hsp83*, *nanos*, *orb*, and *Pgc* can be detected only in pole cells.

During the syncytial and cellular blastoderm stages, zygotic synthesis of RNA commences. Several of these zygotically synthesized transcripts, including *crumbs*, *even-skipped*, *fushi tarazu*, *hairy*, *runt*, and *wingless* are apically localized in the blastoderm (64–69), an epithelium surrounding the syncytial yolk mass of the zygote.

Xenopus Oocytes

As in *Drosophila*, maternally synthesized gene products play a key role in the development of the *Xenopus* embryo (reviewed in 70). Zygotic transcription initiates at the 4000-cell mid blastula stage. Unlike in *Drosophila*, however, synthesis of maternal molecules occurs in the oocyte itself. Thus the issue of transport into the oocyte from interconnected nurse cells does not arise.

DEVELOPMENT OF THE OOCYTE The *Xenopus* oocyte is initially a small spherical cell of 30 μm diameter when it is produced by mitosis of a stem cell, the oogonium (71). However, even at this stage, its nucleus and organelles are asymmetrically distributed (72, 73). Unlike *Drosophila* oogenesis, which lasts just over a week, *Xenopus* oogenesis lasts three years, although most of the

synthesis of oocyte contents occurs in the third year (71). The oocyte reaches a final diameter of approximately 1.5 mm (71).

An early indicator of asymmetry is the mitochondrial cloud or Balbiani body (71). It is composed of clumps of mitochondria, rough endoplasmic reticulum, and dense granules that initially are evenly distributed around the periphery of the germinal vesicle in early stage I oocytes (~80 μm diameter). By the end of stage I these components condense on one side of the germinal vesicle as a cap-like structure that grows and assumes a spherical shape. Beginning in stage II, the mitochondrial cloud moves toward the future vegetal pole initially changing shape to become disk-like and then reorganizing into a wedge-like shape (late stage II/early stage III). Subsequently its components become localized to the vegetal cortex of the oocyte during stage III/IV.

The mitochondrial cloud probably functions in the accumulation and localization of material needed for the formation of germ plasm at the vegetal pole of the early embryo (reviewed in 70, 74). In structure and function the *Xenopus* germ plasm is comparable to the *Drosophila* posterior polar plasm, and it contains germinal granules that function in germ-cell determination. However, while *Drosophila* polar granules are sufficient for the induction of germ cells (75, 76), *Xenopus* primordial germ cells are not irreversibly determined (77). Preliminary evidence indicates that certain RNA and protein components of the *Drosophila* and *Xenopus* germinal granules are evolutionarily conserved (70, 78, 79) and that in both cases RNA localization is an important mechanism used to locally assemble these structures.

The oocyte cytoskeleton is symmetric early in oogenesis. Until stage II the germinal vesicle appears to serve as the only MTOC with microtubules emanating radially toward the plasma membrane (80). This array loses its symmetry as the germinal vesicle moves toward the future animal pole and the mitochondrial cloud starts condensing at the opposite (vegetal) side. At this time microtubules start to concentrate at the vegetal side of the germinal vesicle, colocalizing with the wedge-shaped mitochondrial cloud by late stage II (77). The germinal vesicle completes movement to the animal hemisphere by stage V/VI and at this time the microtubule array disappears.

RNA LOCALIZATION PATTERNS The first collection of localized RNAs was reported for *Xenopus* oocytes. Three animal hemisphere-enriched RNAs (*An1*, *An2*, *An3*) and one vegetal hemisphere-localized RNA (*Vg1*; Figures 3 and 4) were identified in a molecular screen for cDNAs representing mRNAs differentially distributed along the animal-vegetal axis (5).

The animal hemisphere (*An*)-enriched RNAs are not tightly localized within the animal hemisphere but are at least fourfold enriched in this hemisphere

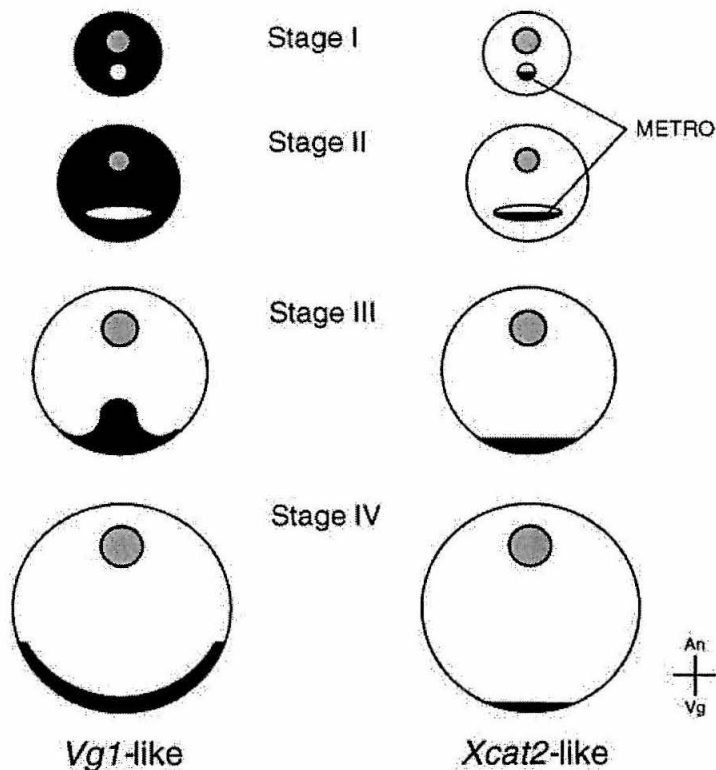


Figure 3 Localization of transcripts during *Xenopus* oogenesis. Transcript distribution patterns are shown in black, on the left for transcripts that show a *Vg1*-like pattern and on the right for transcripts that show an *Xcat-2*-like distribution pattern. Oocytes from stages I–IV are schematized. An, animal pole; Vg, vegetal pole. The germinal vesicle (oocyte nucleus) is shown in gray and the METRO as a white circle (stage I) or ellipsoid (stage II). Drawings of oocytes are after Kloc & Etkin (90).

relative to their vegetal concentration. Generally distributed maternal RNAs are twice as abundant in the animal than in the vegetal hemisphere (5). Thus the *An* RNAs are enriched in the animal hemisphere at least twofold versus other maternal RNAs. There are over a dozen known examples of *An* RNAs, all with similar distribution patterns: *An1a* (5, 81), *An1b* (5, 81), *An2* (5, 82), *An3* (5), *An4a* (83), *An4b* (83), β -*TrCP* (83), *G protein* (84), *oct60* (85), *PKC- α* (86), *xl-21* (87), *Xlan-4* (88), and *Xlcaax-1* (89). Unfortunately, reported in situ RNA hybridization data are lacking, making detailed comparisons of distribution patterns impossible.

In contrast to the *An* RNAs, the vegetally localized RNAs exhibit highly restricted distribution patterns. Careful observations of the patterns of localization

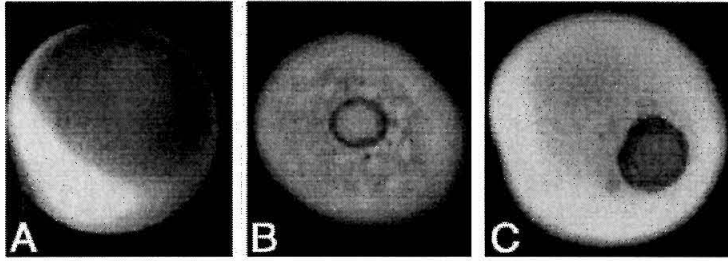


Figure 4 Localized transcripts in *Xenopus* oocytes. **A:** *Vg1* RNA; **B:** *Xcat-2* RNA; **C:** *Xlsirt* RNA. All images are of whole mount RNA tissue in situ hybridizations to either late stage III (**A**) or early stage II (**B, C**) oocytes. In **A**, the vegetal pole points toward the top right; in **B** and **C** the vegetal tip of the oocyte is at the center of the transcript distribution (i.e. the oocytes are viewed from the vegetal side). The small patches of *Xcat-2* RNA that are radially symmetrically distributed around the vegetal ring of transcripts are in the islands of germ plasm.

in situ in whole mounts have suggested two or three distinct patterns (70, 90–92) exemplified by *Vg1*, *Xcat-2*, and, possibly, *VegT/Antipodean*.

Four RNAs show the *Vg1*-like pattern of localization: *Vg1* (Figures 3 and 4); and *Xcat-4*, *B12*, and *B9* (70). *Vg1* RNA is initially distributed uniformly in the oocyte cytoplasm and is excluded from the mitochondrial cloud during stages I and II (93). During late stage II/early stage III, *Vg1* transcripts accumulate in a wedge-like pattern toward the vegetal pole before becoming restricted to the vegetal cortex by late stage III (93–95). Finally, at stage IV, *Vg1* RNA is tightly localized to the cortex of the entire vegetal hemisphere (94, 96). This localization pattern correlates with the dispersion of the mitochondrial cloud (see above).

The second pattern of RNA localization is exhibited by seven RNAs: *Xcat-2*, *Xwnt-11*, *Xcat-3*, *B6*, *B7*, *C10*, and the *Xlsirts* (Figures 3 and 4) (70, 78, 79, 95, 97, 98). This localization process includes passage through what has been called a message transport organizer (METRO) within the mitochondrial cloud (Figure 3) and occurs in three distinct steps (90): (a) movement from the germinal vesicle to the mitochondrial cloud, (b) sorting within the METRO, and (c) translocation and anchoring to vegetal cortex. Localization begins during early oocyte stage I when transcripts appear to be distributed throughout the cytoplasm at low levels with slightly higher concentrations around the germinal vesicle. As the mitochondrial cloud condenses into a sphere during mid stage I, these transcripts are transported to the METRO. For *Xcat-2* this change in pattern is not the result of a reduction of RNA elsewhere, as the total amount of RNA in the oocyte remains constant or even increases (79). Within the METRO the transcripts are sorted such that, for example, *Xcat-2* is localized first, followed by *Xlsirts*, and then *Xwnt-11* (70, 79, 90, 99). By late stage I,

when the METRO is disc-like, *Xcat-2* RNA is in the periphery of the disc, *Xwnt-11* RNA is in the center, and *Xlsirts* reside between these two (Figure 3). The METRO moves vegetally such that by stage IV, all three RNAs are localized at the tip of the vegetal pole (70, 79, 90, 99). At this stage, the *Vg1* RNA pattern is quite distinct as it is distributed throughout the vegetal cortex (70, 79, 90, 99).

The third type of localization, typified by *VegT* (*Antipodean*), appears to deviate from both of these patterns, although there is some discrepancy in the distributions described in two reports (91, 92). *VegT/Apod* maternal transcripts are initially uniform in the cytoplasm in stage I. Later they appear to move to the vegetal pole with a timing and pattern similar to *Xlsirts*, *Xcat-2*, and *Xwnt-11* transcripts. One report describes a distribution at late stage III/early stage IV similar to that of *Vg1* (92), while another describes a novel final pattern predominantly in the vegetal yolk (91). The latter distribution would imply a target of localization that is distinct from all other vegetally localized transcripts.

After fertilization, the *B7* transcripts disappear, the *Xlsirt*, *Xcat-2*, and *Xcat-3* transcripts are associated with the germ plasm in the primordial germ cells, and the other transcripts (*B9*, *B12*, *C10*, *Vg1*, *Xcat-4*, and *Xwnt-11*) are all located in the vegetal blastomeres (70, 79, 90, 93, 98, 99; L Etkin, personal communication).

Ascidian Oocytes

Several RNAs are localized in ascidian (*Styela*) oocytes (Table 1). These include *YC* RNA, *PCNA* mRNA, and *ribosomal protein L5* mRNA. *PCNA* mRNA is initially uniformly distributed throughout the previtellogenic oocyte (100). During maturation, *PCNA* mRNA becomes concentrated in the central ectoplasm and cortical regions surrounding the myoplasm but is absent from the myoplasm per se (100). While *PCNA* mRNA can be observed in both the ectoplasm and the myoplasm after the first phase of ooplasmic segregation, which restricts the ectoplasm and myoplasm to the vegetal hemisphere, *PCNA* mRNA is absent from the myoplasm in the two-cell embryo (100). *YC* RNA is distributed throughout the cytoplasm of previtellogenic oocytes (101). However, during early vitellogenesis, *YC* transcripts are localized around the nucleus. They gradually move away from the nucleus as the oocyte increases in size, until they become restricted to the cortex of postvitellogenic oocytes (101). After the first phase of ooplasmic segregation shortly after fertilization, *YC* transcripts are localized in the vegetal cap of myoplasm (101). A third pattern of localization is exhibited by *L5* transcripts, which are concentrated in the cortical myoplasm (except at the animal pole) during oogenesis (102).

After fertilization, *L5* transcripts become restricted to the vegetal myoplasm (102).

Echinoderm Oocytes

There is one example of a maternally synthesized mRNA that is localized in the echinoderm (*Strongylocentrotus purpuratus*) oocyte and early embryo (103). This *SpCOUP-TF* mRNA, which encodes an “orphan” nuclear steroid hormone receptor, is localized subcortically in one hemisphere of the sea urchin oocyte and mature egg. Since there are no markers of the animal-vegetal axis of the egg, the location of *SpCOUP-TF* transcripts in the egg was inferred from their distribution in cleavage stage embryos where the animal-vegetal and oral-aboral axes are evident morphologically. From this inference it was concluded that *SpCOUP-TF* transcripts are localized such that they are restricted to one of the two cells produced by the first cleavage (i.e. lateral to the animal-vegetal axis) and, thus, are fixed at a 45° angle relative to the future oral-aboral axis (103).

Zebrafish Embryos

There is one example of a maternally synthesized mRNA that is localized within the cells of the zebrafish (*Brachydanio rerio*) embryo (209). This mRNA encodes a fish homolog of *Drosophila* Vasa, a DEAD-box RNA helicase that is known to function in germ plasm assembly (see below). Maternally synthesized zebrafish *vasa* transcripts localize to the inner (yolk-most) edges of the cleavage furrows at the first embryonic cell division (209). This localization pattern is maintained through the four-cell stage. From the 8- to the 1000-cell stage, the *vasa* transcripts remain in only four cells (the presumptive primordial germ cells) and are found in intracellular clumps that likely represent the assembling germ plasm. Subsequently, *vasa* transcripts are found in all primordial germ cells and germ cells.

Polarized Somatic Cells

Many cells in addition to oocytes are polarized. Epithelial cells have an apical-basal polarity. Differentiated neurons have dendritic arbors and an axon. Fibroblasts have specialized moving membranes (lamellopodia) at defined surfaces. These classes of cells also show asymmetric distributions of RNAs. However, in most cases, the developmental significance of RNA localization is unknown or, alternatively, transcript localization serves a function in the fully differentiated cell rather than during its development or differentiation. Several RNA localization patterns in these polarized cells are described here.

Although neurons can exhibit very complex and quite varied cytoarchitectures, they are classic examples of polarized cells and generally have an axon

on one side of the cell body (soma) and dendrites on the other. Most neuronal RNAs are present only in the soma and are excluded from dendrites and axons. At least 12 localized neuronal RNAs have been reported (1, 104, 105). These RNAs can be classified into two different patterns. The first is somatodendritic: *MAP2* (106); *BC-1* (107); *BC-200* (108); *CaMKII- α* (109); *IP3 receptor* (110); and *Arc*, *FI/GAP43*, and *RC3* (104) RNAs. The second is axonal: *BC-1* (111), *tau* (112), *tropomyosin-5* (113), *vasopressin/oxytocin* (114, 115), *prodynorphin* (116, 117), and *odorant receptor* (118, 119) RNAs. In almost all cases these RNAs are localized in differentiated neurons. The exception, *tropomyosin-5* (*Tm5*) RNA, is localized prior to any structural polarities at the future axonal pole of differentiating neurons (113). In mature neurons *Tm5* RNA is present only in the soma (113).

Several types of cells have defined areas of membrane devoted to a particular function. Myelinating membranes of oligodendrocytes and Schwann cells have associated myelin basic protein (MBP) mRNA (120, 121). mRNA for vacuolar H⁺-ATPase subunits is localized to the bone resorption membranes of osteoclasts (122). Lamellopodia of fibroblasts (123) and myoblasts (124) contain localized cytoplasmic β -actin mRNA. Apical ends of villar epithelial cells also have high concentrations of *actin* mRNA (125). In these cases, the distribution of mRNA likely follows the differentiation of these cell types rather than playing a role during their differentiation.

In *Drosophila* the location of plus-end (kinesin)- and minus-end (Nod)-directed microtubule motors provides a readout of the polarities of various cell types. Localization of these motors within oocytes was mentioned earlier. In addition, these motors localize to opposite ends of polarized cells (36): epithelia (Nod is apical and kinesin is basal), mitotic spindles (Nod is at the poles), neurons (Nod is dendritic and kinesin is axonal), and muscle (Nod is at the center and kinesin at attachment sites). As mentioned previously, several mRNAs (e.g. *crumbs*, *even-skipped*, *fushi tarazu*, *hairy*, *runt*, and *wingless*) are apically localized within undifferentiated epithelia such as the embryonic blastoderm (64–69). In addition, mRNAs (e.g. *sevenless*) are localized within the developing epithelium of imaginal discs such as the eye disc (126).

It has been reported that *prospero* and *inscuteable* mRNAs are localized within embryonic *Drosophila* neuroblasts (127). The *inscuteable* transcripts are apically localized during interphase of the neuroblast cell divisions, while *prospero* transcripts are apically localized at interphase but are basal from prophase to telophase. Basal *prospero* RNA is segregated into one daughter cell (the ganglion mother cell).

The *S. cerevisiae* *ASH1* mRNA is localized within yeast cells at the site of the future bud and is segregated into the daughter cell (128, 129).

MECHANISMS OF RNA LOCALIZATION

This section focuses on general classes of RNA localization mechanisms. Specific details of *cis*-acting sequences and *trans*-acting factors that function in RNA localization are reviewed in the following section.

Nucleo-Cytoplasmic Transport

An obvious way to achieve cytoplasmic RNA localization is to export transcripts vectorially from only one side of the nucleus and then to transport or anchor them in the cytoplasm on that side of the nucleus. Substantial progress has been made recently in understanding the mechanisms of nucleo-cytoplasmic transport (130); however, studies of vectorial aspects of transport from the nucleus are in their infancy.

In general, it has been difficult to establish vectorial nucleo-cytoplasmic transport for particular transcripts due to experimental limitations. An exception is the case of pair-rule gene transcripts (*hairy* and *fushi tarazu*) in the cellularizing blastoderm of *Drosophila* (65, 131). Here it was possible to use mutations to produce two layers of nuclei (or displaced nuclei) in the cortex of the syncytial blastoderm and, thus, to show—for the inner nuclei—that transcripts are vectorially exported even in the absence of normal apical cytoskeletal structures. The fact that this is possible suggests that the nuclei themselves have a polarity independent of the cytoplasmic cytoskeleton. Moreover, this directed export depends on the 3'-UTR (65), suggesting that it is specific to these transcripts (see below for a discussion of the role of 3'-UTRs).

A second example of vectorial nucleo-cytoplasmic export may be the *Drosophila gurken* mRNA that is localized dorso-anterior to the nucleus in stage 8 oocytes. The *gurken* transcripts are synthesized in the oocyte nucleus itself (R Cohen, personal communication), and the K10 and Squid proteins may function in vectorial transport of the *gurken* mRNA (see below).

Transport from One Cell Type into Another

A second class of localization mechanism applies during *Drosophila* oogenesis. As outlined previously, RNAs are transported from the nurse cells into the oocyte through intercellular bridges known as ring canals. Nurse cells connect only to the presumptive anterior pole of the oocyte, so that the imported RNAs first arrive at the oocyte's anterior pole. It is likely that anteriorly localized RNAs (e.g. *bicoid*) are trapped at the anterior pole when they enter the oocyte (WE Theurkauf, TI Hazelrigg, personal communication). The fact that mutants in which nurse cells connect to the oocyte at both poles result in bipolar transport into the oocyte and trapping of *bicoid* RNA at both poles (42) supports this hypothesis. Recent experiments in which so-called localization particles were followed by time-lapse confocal microscopy supports this hypothesis further

(WE Theurkauf, TI Hazelrigg, personal communication). In contrast to the entrapment seen for anterior-localized RNAs, those that are localized to the posterior pole are actively transported there in association with the cytoskeleton or are localized there by other mechanisms such as degradation-protection (see below).

Transport Out of Mitochondria

The posterior polar plasm of *Drosophila* oocytes and early embryos contains large, non-membrane-bound organelles known as polar granules, which are involved in germ cell formation and specification (see below). Mitochondria are found in close association with the polar granules. One of the more remarkable examples of a localized RNA is the *Drosophila* 16S mitochondrial large ribosomal RNA (*mtlrRNA*), which is encoded by the mitochondrial genome (132). This RNA appears to be exported from the mitochondria into the cytoplasm within the posterior polar plasm and to be associated with polar granules (61, 133–137). Indeed, given the apposition of polar granules and mitochondria, the *mtlrRNA* may in fact be exported vectorially out of mitochondria directly into or onto the polar granules. The function of the *mtlrRNA* in the polar granules is unclear, although it has been implicated in pole cell formation (133). There is some disagreement, however, about whether a high local concentration of *mtlrRNA* is indeed necessary for pole cell formation (135–137).

Generalized Degradation with Localized Protection

It was postulated several years ago that one mechanism by which a generalized RNA distribution could be converted to a restricted pattern was through degradation of the RNA throughout the cell except at the site of localization (138). Several *Drosophila* transcripts represent variants of this type of process. For example, while the bulk of maternally synthesized *nanos* and *cyclin B* transcripts are concentrated in the posterior polar plasm of the early embryo, a subset of these transcripts remains unlocalized (62, 139–141). The posteriorly localized transcripts are taken up into the pole cells when they bud, while the unlocalized transcripts are degraded (62, 139–141). Similarly, maternally synthesized *Hsp83* transcripts are generally distributed in the early embryo (61, 63, 142; SR Halsell, A Bashirullah, RL Cooperstock, WW Fisher, A Karaiskakis, HD Lipshitz, manuscript in preparation). *Hsp83* transcripts in the posterior polar plasm also are taken up into the pole cells when they bud, while the remaining transcripts are degraded (61, 63, 142; SR Halsell, A Bashirullah, RL Cooperstock, WW Fisher, A Karaiskakis, HD Lipshitz, manuscript in preparation). There is a close correlation between translational repression of unlocalized *nanos* transcripts and their degradation (reviewed in 144). Under normal conditions, the polar granules are necessary and sufficient for protection of *nanos*, *cyclin B*, and *Hsp83* transcripts from degradation at the posterior (56, 60, 63).

Another example of transcript destabilization and localization may be maternally synthesized *PCNA* mRNA in the ascidian oocyte. There is sequence complementarity between a non-protein-coding RNA, *YC*, whose 3' end is complementary to the 3'-UTR of the *PCNA* RNA (100) as well as to the 5'-UTR of *ribosomal protein L5* RNA (*ScYC26a*) (102). During oogenesis the *YC* RNA is perinuclear, gradually moving to the cortex, and after fertilization the RNA segregates to the myoplasm and associates with the cytoskeleton (101). Uniformly expressed maternal *PCNA* RNA initially overlaps with *YC* RNA but later becomes depleted in the myoplasm (100). Investigators have suggested that the double-stranded *YC-PCNA* RNA hybrid in the myoplasm might somehow destabilize *PCNA* RNA, thus representing an example of RNA localization by degradation-protection. The hypothesis that such double-stranded RNA hybrids destabilize specific RNAs in the myoplasm is, however, confounded by the data for the *L5 ribosomal protein* maternal RNA. Although there is substantial sequence complementarity between *YC* and *L5* RNAs, *L5* RNA is concentrated in myoplasm along with *YC* RNA, rather than destabilized there (102). In this case, the *YC* RNA has been postulated to aid the anchoring of *L5* RNA. Whether *PCNA* RNA localizes by a mechanism that involves hybrid-induced degradation remains an open question.

Directed Cytoplasmic Transport of RNA

Asymmetries in cytoskeletal organization have been described earlier for both *Xenopus* and *Drosophila* oocytes. Further, there is colocalization of specific RNAs with either a minus-end-directed microtubule motor (Nod) or a plus-end-directed motor (kinesin), in particular regions of the *Drosophila* oocyte's cytoplasm (see above). There is now substantial evidence that cytoplasmic RNA transport to specific intracellular destinations is accomplished by both the microtubule- and the microfilament-based cytoskeleton. The following section reviews evidence for a role of the cytoskeleton in anchoring localized RNAs at their intracellular destinations. Here the role of the cytoskeleton in directed cytoplasmic transport is reviewed.

Analysis of intracellular transport mechanisms requires the ability to systematically perturb normal cytoskeletal function. These studies have been aided in *Xenopus* and *Drosophila* by drugs that specifically perturb either the microtubule-based (colchicine, nocodazole, or taxol) or the microfilament-based (cytochalasins) cytoskeleton. In addition, mutations that affect components of the cytoskeleton have led to informative results in *Drosophila* and *Saccharomyces*.

THE ROLE OF THE CYTOSKELETON IN RNA TRANSPORT DURING DROSOPHILA OOGENESIS Localized RNAs have several characteristic and sequential patterns of expression during *Drosophila* oogenesis that correlate with particular aspects of the cytoskeleton, particularly the microtubules (see above).

Over a dozen transcripts are synthesized in the nurse cells and specifically accumulate in the oocyte within early egg chambers prior to their localization [*bicoid* (7), *nanos* (28), *orb* (23), *oskar* (24, 25), *Add-hts* (16), *Bicaudal-C* (18), *Bicaudal-D* (19), *gurken* (21), *Pgc* (26), *K10* (22), *egalitarian* (20), and *tudor* (27)]. Transport of these RNAs into the oocyte is likely to be carried out by minus-end-directed microtubule motors since the MTOC is located in the oocyte during these stages (see above). Although no specific motors have been demonstrated to be involved in this process, the kinesin-like minus-end-directed motor—Nod—localizes first to the oocyte and then to its posterior at the same stages as many of these RNAs are transported into the oocyte and then accumulate at its posterior pole (36). Dynein (a minus-end-directed motor) is also localized to the oocyte at these stages (145) but does not appear to be involved in RNA transport and localization (146). During these stages, several RNAs are present in detergent insoluble fractions (e.g. *bicoid*, *oskar*, *Bicaudal-D*, *K10*, *orb*) indicating association with the cytoskeleton (147). Moreover, the association of *bicoid*, *oskar*, and *Bicaudal-D* RNAs with the cytoskeleton is sensitive to colchicine and not to cytochalasins, indicating that microtubules but not microfilaments are involved in their transport and localization (37, 147).

The phenotypes of *orb*, *egalitarian*, and *Bicaudal-D* mutants suggest a role in oocyte specific RNA accumulation. Egalitarian and Bicaudal-D proteins are made in nurse cells and are transported to the posterior of the oocyte presumably along minus-directed microtubules (20). The distribution of Egalitarian and Bicaudal-D proteins parallels that of the RNAs that are transported into the oocyte at these stages. Microtubule inhibitors result in delocalization of Egalitarian protein (20). Moreover, in *egalitarian* mutants *oskar* and *orb* RNA are no longer associated with the cytoskeleton (147). This indicates that Egalitarian and Bicaudal-D proteins may be involved—directly or indirectly—in transporting localized RNAs along microtubule networks into and to the posterior of the oocyte.

Mutations in genes required for early localization also perturb oocyte polarity; *egalitarian* and *Bicaudal-D* mutations cause all 16 cells of the cyst to become polyploid nurse cells; thus oocyte-specific accumulation of transcripts cannot occur because there is no oocyte (20, 148). Orb is required for oocyte polarity, and in *orb* mutants, oocytes are located at ectopic positions within the egg chamber (149). In *orb* mutant oocytes certain RNAs (*orb*, *oskar*) are still localized—albeit at abnormal positions—whereas others are not localized at all (*Add-hts*, *Bicaudal-D*, *K10*) (149). It is possible that Orb protein is required to establish microtubule polarity, whereas Egalitarian and Bicaudal-D are necessary for its maintenance.

As described above, the majority of RNAs transported into and localized in the oocyte have in common early transport from the nurse cells (stage 1–5),

transient localization to the posterior (stage 6), and subsequent localization to the anterior (stages 7–8). In addition, *oskar* and *Pgc* transcripts move back to the posterior pole of the oocyte at stage 9, whereas the *bicoid* and *Add-hts* RNAs never show the early posterior localization but are either always anteriorly localized (*bicoid*) or are initially localized throughout the cortex and subsequently localize to the anterior (*Add-hts*). These data suggest that a default transport and localization mechanism is carried out by minus-end-directed microtubule motors, and that certain RNAs (*bicoid*, *Add-hts*, *oskar*, *Pgc*) initially use this mechanism to enter the oocyte but then engage a different localization machinery. Since *bicoid* and *oskar* RNA transport and localization are best understood and exemplify distinct localization mechanisms, they are discussed below.

bicoid RNA is localized at the anterior pole of the oocyte by stage 8 of oogenesis and remains anterior until the late cleavage stage of embryogenesis when it is degraded. During its translocation from the nurse cells into the oocyte, it is apically localized within the nurse cells (32). Both apical nurse cell localization and anterior oocyte localization are sensitive to microtubule depolymerizing drugs (colchicine, nocodazole, tubulazole C) but not to inhibitors of F-actin polymerization (cytochalasin D and B) (150). Recent evidence suggests that transport of *bicoid* RNA into the oocyte actually involves several distinct steps that might be mediated by distinct localization mechanisms; for example, two distinct microtubule-dependent steps drive *bicoid* RNA localization particles within the nurse cell cytoplasm (WE Theurkauf, TI Hazelrigg, personal communication), but transport through the ring canals into the oocyte is resistant to both microtubule and actin filament inhibitors (WE Theurkauf, TI Hazelrigg, personal communication). The Exuperantia protein may mediate this microtubule-independent transport (151). The cytoskeletal association of *bicoid* transcripts is stage specific (147). During early oocyte accumulation, *bicoid* transcripts are associated with the cytoskeleton (i.e. the detergent-insoluble fraction). However, during stages 8–11, when *bicoid* transcripts are at the anterior margin of the oocyte, they are not cytoskeleton associated. This observation supports the idea that anchoring at the anterior pole at these stages is accomplished by some other structures. Later, during stage 14, *bicoid* RNA is localized in a tight cap at the anterior, is again associated with the microtubule-based cytoskeleton, and its localization is again sensitive to colchicine. In early embryos, *bicoid* RNA is no longer restricted to the cortex and is not associated with the cytoskeleton (147).

A kinesin- β -galactosidase fusion protein localizes to the posterior (41) at stages 8–9, indicating that microtubules traverse the antero-posterior axis of the oocyte at these stages and are oriented with their plus ends at the posterior (41). This localization coincides with the initiation of *oskar* and *Pgc* translocation

from the anterior pole of the oocyte to its posterior. Thus it is likely that *oskar* and *Pgc* switch from the use of minus-end-directed microtubule motors to the use of plus-end-directed ones in order to achieve transport to the posterior.

Posterior localization of the kinesin- β -galactosidase fusion protein is lost once ooplasmic streaming begins (stage 10) and is absent in *capuccino* and *spire* mutant oocytes that undergo premature streaming (41, 52). In *capuccino* and *spire* mutants *oskar* RNA is not localized to the posterior during stages 8 and 9, but instead *oskar* RNA is uniformly distributed throughout the oocyte (24, 25). These mutants cause an early cytoplasmic streaming during stage 7 and 8 instead of 10B (52), suggesting that premature assembly of microtubules into the parallel arrays in the subcortex drives cytoplasmic streaming (52). In other words, *oskar* RNA does not localize to the posterior in *capuccino* and *spire* mutants because these mutants omit the stage during which antero-posterior axial organization of microtubules is used for directed transport of *oskar* RNA to the posterior.

Evidence suggests a role for the actin-based cytoskeleton at the anterior of the oocyte in transfer of RNAs to the microtubules that run from the anterior to the posterior pole. In oocytes that are mutant for a component of the actin-based cytoskeleton—cytoplasmic (nonmuscle) tropomyosin II (*cTmII*)—*oskar* RNA remains anteriorly localized at stage 9 and never localizes posteriorly (152, 153). This observation suggests a role for *cTmII*—and possibly the actin-based cytoskeleton—in transfer of *oskar* RNA to the axial microtubules. Staufen protein similarly fails to translocate posteriorly in *cTmII* mutants (152), suggesting that the entire transport particle containing Staufen protein and *oskar* RNA fails to be transferred to the posterior translocation apparatus.

THE ROLE OF THE CYTOSKELETON IN RNA TRANSPORT DURING XENOPUS OOGENESIS As discussed above, the dynamics of transcript localization to the vegetal pole of *Xenopus* oocytes can largely be classified into two different patterns exemplified by *Vg1* and *Xcat-2* RNAs.

Xcat-2 transcripts are distributed uniformly in early *Xenopus* oocytes (79) and are then sequestered into the METRO region of the mitochondrial cloud along with *Xwnt-11*, *Xlsirt*, and other RNAs (70, 90). This step appears to be mediated by selective entrapment of these RNAs, possibly similar to posterior polar-granule-localized RNAs in *Drosophila* (see below). Once localized to the METRO, *Xcat-2* accompanies the mitochondrial cloud to the vegetal pole (90). *Xcat-2* RNA then relocates to form a disc-like pattern at the tip of the vegetal pole (90).

Vg1 RNA is initially generally distributed in the oocyte and later localizes in the wedge-shaped pattern that overlaps but differs from that of *Xcat-2* RNA at the vegetal pole (90). Accumulation of *Vg1* to the vegetal pole requires

functional microtubules but not actin microfilaments (94). Later *Vg1* RNA is found throughout the cortex of the vegetal hemisphere, unlike *Xcat-2*, which is localized to a more restricted area at the vegetal pole (90). During this late stage, *Vg1* RNA is enriched 30- to 50-fold in the detergent-insoluble fraction (96). Moreover, this association and cortical *Vg1* RNA localization are not sensitive to microtubule-depolymerizing drugs (nocodazole and colchicine) but rather to microfilament-disrupting agents (cytochalasin B) (94). This is an indication of a two-step localization mechanism for *Vg1* RNA where microtubules are required for translocation and actin filaments for anchoring (94). Recent evidence indicates that *Vg1* RNA is associated with the endoplasmic reticulum (ER) and that *Vg1* RNA-ER complexes move to the vegetal pole along with the mitochondrial cloud in a microtubule-dependent fashion (154).

Xcat-2 RNA injected into later oocytes is able to localize cortically without prior association with the METRO (99). This localization is dependent on microtubules and cannot occur in late oocytes (stage VI) when microtubules are no longer present (99). Moreover, the *cis*-acting elements within the *Xcat-2* 3'-UTR that are required for METRO localization and cortical localization are different but overlapping (79, 99) (see below). In addition, injected *Xcat-2* transcripts that localize to the vegetal cortex without METRO do so in a pattern similar to *Vg1* (throughout the vegetal hemisphere) but different from that of endogenous *Xcat-2* transcripts (99). Thus the differences in *Vg1* and *Xcat-2* localization patterns are a consequence of the fact that *Xcat-2* is normally associated with the METRO, rather than in some inherent difference in their ability to associate with the microtubule-based cytoskeleton.

ROLE OF THE CYTOSKELETON IN RNA TRANSPORT IN OTHER CELL TYPES Observations of localized RNAs in living neurons in culture have suggested that they are present in particles composed of several RNAs and proteins including polyribosomes (155). These particles translocate inside the cell in a microtubule- but not microfilament-dependent manner (155). Similar studies with *MBP* RNA injected into oligodendrocytes in culture indicate that the initially homogeneous *MBP* RNA becomes organized into granules that align on microtubule tracks in the peripheral processes (156). Endogenous *MBP* RNA is seen in granules and fractionates with the insoluble fraction in cell extracts, consistent with an association of "transport" granules with the cytoskeleton (156).

Mammalian *tau* mRNA is localized to the proximal hillock of axons (112). This localization is mediated by the *tau* 3'-UTR (see below) and depends on microtubules (157). Interestingly, *in vitro* synthesized *tau* 3'-UTR injected into *Xenopus* oocytes localizes to the vegetal pole in a pattern identical to *Vg1* RNA (158). Moreover, this localization is dependent first on microtubules and then on

actin microfilaments, as for *Vg1* RNA (158). This observation demonstrates that once an RNA associates with the cytoskeletal transport apparatus, it localizes according to the type of cell in which it is. This occurs even if that RNA normally would not be present in this cell type. Thus the role of the cytoskeleton in RNA localization is highly conserved across evolution (see below).

RNA localization also occurs in the yeast *S. cerevisiae*. In this budding yeast, *ASH1* mRNA is localized first to the future bud site and then to the daughter cell by a mechanism involving actin microfilaments (128, 129). The role of microfilaments was demonstrated genetically using mutants in actin, myosin, profilin, and tropomyosin (which form part of the microfilament network). In contrast, disruption of microtubules by tubulin mutants, or disruption of the process of budding with *MYO2* mutants, has no effect on *ASH1* transcript localization.

In various somatic cells (e.g. fibroblasts and myoblasts) β -actin mRNA is localized to moving membranes (123, 124). This localization is not dependent on microtubules or intermediate filaments but on microfilaments (123). Both RNA transport and anchoring are dependent on the actin cytoskeleton (123).

The data described above indicate a key role for microtubules in directed mRNA transport, especially in *Drosophila* and *Xenopus* oocytes but also in polarized cells such as neurons and glia. In several cases, microfilaments also play a crucial role in RNA localization. However, it is unclear whether the instances of microfilament-based RNA localization indicate a role in directed RNA transport versus in entrapment/anchoring of the RNA at the site of localization (see below).

Entrapment/Anchoring of RNA at the Site of Localization

At stage 10B of *Drosophila* oogenesis, the microtubules in the oocyte assemble into subcortical arrays that direct circumferential ooplasmic streaming (see above). Thus at these stages, RNAs cannot be localized to the posterior by directed transport on axial microtubules. Localized RNAs most likely are trapped at the posterior as they circulate through the oocyte cortex along with unlocalized components of the cytoplasm. In support of this hypothesis, it has been shown that, while long-range transport of injected *oskar* RNA to the posterior requires microtubules (159), local injection of *oskar* RNA near the posterior pole of large (stage 10–11) oocytes or anywhere in smaller (stage 9) oocytes results in posterior localization in a microtubule-independent process. This observation suggests that short-range RNA transport and/or local entrapment of RNA is not dependent on microtubules. Trapping of injected *oskar* transcripts at the posterior pole fails in *cTmII* mutant oocytes (159), consistent with a role for the actin-based cytoskeleton in this process.

Egalitarian and Bicaudal-D may also be required for posterior anchoring or trapping of RNAs such as *oskar*. In a situation where Bicaudal-D is eliminated during late oogenesis (160), *oskar* RNA is initially localized normally but then is lost from the posterior pole. In these mutant oocytes kinesin- β -galactosidase protein localizes normally to the posterior; therefore, the microtubule-based cytoskeleton involved in posterior transport is not disrupted. Posterior RNA localization occurs independent of Bicaudal-D, but maintenance of localization is dependent on Bicaudal-D function. Bicaudal-D may be involved in anchoring of RNA at the posterior pole of the oocyte, where it may function in a complex with Egalitarian (20).

Anchoring of RNAs at the posterior pole of the *Drosophila* oocyte also requires the integrity of the polar granules. These are large non-membrane-bound organelles composed of RNA and protein. Many posteriorly localized RNAs are either components of the polar granules or are associated with the granules (reviewed in 142). Mutations that disrupt the posterior polar granules (e.g. *capuccino*, *oskar*, *spire*, *staufen*, *tudor*, *valois*, and *vasa*) cause delocalization of posteriorly localized RNAs while ectopic assembly of polar granules at the anterior pole of the oocyte results in anterior localization of RNAs normally localized to the posterior (reviewed in 142), with the possible exception of the *mtlrRNA* (137). Developmental functions of the posterior polar granules and their associated localized RNAs are considered below.

In *Xenopus* oocytes, anchoring of *Vg1* RNA to the vegetal cortex of stage IV oocytes requires microfilaments (94), which as for *Drosophila*, implicates the actin-based cytoskeleton in anchoring of RNA. Anchoring of *Vg1* RNA also involves other—non-protein-coding—localized RNAs, *Xlsirts* (161). Injection of oligonucleotides complementary to *Xlsirt* transcripts causes delocalization of anchored *Vg1* RNA in a manner similar to delocalization by F-actin-disrupting drugs (161). This observation indicates a connection between *Xlsirt* RNA, *Vg1* RNA, and F-actin; however, no direct interactions have been demonstrated. A role for the noncoding *YC* RNA in anchoring *L5* RNA in the myoplasm of the ascidian oocyte and early embryo has also been postulated (102). However, no experimental evidence supports this hypothesis.

Finally, for *ASH1* RNA in yeast (128, 129) as well as for β -actin mRNA in mammalian somatic cells (123), the actin-based cytoskeleton is necessary for localization (see above). However, the mechanism of localization of these RNAs is not clear; it has not yet been determined whether localization is by selective entrapment or by directed transport.

RNA Transport/Anchoring Particles

Specific *trans*-acting factors that interact with localized RNAs are discussed later in a separate section. Large ribonucleoprotein RNA transport particles

have been visualized at the light microscope level in several systems. For example, *bicoid* RNA is transported from the nurse cells into the oocyte in particles that contain Exuperantia protein (162; WE Theurkauf, TI Hazelrigg, personal communication). Maintenance of *bicoid* transcripts at the anterior pole, as well as transport of *oskar* RNA to the posterior pole, likely involves particles that contain Staufen protein (163, 164). In *Xenopus*, RNA-containing transport particles have been visualized (90, 99). In neurons and glia, large transport particles containing *tau* RNA (157) and *MBP* RNA (156), respectively, have been identified. Particles containing *ASH1* mRNA have been detected in *S. cerevisiae* (129). The polar granules of *Drosophila* and the germinal granules of *Xenopus* are very large (organelle-sized) ribonucleoprotein (RNP) particles that are involved in anchoring localized RNAs at the posterior and vegetal poles of *Drosophila* and *Xenopus* oocytes, respectively. Several of the particles mentioned here contain not just proteins and mRNAs, but also non-protein-coding RNAs (26, 90, 97, 134, 155).

CIS-ACTING ELEMENTS THAT TARGET RNAs FOR LOCALIZATION

In principle, there are two mechanisms by which an RNA molecule could be targeted for cytoplasmic localization. An RNA element or elements could be recognized by the localization machinery. Alternatively (only in the case of mRNAs), the polypeptide product of the RNA might be recognized and the RNA translocated intracellularly along with the polypeptide. The latter mechanism—through recognition of the signal peptide by the SRP apparatus—may be used to bring mRNAs that encode secreted or transmembrane proteins into association with the endoplasmic reticulum (reviewed in 165). All other defined cytoplasmic RNA localization mechanisms involve recognition of RNA elements, particularly in the 3'-UTR of mRNAs. This section summarizes the methods used to map *cis*-acting sequence elements within localized RNAs. Generalities about the location of such elements within the RNAs are then drawn, and specific features of these elements are discussed. A subsequent section focuses on *trans*-acting factors that interact with these elements.

Mapping of Cis-Acting Elements in Localized RNAs

The general method used to map *cis*-acting sequences that function in RNA localization is to produce hybrid RNAs that include an exogenous reporter sequence (e.g. part of the *E. coli* β -galactosidase RNA) and part or all of the RNA under study. These hybrid transcripts are introduced into the cell type of interest, and the reporter sequence is used as a tag to assay localization of the hybrid transcript. Initially the location of the transcripts was assayed by isolating parts of cells and carrying out RNase protection assays for the presence of the

transcripts (166). However, this method was replaced by the use of in situ hybridization with antisense reporter RNA probes (e.g. antisense *β -galactosidase* RNA probes) either in tissue sections or whole mounts. More recently—in the case of injected in vitro transcribed RNAs that have been fluorescently tagged—it has been possible to visualize the injected RNAs directly by fluorescence microscopy (159). Elements involved in various aspects of localization are then mapped further by testing a series of RNAs that carry deletions or mutations in the region that confers localization. Using these methods, *cis*-acting sequences sufficient (i.e. that are capable of conferring localization) or necessary (i.e. that when deleted result in failure of localization) can be mapped. Additional information may be gained by performing sequence alignments of the region of interest among different species. Conserved domains may represent important *cis*-acting elements required for localization (167).

Methods available for introducing the hybrid RNA into the cell-type of interest vary depending on the system. In *Drosophila* transgenic flies can be obtained that synthesize the hybrid transcripts in the correct cell type and often at the correct developmental stage. This can be accomplished using an inducible promoter, a cell-type-specific promoter, or the promoter of the relevant endogenous gene. Thus there is seldom any question as to the in vivo significance of the results obtained. In many cases mutations exist that eliminate or reduce the function of the endogenous gene. This then enables one to test whether a transgene carrying all of the endogenous regulatory and protein coding sequences rescues the mutant phenotype. If so, then transgenes in which specific RNA elements are deleted can be assayed for phenotypic rescue or lack thereof; thus both the effects on RNA localization, and the phenotypic consequences of disrupting that localization, can be tested simultaneously.

A second common method for introducing the hybrid transcripts into the host cytoplasm is by injection of in vitro transcribed RNA. This has been done occasionally in *Drosophila* (60, 159) but is most common in *Xenopus* oocytes where transgenic technology is still rather primitive. In both *Drosophila* and *Xenopus*, the large size of the oocyte enables the injected RNA to be introduced at a specific location within the cell.

A third method, used mostly for analyses of somatic cells in culture, is to transfect expression plasmids carrying the hybrid transcription unit into the cells, to wait for transcription and possible localization to occur, and then to assay the distribution of the hybrid RNAs.

Cis-Acting Sequences for Localization Map to the 3'-Untranslated Region of mRNAs

Table 2 lists localized RNAs in which *cis*-acting localization elements have been mapped. For all mRNAs studied to date, sequences that are necessary for localization are found in the 3'-untranslated region (3'-UTR). In many cases,

Table 2 *Cis*-acting localization elements

Species	Transcript name	Localization signal(s)	Sufficient subregions (subelements)	Reference
<i>Drosophila</i>	<i>Add-hts</i>	3'-UTR (345 nt)	345 nt sufficient (ALE1 = 150 nt)	— ^a
	<i>bicoid</i>	3'-UTR (817 nt)	625 nt sufficient (BLE1 = 53 nt)	166, 176
	<i>Cyclin B</i>	3'-UTR (776 nt)	94 nt + 97 nt (TCE = 39 nt)	182
	<i>even-skipped</i>	3'-UTR (190 nt)	163 nt (124 nt in UTR)	65
	<i>fushi tarazu</i>	3'-UTR (455 nt)	Not defined	65
	<i>hairy</i>	3'-UTR (816 nt)	Not defined	65
	<i>Hsp83</i>	3'-UTR (407 nt)	107 nt sufficient (protection)	— ^b
	<i>K10</i>	3'-UTR (1400 nt)	44 nt (TLS) sufficient	181
	<i>nanos</i>	3'-UTR (849 nt)	543 nt sufficient (localization) (TCE = 90 nt translational control) (SRE = 60 nt translational control)	43, 141, 185
	<i>orb</i>	3'-UTR (1200 nt)	280 nt sufficient	169
	<i>oskar</i>	3'-UTR (1043 nt)	924 nt sufficient (localization) (BRE = 71 nt translational control)	168, 184
	<i>wingless</i>	3'-UTR (1083 nt)	363 nt sufficient	— ^c
	Mammals	<i>β-actin</i>	3'-UTR (591 nt)	54 nt or 43 nt sufficient (43 nt less active)
<i>BC1</i>		5' region (152 nt)	62 nt sufficient	173
<i>CaMKIIα</i>		3'-UTR (3200 nt)	Not defined	109
<i>tau</i>		3'-UTR (3847 nt)	1395 nt sufficient (VgRBP-binding region = 624 nt)	157, 158
Xenopus	<i>Vgl</i>	3'-UTR (1300 nt)	340 nt (VgLE) sufficient (85 nt repeat)	170, 183
	<i>TGF β-5</i>	3'-UTR (1102 nt)	Not defined	198
	<i>Xcat-2</i>	3'-UTR (410 nt)	150 nt (mitochondrial cloud) 120 nt (vegetal cortex)	99
	<i>Xlsirt</i>	3–12 repeat sequences (79–81 nt)	Two copies of repeat sufficient	97
Yeast	<i>ASH1</i>	3'-UTR	250 nt sufficient	128

^aKL Whittaker, D Ding, WW Fisher, HD Lipshitz, manuscript in preparation.^bSR Halsell, A Bashirullah, RL Cooperstock, WW Fisher, A Karaiskakis, HD Lipshitz, manuscript in preparation.^cH Krause, personal communication.

these 3'-UTR elements are also sufficient for localization. Examples of mRNAs that contain such localization elements in *Drosophila* include anteriorly localized transcripts such as *bicoid*, *Add-hts*, and *K10* (22, 166; KL Whittaker, D Ding, WW Fisher, HD Lipshitz, manuscript in preparation), posteriorly localized transcripts such as *oskar*, *nanos*, *orb*, *Cyclin B*, and *Hsp83* (43, 60, 142, 168, 169; SR Halsell, A Bashirullah, RL Cooperstock, WW Fisher, A Karaiskakis, HD Lipshitz, manuscript in preparation), and apically localized pair-rule gene transcripts such as *even-skipped*, *fushi-tarazu*, *hairy*, and *wingless* (65). *Xenopus* also provides examples such as *Vg1*, *TGF β -5*, and *Xcat-2* (99, 170). Interestingly, the rat *tau* RNA's 3'-UTR, which confers localization to the proximal hillock of rat axons, also mediates vegetal localization in *Xenopus* oocytes (158). The chicken β -actin 3'-UTR contains a *cis*-acting element sufficient for peripheral localization in chicken embryonic fibroblasts and myoblasts (171). The presence of localization tags in the 3'-UTR adds to the list of 3'-UTR *cis*-acting elements involved in posttranscriptional mRNA regulation via control of stability, cytoplasmic polyadenylation, and translation (172).

Cis-Acting Sequences for Localization Map Within Non-Protein-Coding RNAs

Non-protein-coding RNAs also contain discrete elements that target the RNAs for localization (Table 2). Such elements have been mapped in *Xenopus Xlsirt* (97) and in neuronal *BC-1* RNAs (173).

Alternative Splicing Can Generate Localized vs Unlocalized RNA Isoforms

Drosophila Cyclin B transcripts exemplify the importance of alternative splicing of sequences that target localization (60). Alternative splicing within the 3'-UTR generates two *Cyclin B* mRNA isoforms that differ by 393 nucleotides (nt). The shorter splice variant is synthesized preferentially during early oogenesis and is present throughout the pro-oocyte until stages 7–8. The longer splice variant is synthesized in the nurse cells later in oogenesis, during stages 9–11. It is then transported into the oocyte, with an initially uniform distribution and is later concentrated at the posterior pole (60, 61). The transcript also exhibits perinuclear localization in the syncytial embryo. Posterior localization of the long *Cyclin B* mRNA isoform is directed by the additional sequences spliced into its 3'-UTR relative to the short mRNA isoform (which is unable to localize) (60).

Alternative splicing also plays a role in the localization of *Add-hts* transcripts. Three classes of *Add-hts* contain unique 3'-UTRs introduced by alternative splicing (KL Whittaker, D Ding, WW Fisher, HD Lipshitz, manuscript in preparation). This alternative splicing also introduces variability in the

carboxy-terminal regions of the encoded Adducin-like protein isoforms (174; KL Whittaker, D Ding, WW Fisher, HD Lipshitz, manuscript in preparation). Only one of the mRNA variants, N4, exhibits transport into and localization within the oocyte (16; KL Whittaker, D Ding, WW Fisher, HD Lipshitz, manuscript in preparation). The N4 3'-UTR is necessary and sufficient for this transport and localization, suggesting that use of alternative 3'-UTRs is one mechanism by which different *Add-hts* protein isoforms are restricted to different subsets of the nurse cell–oocyte complex (KL Wittaker, D Ding, WW Fisher, HD Lipshitz, manuscript in preparation).

Although not a consequence of alternative slicing, two *actin* RNA isoforms, encoding α - and β -actin, possess isoform-specific 3'-UTRs that can confer differential intracellular targeting (175). β -*actin* transcripts are localized to the leading lamellae in both differentiating myoblasts and small myotubes, while α -*actin* transcripts associate with a perinuclear compartment.

Discrete Localization Elements

In the case of *bicoid* RNA, discrete elements within the 3'-UTR have been defined that confer distinct aspects of the RNA localization pattern. A decade ago a 625-nt subset of the *bicoid* 3'-UTR was found to be sufficient for anterior localization (166). At that time it was suggested that the secondary structure of the 3'-UTR, which can be folded into several long stem-loops, might be recognized by the localization machinery. Subsequent evolutionary sequence comparisons supported this hypothesis since the secondary structure appears to be conserved in distant *Drosophila* species (*melanogaster*, *teissieri*, and *virilis*) despite the fact that the primary sequence of these 3'-UTRs has diverged by up to 50% (167). Further, the 3'-UTR from one species can direct anterior localization in a distant species (167). There is complementarity between two single-stranded regions predicted in the secondary structure, implying that tertiary base-pairing interactions might also be important (167).

Subsequent analyses followed two different routes. In one set of experiments, deletions were used to define an approximately 50-nt region, called *bicoid* localization element 1 (BLE1), which is necessary and sufficient (when present in two copies) to direct nurse cell–oocyte transport and anterior transcript localization during mid-oogenesis (176). However, anterior localization is lost later. BLE1 interacts with Ex1 protein, which might function in localization to the anterior of the oocyte (177) (see below). In addition, linker scanning and point mutational analyses were used to define regions of the 3'-UTR that are important for anterior localization late in oogenesis and in the early embryo (163, 164). These regions interact with the double-stranded RNA-binding protein Staufen (178, 179), which functions to anchor *bicoid* RNA at the anterior of the late-stage oocyte and early embryo (see below). This is accomplished in

part by promoting quaternary (inter-3'-UTR) interactions via the complementary single-stranded regions mentioned earlier (164).

Although not yet as well characterized as *bicoid*, it has similarly been possible to map discrete elements in other 3'-UTRs that direct subsets of the localization pattern. For example, the N4 isoform of *Add-hts* mRNA is transported from the nurse cells into the oocyte starting in the germarium, then localized cortically in the oocyte (stages 7–8) and to the anterior pole (stage 9) (16, 44, 45, 180). In this case, a central (100–150 nt) element of the 3'-UTR, *Add-hts* localization element 1 (ALE1), is necessary and sufficient for nurse cell–oocyte transport as well as for cortical localization within the oocyte (KL Whittaker, D Ding, WW Fisher, HD Lipshitz, manuscript in preparation). The region that includes ALE1 comprises the most extensive predicted secondary structure within the *Add-hts* N4 3'-UTR (KL Whittaker, D Ding, WW Fisher, HD Lipshitz, manuscript in preparation). When additional, adjacent parts of the N4-3'-UTR are added to ALE1, anterior localization is conferred starting at stage 9 (KL Whittaker, D Ding, WW Fisher, HD Lipshitz, manuscript in preparation). The *K10* 3'-UTR reveals several long inverted repeats, suggesting that it forms extensive secondary structure (22). A short region within the *K10* 3'-UTR, TLS (transport/localization sequence, 44 nt in length) is predicted to form a stem-loop structure and is necessary and sufficient for nurse cell–oocyte transport and anterior localization (181). Mutations that disrupt this structure block transport and localization, while compensatory mutations that preserve the structure restore these processes.

With respect to posteriorly localized RNAs, it has also been possible in some cases to map discrete localization elements. For example, as mentioned above, a 181-nt element in the long isoform of *Cyclin B* mRNA is necessary for posterior localization (182). Similarly, a 107-nt element in the *Hsp83* 3'-UTR is necessary and sufficient for association with the posterior polar plasm (SR Halsell, A Bashirullah, RL Cooperstock, WW Fisher, A Karaiskakis, HD Lipshitz, manuscript in preparation).

Repeated/Redundant Localization Elements

In the examples described above it was possible to define discrete, relatively small (<150 nt) localization elements that confer specific aspects of localization. In other instances, while discrete elements have been identified that direct localization, there is some redundancy in the system such that more than one localization element capable of conferring a particular aspect of the localization pattern, is present in the RNA.

An example comes from the *Xenopus Vg1* 3'-UTR. A 340-nt region within the 3'-UTR is necessary and sufficient for vegetal localization of *Vg1* RNA (170). Deletion analysis indicates that there is considerable redundancy within

this region but that critical elements can be defined that lie at each end (183). An 85-nt subelement from the 5' end of the region, when duplicated, is sufficient to direct vegetal localization (183).

A second example is in the *orb* 3'-UTR (169). In early oogenesis, *orb* transcripts accumulate preferentially in the pro-oocyte (stage 1). They localize transiently to the oocyte posterior (stages 2–7) and then to the oocyte anterior (stages 8–10). A 280-nt element is sufficient to confer oocyte accumulation, posterior localization, and then anterior localization. Further analysis has shown that when the element is split in two, each half on its own confers oocyte accumulation, although the level of accumulation is reduced relative to the intact element (169). Several possibilities could account for this result. Each element may constitute an independent binding site for the localization machinery, and the presence of both elements might recruit more localization factors. Alternatively, the two elements may interact with each other to present a better binding site and recruit a single binding factor.

A third example comes from analysis of the chicken β -*actin* 3'-UTR (171). β -*actin* mRNA is localized to the leading edge of lamellae in chicken embryonic fibroblasts and myoblasts. A so-called peripheral zipcode element consisting of the first 54 nt of the 3'-UTR is sufficient to direct localization of a heterologous transcript. When this element is deleted from the full-length 3'-UTR, the transcript is still able to localize, suggesting the presence of a redundant element. An inspection of the remainder of the 3'-UTR revealed a region of homology to the 54-nt zipcode within a more 3'-located 43-nt sequence. When this 43-nt region is present on its own, it is able to direct localization, albeit less effectively than the 54-nt element. These data suggest functional redundancy, but a functional analysis gave complicated results. Transfection of oligonucleotides complementary to each element individually significantly reduced localization (171). This observation may suggest that both elements are required in their natural context to mediate localization and, therefore, that they are not fully redundant. However, each element can mediate localization in isolation. In addition, antisense oligonucleotides used may have recognized both elements (since they share sequence homology) and thus simultaneously inactivated both localization elements.

A final case of repetition comes from the noncoding *Xlsirts*. These RNAs include repeated sequence elements flanked by unique sequences. The repeated element is 79–81 nt long and is tandemly repeated 3–13 times (97). Vegetal localization can be conferred by as few as two of the 79-nt sequence elements (97).

Dispersed/Nonredundant Localization Elements

In contrast to the aforementioned examples, in some cases it has been difficult to map discrete localization elements. For example, the *nanos* 3'-UTR contains

a 547-nt region that is necessary and sufficient to confer localization (43). Two overlapping subregions map within this larger region, either of which are capable of conferring localization. However, these subregions are 400 and 470 nt in length, respectively, and cannot be subdivided without disrupting localization (43). Another possible example is the 1043-nt *oskar* 3'-UTR (168). In this case deletions have been used to define elements necessary for distinct aspects of *oskar* RNA localization. However, it has been difficult to demonstrate sufficiency of individual elements for any specific aspect of localization (168).

In principle, several scenarios might prevent definition of discrete and small (<150 nt) elements sufficient for localization. For example, there might be several dispersed elements, each necessary for localization, distributed over a large region. Deletion of any one of these elements would disrupt localization. Alternatively, the arrangement of specific localization elements within the larger region or the secondary structure of the RNA might preclude the use of gross deletional studies to define subregions sufficient for localization.

Additive Function of Localization Elements

Implicit in much of the preceding discussion is the fact that different subsets of the RNA confer different aspects of the localization pattern. In other words, localization elements act additively. Examples already mentioned are the *bicoid* 3'-UTR, which has distinct elements for early (BLE1) vs later (Staufen-mediated) localization to the anterior pole, and the *Add-hts* N4 3'-UTR, which has an early transport and cortical localization element (ALE1) and distinct elements that function in anterior localization. In each case, the combination of the defined elements (with possible contributions from other undefined elements) directs localization with the correct spatial and temporal dynamics.

Elements That Function in Translational Control During or After Localization

Several localized RNAs in the *Drosophila* oocyte are not translated until they are localized. For example, *oskar* RNA is not translated until it is localized to the posterior pole of the stage 9 oocyte. Translation of unlocalized *oskar* RNA leads to major developmental defects. Thus there is an intimate and important link between localization and translational control of *oskar* RNA. Sequence elements for translational control are separable from those that function in localization per se. Elements known as Bruno response elements (BREs) have been mapped within the *oskar* 3'-UTR and are necessary and sufficient for preventing translation of unlocalized RNA. Three discrete segments (A, B, and C) within the 3'-UTR bind an 80-kDa protein (Bruno) that mediates translational repression (discussed in the next section) (184). These segments share a conserved 7- to 9-nt sequence [U(G/A)U(A/G)U(G/A)U] that is present as a

single copy in elements A and B, and in two copies in element C. Mutation of this sequence abolishes binding of Bruno and thus translational repression of unlocalized *oskar* RNA (184).

A second example comes from the *nanos* RNA. Unlike *oskar* RNA, which becomes tightly localized to the posterior pole of the oocyte, some unlocalized *nanos* RNA always exists in the embryo even after most of it is localized to the posterior. This unlocalized *nanos* RNA must be translationally repressed in order to prevent pattern defects in the early embryo (43, 139–141, 185). This translational repression is mediated by a 184-nt translational control element (TCE) in the *nanos* 3'-UTR (140) that contains two separable Smaug recognition elements (SREs), which bind a translational repressor to be described in the next section (141). These elements map within evolutionarily conserved regions of the *nanos* 3'-UTR (185). SRE1 lies between nucleotides (nt) 25 and 40 (141) within a 90-nt region (nt 1–90 of the 3'-UTR), which was shown independently to confer translational repression (185). SRE2 maps to nt 130–144, downstream in the 3'-UTR (141), within an adjacent 88-nt region (nt 91–178), which independent analyses showed has limited ability to repress translation (185). The SREs can form stem-loops (14–23 nt in length) with a highly conserved loop sequence (CUGGC) while the stem sequence is not conserved. Point mutations in the loops abolish binding of Smaug protein and eliminate translational repression of *nanos* RNA.

The BREs in the *oskar* 3'-UTR and the SREs in the *nanos* 3'-UTR are clear examples of discrete elements that are repeated within the 3'-UTRs and are largely functionally redundant.

A translational control element has also been mapped within the *Cyclin B* 3'-UTR, to a 39-nt region distinct from the posterior localization element (see above) (60, 182). In this case, the translational control element represses translation of localized maternal *Cyclin B* mRNA until late stage 14, about 11 h after fertilization. Deletion of the element results in premature translation, starting an hour after fertilization (182). The functional significance of this translational control has not been determined.

Primary, Secondary, Tertiary, and Quaternary Structures

A final question to be addressed here is the nature of the localization and translational control elements themselves. That is, is it the primary, secondary, tertiary, or quaternary structure that is recognized by the localization and translational control machinery? Instances of each of these possibilities have been mentioned in the preceding discussion. Several conserved primary sequence elements have been defined. For example, the SREs in the *nanos* 3'-UTR include a highly conserved loop sequence (CUGGC) recognized by Smaug (141), and the BREs in the *oskar* 3'-UTR contain a highly conserved sequence

[U(G/A)U(A/G)U(G/A)U] important for Bruno binding (184, 186). Similarly, a conserved sequence in *Vg1* and several other 3'-UTRs (*TGF β -5*, *Xwnt-11*, *Xlsirt*, *tau*, *oskar*, *nanos*, and *gurken*) has been implicated in localization (187). As mentioned above, the chicken β -actin 3'-UTR contains two regions that confer peripheral localization (171); these regions each contain two conserved motifs (GGACT and AATGC).

The importance of RNA secondary structure in localization has been clear for some time (e.g. *bicoid* 3'-UTR) (166, 167). Conserved primary sequence elements are often parts of a stem-loop (e.g. SREs) and are likely to be bound by factors that interact with single-stranded RNA. Other examples of important stem-loop structures are the *K10* TLE (181) and, possibly, the *Add-hts* ALE1 (KL Whittaker, D Ding, WW Fisher, HD Lipshitz, manuscript in preparation).

Initially it was proposed that tertiary structure is also important for localization based on the discovery of complementarity between two loops within stem-loop III of the *bicoid* 3'-UTR (166, 167). These complementary regions actually undergo quaternary interactions (i.e. between different 3'-UTR molecules) mediated by the double-stranded RNA-binding Staufen protein (see below) (163, 164).

TRANS-ACTING FACTORS INVOLVED IN RNA LOCALIZATION AND TRANSLATIONAL CONTROL OF LOCALIZED RNAs

The previous section outlined the *cis*-acting sequences that function in RNA localization. It also discussed the sequences involved in localization as well as the elements involved in translational control of mRNAs during or after localization. Here, the focus is on *trans*-acting factors that function during RNA localization. These factors can function in RNA localization per se or in translational control during or after localization. The latter class of factors is included only if translational control is related directly either to the localization process or to the functional significance of RNA localization.

Identification of Trans-Acting Factors

Three strategies have led to the identification of *trans*-acting factors that function in RNA localization and/or translational control of localized RNAs. The first strategy, genetic definition of genes involved in RNA localization followed by molecular cloning of the genes and molecular biological and biochemical analyses of their encoded products, is restricted to *D. melanogaster* and *S. cerevisiae*. Examples are *Drosophila* Bicaudal-C, Bicaudal-D, Exuperantia, Homeless, K10, Squid, Staufen, Swallow, and Vasa. Although this strategy ensures that the gene product is involved in RNA localization, it cannot be

determined at the outset whether the effects on RNA localization are direct or indirect.

A second strategy proceeds in the opposite direction by starting with biochemical searches for factors that bind defined RNA elements involved in localization and/or translational control. Ultimately, the gene encoding the identified factor is cloned and, in *Drosophila*, also mutated in order to assay function of the endogenous protein. With this method, it is known from the outset that the factor interacts directly with the target RNA; however, one has no assurance that the identified protein will indeed function in RNA localization/translational control rather than in some other aspect of RNA metabolism. Examples of *trans*-acting factors identified in this way are Bruno, Smaug, and Exl in *Drosophila*, and Vg1 RBP and Vera in *Xenopus*.

A final approach (not so much a strategy) that has led to the identification of factors involved in RNA localization has derived from molecular screens for gene products (RNA or protein) with interesting intracellular distributions (e.g. localization) or with interesting molecular homologies (e.g. RNA-binding motifs). In this case, as for the second strategy described above, one has no prior indication that the gene product functions in localization or translational control. However, if it is present in the right place at the right time, and possesses the appropriate molecular properties, the gene product may have a function in the process of interest. Examples of gene products identified in this way are Oo18 RNA-binding protein (Orb) and *Pgc* RNA in *Drosophila*, the *Xlsirt* RNAs in *Xenopus*, and the *YC* RNA in ascidians.

Factors That Interact Directly with Defined RNA Elements

STAUFEN PROTEIN (*DROSOPHILA*) Alleles of the *staufen* gene were first recovered as maternal effect mutations with defects in anterior and posterior (abdominal) pattern in the *Drosophila* embryo (188). It was implicated in *bicoid* RNA localization to the anterior since *bicoid* RNA is partially delocalized in early embryos produced by mutant mothers (7, 32, 189). In *staufen* mutants *oskar* RNA is maintained at the anterior of the oocyte until stage 10 when it delocalizes (25) (in wild-type oocytes *oskar* RNA is transported from the anterior pole to the posterior by stage 9). Therefore, *staufen* is essential for initiation of posterior transport of *oskar* RNA. Moreover, weak *staufen* alleles show normal posterior localization of *oskar* RNA at stage 9, but the posterior localization is lost in later oocytes (stage 11) indicating that Staufen is also required to maintain posteriorly localized *oskar* RNA (190). During oogenesis Staufen protein first appears uniformly in stage 3–4 egg chambers, and by stage 8 it is present in a ring at the oocyte anterior as well as at the posterior of the oocyte (179). By stage 10B Staufen protein is at the posterior pole of oocyte; therefore, *oskar*

RNA and Staufen protein colocalize. In the early embryo, Staufen protein colocalizes with *oskar* RNA at the posterior pole and with *bicoid* RNA at the anterior pole (179).

Staufen is a double-stranded RNA-binding protein (178). Varying the amount of the Staufen target RNAs (*bicoid* or *oskar*), or of Staufen protein, indicates that the amount of Staufen protein recruited to the anterior or posterior pole depends on the amount of *bicoid* or *oskar* RNA present; thus the RNA targets rather than Staufen protein are limiting. Injected in vitro transcribed *bicoid* 3'-UTR RNA recruits Staufen protein into particles that colocalize with microtubules near the site of injection in the early embryo (163). The formation of these particles requires specific 3'-UTR elements previously defined as important for *bicoid* RNA localization (see above). Specifically, evidence suggests that two single-stranded regions of stem-loop III within the *bicoid* 3'-UTR form intermolecular double-stranded RNA hybrids (i.e. via quaternary interactions) that are bound by Staufen protein (164). Staufen protein also interacts later in embryogenesis with the *prospero* 3'-UTR in neuroblasts and is necessary for basal localization of *prospero* transcripts (127).

Given that Staufen interacts with the best-characterized 3'-UTRs of localized RNAs (those in *bicoid* and *oskar* RNAs), that it is an RNA-binding protein, and that mutations exist both in the *staufen* gene and in the genes that encode its target RNAs, Staufen is by far the best-understood *trans*-acting factor involved in RNA localization.

EXL PROTEIN (*DROSOPHILA*) BLE1 is a 53-nt element in the *bicoid* 3'-UTR that is sufficient (when present in two copies but not one) to direct early nurse cell–oocyte transport and anterior localization of RNA (see above) (176). 2xBLE1 was used in UV-crosslinking assay to search for directly interacting proteins (177). A single protein of 115 kDa (Exl) was found to bind 2xBLE1 but not 1xBLE1, consistent with a role in localization. Definition of Exl-binding sites within BLE1 and mutation of these sites gave results consistent with a role for Exl in BLE1-mediated anterior localization. Exl might interact directly with BLE1 in the *bicoid* 3'-UTR during localization, and it might mediate Exuperantia protein interaction with *bicoid* RNA in the localization particles (177) (see below for discussion of Exuperantia). To date, the gene encoding Exl has not been cloned, and mutations in the gene have not been identified.

BRUNO PROTEIN (*DROSOPHILA*) Bruno, an 80-kDa protein, was identified in a UV-crosslinking screen for *trans*-acting factors that bind the *oskar* 3'-UTR (184). There are three binding sites (BREs) in the *oskar* 3'-UTR that share a 7- to 9-nt motif. Mutations in these elements abolish Bruno binding in vitro

(184). Endogenous *oskar* mRNA is translated only after the transcript is localized to the posterior of the oocyte in stages 8–9 (184). An *oskar* [BRE⁻] transgene results in premature translation of *oskar* RNA during stages 7–8, prior to *oskar* RNA localization, producing gain-of-function phenotypes (double-posterior or posteriorized embryos) (184), consistent with spatially inappropriate Oskar protein expression (75, 76). BRE elements can confer translational repression on a heterologous transcript (184). Bruno-mediated translational control of other transcripts is suggested by the ability of Bruno protein to bind *gurken* RNA (184).

The gene encoding Bruno was recently cloned (186). The sequence reveals RNP/RRM-type ribonucleoprotein RNA-binding domains consistent with direct interaction with RNA. The RNP/RRM-domain RNA-binding motif was first defined in yeast mRNA poly(A)-binding protein and mammalian hnRNP protein A1 (reviewed in 191). The gene encoding Bruno is a previously identified genetic locus, *arrest*, which is necessary for female as well as male fertility (192, 193). This observation, together with the fact that *arrest* mutants display defects in oogenesis prior to the time that Bruno binds *oskar* RNA, suggests that Bruno regulates other transcripts in addition to *oskar* RNA.

Bruno also interacts with Vasa protein as assayed by far-Western analysis (186). Vasa is itself an RNA helicase related to eIF-4A, which functions in translation initiation (194–196). This suggests a possible mechanism for Bruno; Bruno may protect *oskar* RNA from premature translational activation by the Vasa protein (186).

Identification and cloning of Bruno, and its correlation with a previously identified genetic locus, is the first instance in which a *trans*-acting factor involved in translational control of a localized RNA has been identified biochemically and then studied both molecularly and genetically.

SMAUG PROTEIN (*DROSOPHILA*) As described above, translational repression of unlocalized *nanos* mRNA (43, 140, 141) is accomplished through two elements that bind in vitro to Smaug, a 135-kDa protein (141). Mutation of these SREs abolishes Smaug binding in vitro. Embryos from *nanos* [SRE⁻] transgenic mothers lose head structures, which is consistent with translation of *nanos* RNA throughout the embryo rather than solely at the posterior (141). Smaug binding alone is sufficient to mediate translational repression since a transgene containing three SREs but no other part of the *nanos* 3'-UTR is translationally repressed (141). The gene encoding Smaug has not been cloned.

VG1 RNA-BINDING PROTEIN (RBP) (*XENOPUS*) UV crosslinking has also been used to identify *trans*-acting factors that bind to the *Vg1* 3'-UTR, which functions in vegetal localization of *Vg1* RNA in *Xenopus* oocytes (197). The crosslinking experiments led to the identification of a 69-kDa protein called Vg1

RNA-binding protein (RBP). Vg1 RBP may also bind in vitro to the 3'-UTR of a second vegetal pole-localized RNA, *TGF β -5* (187, 197), but not to *An2* RNA, which is localized to the animal hemisphere. The precise role of Vg1 RBP in vegetal RNA localization is not clear. Evidence indicates that it mediates the association of *Vg1* RNA with microtubules (199), which are necessary for vegetal RNA localization (see above). Based on the results of UV-crosslinking experiments Vg1 RBP is likely to be a member of an RNP complex containing up to six proteins plus *Vg1* mRNA (200). Six protein bands (one of which is likely to be Vg1 RBP) were identified from stage II–III oocyte extracts, corresponding to the period during which *Vg1* RNA is localized (200). Fewer proteins were labeled in earlier and later stage oocyte extracts, at times during which *Vg1* RNA is not being localized.

VERA PROTEIN (*XENOPUS*) In a search for *trans*-acting factors that bind the *Vg1* localization element a new 75-kDa protein, Vera, was purified (154). A mutant form of the *Vg1* localization element (deleted for three out of four repeated sequence motifs) that does not bind Vera in vitro exhibits impaired localization in vivo (154). Vera protein co-sediments with Trap- α , an integral membrane protein associated with the protein translocation machinery of the endoplasmic reticulum (ER) (154). Vera may link *Vg1* mRNA to the vegetal ER subcompartment while the ER (along with *Vg1* RNA) is transported via microtubules to the vegetal pole.

Other Factors That Function in RNA Localization

EXUPERANTIA PROTEIN (*DROSOPHILA*) The genetic analyses that led to the identification of *staufer* as functioning in *bicoid* RNA localization also led to the identification of *exuperantia* (188, 189). The first observable *bicoid* RNA localization defect in *exuperantia* mutants is loss of apical transcript localization in nurse cells (32) at a stage at which Exuperantia protein is localized around the nurse cell nuclei (201, 202). Exuperantia protein is highly concentrated in the anterior cortex of the oocyte between stages 8 and 10 (162, 201). In stage 10 egg chambers mutant for *exuperantia*, *bicoid* RNA delocalizes from the anterior of the oocyte (7, 150). In late oocytes (stage 14) mutant for *exuperantia*, *bicoid* RNA is released from the microtubule-based cytoskeleton (147). However, Exuperantia protein is not present in late oocytes or in embryos, indicating that Exuperantia is involved in establishing but not in maintaining anterior *bicoid* RNA localization (201, 202).

Visualization of an Exuperantia-GFP fusion protein in live oocytes (162) demonstrates that Exuperantia is present in large particles that are transported from the nurse cells into the oocyte through the ring canals (see above). Transport of these Exuperantia-containing particles appears to be a multistep process: Colchicine-sensitive steps are transport within the nurse cells and

anchoring at the anterior of the oocyte; whereas transport through the ring canals into the oocyte is insensitive to both microtubule and microfilament inhibitors (162; WE Theurkauf, TI Hazelrigg, personal communication). Exuperantia may function in this microtubule-independent transport of *bicoid* transcripts through the ring canals into the oocyte (151).

Taxol stabilizes microtubules and causes aberrant microtubule bundles in the oocyte that contain ectopically localized *bicoid* transcripts (150). Taxol-treated *exuperantia* mutant oocytes do not exhibit ectopic *bicoid* transcript localization (150). The microtubule networks in *exuperantia* oocytes are normal. These results are consistent with *bicoid* RNA association with ectopic microtubules requiring Exuperantia protein.

Deletion of the *cis*-acting element BLE1 from the *bicoid* 3'-UTR mimics the *bicoid* transcript delocalization defects caused by *exuperantia* mutants (176). However, BLE1 specifically binds a protein called Exl (see above) and Exuperantia alone can bind RNA only nonspecifically (177). Exuperantia protein may interact with Exl protein in *bicoid* RNA localization particles. While Exuperantia does not interact specifically with *bicoid* RNA, it does function specifically in *bicoid* RNA localization; other anteriorly localized RNAs such as *Add-hts*, *Bicaudal-D*, *K10*, and *orb* are not delocalized in *exuperantia* mutant oocytes (16, 37).

SWALLOW PROTEIN (*DROSOPHILA*) The third genetic locus initially shown to be necessary for *bicoid* transcript localization during oogenesis is *swallow* (7, 189). Subsequent analyses implicated it in the cortical and anterior localization of a second RNA, *Add-hts* (16, 174; KL Whittaker, D Ding, WW Fisher, HD Lipshitz, manuscript in preparation). The *swallow* locus is not necessary for the transient anterior positioning of other RNAs such as *Bicaudal-D*, *K10*, and *orb* (37). Swallow protein maintains cortical localization of transcripts such as *bicoid* and *Add-hts* as well as of RNPs such as the polar granules (44, 45). With regard to *bicoid*, Swallow appears to be involved in maintaining rather than establishing *bicoid* transcript association with microtubules since taxol-treated *swallow* oocytes exhibit ectopic *bicoid* transcript localization (150). The Swallow protein may possess a highly divergent RNP/RRM motif suggestive of a direct interaction with RNA (203). Swallow protein is distributed throughout the oocyte at stages 5–7 and at its anterior cortex at stages 8–10, consistent with localization of *Add-hts* and *bicoid* RNAs to these regions (44, 45, 204).

OSKAR PROTEIN (*DROSOPHILA*) Nonsense mutants such as *oskar*⁵⁴ show abnormal *oskar* RNA localization (24, 25). In these mutants *oskar* RNA localizes to the posterior in stage 8 but subsequently delocalizes, indicating a role for Oskar protein in anchoring *oskar* RNA at the posterior. Directly or indirectly,

Oskar protein's role in *oskar* transcript localization is mediated by the *oskar* 3'-UTR since a chimeric *oskar* 3'-UTR construct localizes to the posterior and is maintained there in wild type but fails to be maintained there in an *oskar*⁵⁴ mutant (190). Further support for this scenario is the observation that in *D. melanogaster*, a transgenic *D. virilis oskar* RNA is able to localize to the posterior but fails to maintain its position at the oocyte posterior in the absence of *D. melanogaster* Oskar protein (205). *D. virilis* Oskar can direct posterior abdominal patterning but not pole-cell formation. This observation indicates that pole-cell formation may require a high concentration of Oskar protein and that this is provided for by anchoring high concentrations of *oskar* RNA at the posterior. Oskar protein nucleates the formation of the posterior polar granules, organelles that function in germ-cell formation and specification (see below). Oskar protein may interact directly with the *oskar* RNA's 3'-UTR to maintain transcript localization. Alternatively, Oskar function may be indirect in nucleating formation of polar granules that in turn are needed for *oskar* RNA localization.

VASA PROTEIN (*DROSOPHILA*) Vasa protein is a component of the perinuclear "nuage" material in the nurse cells and also of the polar granules at the posterior pole of the *Drosophila* oocyte (194, 196, 206–208). Loss of *vasa* function results in destabilization of the polar granules and delocalization of posteriorly localized RNAs (188, 194, 196, 206–208). Vasa protein is a founding member of the DEAD-box family of ATP-dependent RNA helicases (194, 207), and it binds duplex RNA (196). There is no evidence for specific binding of Vasa to any localized RNA; however, far-Western analysis has demonstrated that Vasa protein interacts directly with Bruno protein, which in turn binds directly to the BRE translational control elements in the *oskar* RNA's 3'-UTR (see above) (186). Transcripts encoding the zebrafish homolog of Vasa are localized subcellularly beginning at the two-cell stage and segregate into the primordial germ cells (209). This observation suggests likely evolutionary conservation of Vasa function in metazoan germ plasm.

HOMELESS PROTEIN (*DROSOPHILA*) Homeless is another member of the DEAD/DE-H family of RNA-binding proteins (40). Its amino terminal portion contains a region that bears homology to yeast splicing factors PRP2 and PRP16 and to the *Drosophila* Maleless protein (40). Transport and localization of *gurken*, *oskar*, and *bicoid* transcripts are severely disrupted in *homeless* mutant ovaries, which also contain reduced amounts of *K10* and *orb* transcripts (40). In contrast, *Bicaudal-D* and *Add-hts* transcript localization is unaffected (40). It is unknown whether Homeless protein interacts directly with any of the affected transcripts.

ORB PROTEIN (*DROSOPHILA*) Orb protein contains two RNP/RRM-type RNA-binding domains and functions in antero-posterior and dorso-ventral patterning during *Drosophila* oogenesis (23, 149, 210). *orb* mutants affect the transport and localization of several RNAs including *Add-hts*, *Bicaudal-D*, *K10*, *gurken* and *oskar* (149, 210). For example, in wild-type oocytes during stages 8–10, *gurken* mRNA is usually restricted to the dorsal side of the nucleus at the antero-dorsal pole. In *orb* mutants, however, *gurken* transcripts are present throughout the entire anterior of the oocyte. In the wild type, *oskar* mRNA is localized to the posterior pole of the oocyte. In *orb* mutants *oskar* transcripts are distributed throughout the oocyte. Direct binding of Orb protein to either RNA has not been demonstrated.

SQUID PROTEIN (*DROSOPHILA*) Squid is a member of the hnRNP family of RNA-binding proteins and was identified as functioning in dorso-ventral axis formation (211). There are three protein isoforms that share a common amino terminus containing two RNA-binding motifs. Two of these isoforms, Squid-A and Squid-B, are present in the oocyte. Squid is required for the correct dorso-anterior localization of *gurken* mRNA in the oocyte. In *squid* mutant ovaries, *gurken* transcripts are localized throughout the anterior of the oocyte rather than just antero-dorsally (211). Since *gurken* is unusual in that it is transcribed in the oocyte nucleus (R Cohen, personal communication), Squid's function in *gurken* transcript localization may initiate in the oocyte nucleus. It is unknown whether Squid interacts directly with the *gurken* mRNA or with the *gurken* pre-mRNA. As for K10 (below), Squid may function in vectorial transport of *gurken* transcripts out of the oocyte nucleus.

K10 PROTEIN (*DROSOPHILA*) *K10* gene function is required during stage 8 of oogenesis for localization of *gurken* mRNA adjacent to the oocyte nucleus at the antero-dorsal tip of the oocyte (21, 212). K10 protein is restricted to the oocyte nucleus (213) but does not regulate *gurken* transcript production or stability (212). Since *gurken* is transcribed in the oocyte nucleus (R Cohen, personal communication) and becomes restricted to the oocyte cytoplasm dorso-anteriorly to the oocyte nucleus, K10 protein might function specifically in vectorial nucleo-cytoplasmic transport of *gurken* transcripts (R Cohen, personal communication). Whether this function is through direct interaction with the *gurken* mRNA is not known at present.

BICAUDAL-C PROTEIN (*DROSOPHILA*) Mutations that reduce *Bicaudal-C* gene dosage result in defects in RNA localization in the oocyte: Most *oskar* RNA remains at the anterior pole of the oocyte and early embryo instead of being transported to the posterior by stage 9 (18). Possibly as a consequence, in these *Bicaudal-C* mutants, *nanos* RNA is localized ectopically near the anterior pole

in patches on the dorsal and ventral sides rather than at the posterior pole as in wild type (18). These embryos develop a bicaudal (double-abdomen) phenotype. *Bicaudal-C* mutations have no effect on *gurken* or *orb* transcript localization to the anterior pole. Females homozygous for strong *Bicaudal-C* alleles produce oocytes that do not form anterior chorion as a consequence of defects in follicle cell migration over the oocyte anterior. Bicaudal-C is a transmembrane protein that has two conserved cytoplasmic domains (18): an Eph domain that is present in transmembrane receptor tyrosine kinases and is involved in signal transduction, and a KH domain that has been implicated in binding of single-stranded DNA or RNA. Since *Bicaudal-C* RNA is localized to the anterior of the oocyte, it is reasonable to assume that the Eph domain functions in the intercellular signaling from oocyte to follicle cells that programs their migration (18). The KH domain might bind to and interact with the *oskar* transcripts during their localization, possibly functioning in their transfer to the machinery that transports RNA to the posterior (see above) (18).

BICAUDAL-D PROTEIN (*DROSOPHILA*) Bicaudal-D function has been covered with respect to RNA transport and the oocyte cytoskeleton above. The Bicaudal-D protein includes a region with homology to the coiled-coil domains of several cytoskeletal proteins and is required for maintenance of *oskar* RNA localization at the posterior pole of the oocyte (160).

EGALITARIAN PROTEIN (*DROSOPHILA*) In *egalitarian* mutants the *Bicaudal-D*, *orb*, and *K10* RNAs do not accumulate in the oocyte (25). In addition, these RNAs no longer coprecipitate with the cytoskeletal fraction of oocytes as in the wild type (147). Egalitarian protein contains regions homologous to c10G6.1 from *Caenorhabditis elegans*, an EST from *Arabidopsis thaliana*, and ribonuclease D from *Haemophilus influenzae* (20). It is also predicted to include a coiled-coil region. Egalitarian protein localization to and within the oocyte is dependent on microtubules (20). Further, the Egalitarian and Bicaudal-D proteins copurify (20). Egalitarian and Bicaudal-D may be components of the cytoskeletal apparatus involved in RNA localization.

BULLWINKLE (*DROSOPHILA*) Mutations in the *bullwinkle* gene have several defects in posterior body patterning (214, 215). The *bullwinkle* gene is required to localize *oskar* transcripts to the posterior of the oocyte, to maintain *oskar* RNA at posterior, and to regulate the level of *oskar* protein (214, 215). Cloning of the *bullwinkle* gene has not been reported.

AUBERGINE (*DROSOPHILA*) While previously *aubergine* had been implicated in dorso-ventral body patterning (192), two new alleles were identified in a recent genetic screen for genes involved in posterior body patterning (214, 216).

Aubergine functions to enhance the translation of *oskar* mRNA in the ovary, mediated through the *oskar* 3'-UTR (216). *Aubergine*'s enhancement of *oskar* translation is independent of Bruno-mediated repression of translation since an *oskar* [BRE⁻] transgenic RNA still requires *aubergine* function for its translation (216). Cloning and molecular analysis of *aubergine* have not been reported.

XLSIRT RNA (*XENOPUS*) *Xlsirts* are a family of nontranslatable, interspersed repeat transcripts that localize to the vegetal cortex of *Xenopus* oocytes (see above) (97, 161). These RNAs are involved in the localization of *Vg1* but not *Xcat-2* transcripts. It is unknown whether *Xlsirt* and *Vg1* RNAs interact directly or whether *Xlsirt* RNA function in *Vg1* transcript localization is indirect via the cytoskeletal network or as part of a localization particle/organelle.

PGC RNA (*DROSOPHILA*) In *Drosophila* a non-protein-coding RNA, *Pgc*, is a component of the posterior polar granules and is required for pole cells to migrate normally and to populate the gonad (26). Reduction of *Pgc* RNA at the posterior pole results in a reduction in the amount of posteriorly localized *nanos* and *germ cell-less* RNA and Vasa protein (26). It is unknown whether *Pgc* RNA interacts with other posteriorly localized RNAs and/or with protein components of the polar granules.

YC RNA (*STYELA*) As described above, the noncoding *YC* RNA is localized in the yellow crescent of Ascidian eggs and embryos (101). The 3'-UTR of *PCNA* RNA contains a 521-nt region of complementarity to *YC* RNA (100), while the 5'-UTR of *ribosomal protein L5* mRNA exhibits 789 nt of complementarity to *YC* RNA (102). *YC* RNA may interact directly with these two RNAs in vivo (100–102); however, no such interaction has been demonstrated, and its function remains unclear (see above).

Summary

In summary, genetic and molecular strategies have identified a host of *trans*-acting factors that function in transcript localization. To date, although many of these are homologous to known RNA-binding proteins, only a handful have been shown to interact directly with specific localized RNAs. Many localized RNAs have collections of discrete *cis*-acting localization elements that mediate distinct aspects of their localization. It might therefore be predicted that many different *trans*-acting factors will function during localization of any one RNA, each binding to a different type of element and each possibly functioning at a different time and intracellular location. RNA localization particles are likely to consist of these directly interacting factors in addition to numerous others that are involved in linking the RNA to the cytoplasmic translocation machinery

as well as anchoring it at its intracellular target site. It would be surprising if evolution has not also utilized the base-pairing capability of RNA in the translocation and anchoring process.

DEVELOPMENTAL FUNCTIONS OF RNA LOCALIZATION

The cellular functions of RNA localization have been reviewed extensively (see e.g. 1, 217) and so are considered here only briefly. First, for mRNAs, localization directs high-level synthesis of the encoded protein at the site of localization. Thus if protein function requires a high concentration (e.g. *Drosophila* Oskar in the polar granules), this requirement can be met through mRNA localization. Second, localizing an mRNA also excludes protein synthesis from other parts of the cell, thus reducing the amount of protein present in those regions. Often, not only is local protein synthesis directed by mRNA localization, but translational control mechanisms actually prevent translation of unlocalized RNA either during RNA transit to the target site (e.g. *Drosophila oskar* RNA) or of unlocalized RNA that remains after transcript localization is complete (e.g. *Drosophila nanos* RNA).

A third postulated function of mRNA localization is to direct specific protein isoforms to particular regions of the cell. Often this is accomplished by alternative pre-mRNA splicing such that different 3'-UTRs direct different isoforms to different cytoplasmic domains (e.g. *Drosophila Add-hts* RNA). Fourth, intracellular localization is used as a mechanism to segregate RNAs unequally between the products of cell division, particularly when these divisions are asymmetric (e.g. *ASH1* transcripts during yeast budding, *prospero* transcripts during *Drosophila* neuroblast division). Fifth, certain non-protein-coding RNAs are localized (e.g. *Xenopus Xlsirts* or *Drosophila Pgc* RNAs). The detailed role of these RNAs and of their localization is currently under intensive study. These RNAs may serve as structural components of localization particles or organelles such as the germinal granules. Alternatively, they may function in the RNA localization or anchoring process, possibly through sequence complementarity to mRNAs that are being localized.

Specification of the Anterior-Posterior and Dorsal-Ventral Axes of the Drosophila Oocyte

As mentioned above, the *gurken* mRNA is unusual in that it is synthesized in the oocyte nucleus (R Cohen, personal communication). It is localized to the posterior pole of the oocyte at stage 7, then to both the anterior and posterior poles at stage 8, and finally to the antero-dorsal pole from late stage 8 through stage 10 (21, 218). Gurken protein is a TGF α -like secreted growth

factor (21). Establishment of the antero-posterior and dorso-ventral axes of the oocyte is accomplished between stages 7 and 9 of oogenesis through signaling between the oocyte and the surrounding follicle cells (34, 35). The Gurken protein functions as a key signal from the oocyte to the follicle cells in both of these processes. First, due to posterior-localized *gurken* RNA, local production of Gurken protein at the posterior of the oocyte signals to the posterior follicle cells. This signaling is essential for establishing the antero-posterior oocyte axis and the polarization of the oocyte microtubule-based cytoskeleton that plays a crucial role in RNA localization. Subsequently, antero-dorsal localized *gurken* RNA directs local Gurken protein synthesis, enabling oocyte–nurse cell signaling that establishes the dorso-ventral axis of the egg chamber. The dorso-anterior localization of *gurken* mRNA depends on anterior migration of the oocyte nucleus on the polarized microtubule cytoskeleton. Thus the antero-posterior axis is primary and the establishment of the dorso-ventral axis secondary (35). Both axes depend on localization of *gurken* mRNA for localized signaling. If *gurken* mRNA is mislocalized or delocalized, for example, by mutating the *K10*, *squid*, or *orb* genes, severe defects in the formation of both axes result.

Specification of Anterior Cell Fates in the Drosophila Embryo

Shortly after fertilization, *bicoid* mRNA is translated (219, 220). Since the embryo is syncytial, Bicoid protein diffuses away from its site of translation at the anterior pole, forming an antero-posterior protein gradient with its peak at the anterior tip (219, 220). Since Bicoid is a homeodomain-containing transcription factor, its function is to activate zygotic transcription of pattern-specifying genes in the syncytial nuclei in the anterior half of the embryo. It does this in a concentration-dependent fashion (221–223). For example, the *hunchback* gene contains high-affinity Bicoid-binding sites in its transcriptional control region, so its transcription is activated by low as well as high Bicoid concentrations throughout the anterior half of the embryo. In contrast, genes such as *orthodenticle* and *empty spiracles* have lower affinity Bicoid-binding sites and so are activated only by higher Bicoid protein concentrations in the more anterior part of the embryo. In this way, different combinations of zygotic pattern genes are activated in different subsets of the anterior part of the embryo leading to different cell fates within this region (e.g. head more anteriorly, thorax more posteriorly). *Bicoid* mRNA localization controls the amount of Bicoid transcription factor in different regions and thus specifies distinct cell fates. Delocalization of *bicoid* mRNA can be accomplished by mutating genes that encode *trans*-acting factors that function in *bicoid* transcript localization (7, 32, 189) (e.g. *exuperantia*, *swallow*, *staufer*). Delocalization results in lower

levels of Bicoid protein at the anterior pole than in the wild type. As a consequence, acronal and head structures cannot be specified.

Localization of *bicoid* mRNA serves two additional functions. First, mislocalization of *bicoid* RNA to the posterior pole can result in developmental defects in the posterior part of the embryo through cells mistakenly adopting anterior fates (224). Thus a corollary function of anterior *bicoid* transcript localization is to prevent Bicoid protein synthesis in the posterior of the embryo. Translational control mechanisms also prevent Bicoid protein synthesis at the posterior (141, 205, 225). Second, the Bicoid homeodomain protein can function not only as a transcription factor but also can directly bind RNA and translationally repress mRNAs such as *caudal* through interaction with the *caudal* 3'-UTR (226, 227). Thus anterior localization of *bicoid* mRNA and the resultant Bicoid protein gradient creates a reverse gradient of Caudal protein with its peak at the posterior pole. Caudal protein is involved in specifying pattern in the posterior of the early embryo (228, 229).

Specification of Abdominal Cell Fates in the Drosophila Embryo

A key player in abdominal cell fate specification is Nanos, a Zinc-finger-containing protein (56, 230). The *nanos* mRNA is localized at the posterior pole of the late oocyte and early embryo, although some unlocalized RNA is present throughout the embryo (56, 231). After fertilization, the posteriorly localized *nanos* RNA in the syncytial embryo is translated (there is repression of unlocalized *nanos* RNA translation by Smaug protein). This translation leads to a gradient of Nanos protein with a peak at the posterior pole (139–141, 185, 231). Unlike *bicoid*, which controls anterior cell fates by a combination of transcriptional control of target genes and direct translational repression of *caudal* mRNA in the anterior, all of the Nanos protein's effects in abdominal patterning derive from its translational repression of target RNAs. One target, *hunchback* maternal RNA, is distributed uniformly in the early embryo (232, 233) and encodes a Zinc-finger transcription factor that specifies anterior cell fates (234–236). Thus, if Hunchback protein were synthesized in the posterior of the embryo, posterior cells would mistakenly adopt anterior fates. Nanos protein in the posterior of the embryo prevents this by translationally repressing *hunchback* RNA. The Pumilio protein, previously shown to be important for abdominal patterning (237), specifically binds to Nanos response elements (NREs) in the *hunchback* 3'-UTR, recruiting Nanos through protein-protein interactions (140). If *nanos* RNA is misexpressed throughout the embryo by mutation of its SREs, head defects result, probably through repression of *bicoid* translation by Nanos protein since the *bicoid* 3'-UTR also contains NREs (141). Misexpression of high levels of Nanos protein in the anterior results in bicaudal

embryos (231). Thus the combination of posterior localization of *nanos* mRNA and the translational repression of unlocalized *nanos* transcripts plays a crucial role in patterning the abdomen of *Drosophila*.

Assembly of Polar Granules and Specification of Germ Cells in the Drosophila Embryo

oskar mRNA is localized to the posterior pole of the stage 9 oocyte. Translation of *oskar* RNA at this site nucleates the formation of the posterior polar granules and polar plasm (25, 75, 76). The polar granules and posterior polar plasm serve two functions. The first is the anchoring of *nanos* transcripts at the posterior (75, 76). Disruption of the polar granules results in delocalization of *nanos* RNA, translational repression by Smaug, and ultimately the production of embryos without abdomens. The second role of polar granules is to specify the formation of germ (pole) cells and to restrict their formation to the posterior tip of the embryo (25, 75, 76). Disruption of *oskar* function results in an inability to nucleate polar granules and, consequently, absence of pole cells (238). Alternatively, misexpression of Oskar protein throughout the oocyte during *oskar* RNA localization (184, 186), overexpression of *oskar* RNA throughout the oocyte (75), or mislocalization of *oskar* RNA and protein to the anterior pole of the oocyte (76) all result in severe pattern defects. In the latter two situations ectopic pole cells form at or near the anterior of the embryo. The mechanisms by which the polar granules specify the formation and function of the pole cells in the early embryo are not yet fully understood but appear to require the function of several other posteriorly localized RNAs such as *Pgc*, *mtlrRNA*, *nanos*, and *germ cell-less* (26, 57, 133, 134, 136, 137, 239, 240). Thus, both the establishment of the polar granules, and their function in pole cell formation, require RNA localization.

Signaling of Dorso-Ventral Axis and Mesoderm Induction in the Xenopus Embryo

The animal-vegetal axis of the *Xenopus* embryo is established during oogenesis. The three germ layers of the early embryo (ectoderm, mesoderm, and endoderm) are established along the animal-vegetal axis (72, 73). The darkly pigmented animal hemisphere of the oocyte gives rise to ectoderm while the vegetal hemisphere cells become endoderm. The mesoderm is derived from animal hemisphere cells that lie adjacent to the vegetally derived mesoderm. Mesodermal development is not autonomous but is a result of inductive interactions from the endoderm (72, 73).

Asymmetrically distributed RNAs localized to the vegetal hemisphere that encode secreted growth factors such as Vg1 and TGF β -5 have been implicated in mesoderm induction (5, 241–243). The secreted growth factor TGF- β 1 can

act synergistically with another growth factor, bFGF, to induce mesoderm, whereas antibodies against TGF- β 2 can reduce mesoderm induction when injected into *Xenopus* embryos. Since *Vg1* and TGF- β 5 RNAs are localized to the vegetal hemisphere from which the inducing signal derives, and since Vg1 and TGF- β 5 proteins are related, respectively, to TGF- β 1 and 2, these proteins are strong candidates for mesoderm-inducing signals (5, 241–243). Indeed, engineered processed Vg1 protein (in the form of BMP2/4-Vg1 fusion protein) can function as a mesoderm inducer when ectopically expressed in embryos (241, 242).

The orientation of the dorso-ventral axis of the early embryo is not established prior to fertilization. Rather, the sperm entry point in the animal hemisphere establishes this axis in part by causing an oriented cytoplasmic rearrangement (72, 73). This rearrangement relocates interior cytoplasm (endoplasm) relative to the stationary cortical cytoplasm. Treatments, such as UV-irradiation, prevent cytoplasmic rearrangement and ventralize the embryo (i.e. prevent formation of the dorsal-most tissues). Maternal *Xwnt-11* mRNA is localized vegetally in oocytes and early embryos (98). Injection of *Xwnt-11* RNA into embryos that have been ventralized by UV-irradiation substantially rescues the UV-induced defect by inducing formation of dorsal tissues such as somitic muscle and neural tube (98). This observation suggests that Xwnt-11 protein functions during normal embryogenesis in dorso-ventral axis formation and that localization of *Xwnt-11* mRNA and protein may play a role in induction of this axis.

The inductive events discussed previously are complex both at the level of inducing signals and at the level of mesodermal cell fate outcomes. The inability to genetically inactivate genes in *Xenopus* has been a major drawback in defining endogenous factors necessary (rather than sufficient) for induction. Thus the functions during normal development of *Xwnt-11*, *Vg1*, and TGF β -5 RNA localization and of their encoded proteins remain to be determined.

Specification of Cell Fates During Asymmetric Cell Divisions

During *Drosophila* neurogenesis, a stem cell called a neuroblast divides asymmetrically to form a ganglion mother cell (GMC) and another neuroblast. The GMC then divides to form neurons. The Prospero nuclear protein is required for neuronal differentiation (244) and axonal pathfinding (245). The *prospero* mRNA and the Prospero protein are initially apically localized in the neuroblast at interphase but relocate basally from prophase through telophase, thus segregating into the GMC (127, 246, 247). Basal localization of *prospero* RNA requires Inscuteable and Staufen proteins (127), and Staufen binds directly to the *prospero* 3'-UTR (127). The Miranda protein functions as an adapter that links Prospero protein to the basal cell membrane during the asymmetric

neuroblast division (248). Thus RNA and protein localization are used to segregate the Prospero protein into one product of an asymmetric cell division, conferring appropriate neuronal fates upon that cell and its progeny.

Asymmetric segregation of cell fate determinants through mRNA localization has also been described in the budding yeast *S. cerevisiae*. In this case, during cell division the *ASH1* mRNA is localized to the site of the bud and then into the daughter cell that forms there (128, 129). The *ASH1* protein acts as a repressor of the HO endonuclease, which is responsible for mating-type switching (128, 129). Thus localization of the *ASH1* mRNA and its asymmetric segregation into the daughter cell ensures that the daughter cell cannot switch mating type while the mother cell (which does not inherit *ASH1* mRNA) can switch.

EVOLUTIONARY CONSIDERATIONS

Many features of mRNA localization appear to have been conserved during evolution, suggesting that RNA localization is an ancient mechanism for producing cytoplasmic asymmetry. For example, large stereotypic secondary structures in 3'-UTRs that function in *bicoid* transcript localization are evolutionarily conserved and functionally interchangeable between *Drosophila* species separated by over 60 million years (167). Further, the *bicoid* 3'-UTR, which directs anterior RNA localization in the oocyte, can also direct apical transcript localization in epithelia such as the blastoderm (65). Consistent with this observation, *bicoid* RNA is localized apically in the nurse cells prior to its transport into the oocyte during normal development. Thus, at least within the same species, different polarized cell types appear to share localization signals and factors.

More remarkable is the fact that the mammalian *tau* 3'-UTR, which directs *tau* transcript localization to the axons of neurons, can also direct vegetal transcript localization in *Xenopus* oocytes with a pattern and dynamics indistinguishable from *Vg1* transcripts (158). This result suggests that RNA targeting elements and localization machinery are conserved from *Xenopus* to mammals and from oocytes to neurons. Whether this functional conservation extends to the primary RNA sequence level remains to be seen; however, a small sequence element has been reported to be conserved in the 3'-UTR of *tau*, *Vg1*, and several other localized RNAs in mammals, *Xenopus*, and even *Drosophila* (187).

Recently, RNA localization has been reported in the budding yeast, *S. cerevisiae* (128, 129), and functions during budding to confer asymmetric fates on the mother and daughter cells. mRNA localization (e.g. of *prospero* transcripts) can serve a similar function in higher eukaryotes (127). This suggests that the process of RNA localization dates at least to the invention of single-celled organisms with specialized cytoplasmic domains and/or that undergo asymmetric

cell divisions. The demonstration that the yeast *ASH1* mRNA's 3'-UTR carries information for intracellular targeting implies that the position of *cis*-acting localization elements may be conserved in mRNAs from yeast to mammals. Future studies that focus on the identification and analysis of *trans*-acting factors that target RNAs for localization are likely to uncover additional conserved components of the cytoplasmic RNA localization mechanism.

ACKNOWLEDGMENTS

The following kindly shared unpublished or in press results with us: P Macdonald, R Cohen, P Lasko, W Theurkauf, T Hazelrigg, H Krause, R Long, R Singer, P Takizawa, H Tiedge, L Etkin, and K Mowry. Special thanks to L Etkin, University of Texas, for providing the images of *Xenopus* localized RNAs used in Figure 4. We thank S Lewis, L Etkin, and M Kloc for comments on the manuscript. Our research on RNA localization has been funded over the past decade by research grants to HDL from the National Institutes of Health, the National Science Foundation, and currently the Medical Research Council of Canada.

Visit the Annual Reviews home page at
<http://www.AnnualReviews.org>.

Literature Cited

1. Lipshitz HD, ed. 1995. *Localized RNAs*. Austin, TX: Landes/Springer-Verlag
2. Meller VH, Wu K-H, Roman G, Kuroda MI, Davis RL. 1997. *Cell* 88:445-57
3. Herzing LB, Romer JT, Horn JM, Ashworth A. 1997. *Nature* 386:272-75
4. Penny GD, Kay GF, Sheardown SA, Rastan S, Brockdorff N. 1996. *Nature* 379:131-37
5. Rebagliati MR, Weeks DL, Harvey RP, Melton DA. 1985. *Cell* 42:769-77
6. Frigerio G, Burri M, Bopp D, Baumgartner S, Noll M. 1986. *Cell* 47:735-46
7. Berleth T, Burri M, Thoma G, Bopp D, Richstein S, et al. 1988. *EMBO J.* 7: 1749-56
8. Frohnhofer HG, Nüsslein-Volhard C. 1986. *Nature* 324:120-25
9. King RC. 1970. *Ovarian Development in Drosophila melanogaster*. New York: Academic
10. McKearin D, Ohlstein B. 1995. *Development* 121:2937-47
11. Lin HF, Yue L, Spradling AC. 1994. *Development* 120:947-56
12. Lin HF, Spradling AC. 1995. *Dev. Genet.* 16:6-12
13. de Cuevas M, Lee JK, Spradling AC. 1996. *Development* 122:3959-68
14. Stephenson EC. 1995. See Ref. 1, pp. 63-76
15. Cooley L, Theurkauf WE. 1994. *Science* 266:590-96
16. Ding D, Parkhurst SM, Lipshitz HD. 1993. *Proc. Natl. Acad. Sci. USA* 90: 2512-16
17. Yue L, Spradling AC. 1992. *Genes Dev.* 6:2443-54
18. Mahone M, Saffman EE, Lasko PF. 1995. *EMBO J.* 14:2043-55
19. Suter B, Romberg LM, Steward R. 1989. *Genes Dev.* 3:1957-68
20. Mach JM, Lehmann R. 1997. *Genes Dev.* 11:423-35
21. Neuman-Silberberg FS, Schüpbach T. 1993. *Cell* 75:165-74
22. Cheung H-K, Serano TL, Cohen RS. 1992. *Development* 114:653-61
23. Lantz V, Ambrosio L, Schedl P. 1992. *Development* 115:75-88
24. Kim-Ha J, Smith JL, Macdonald PM. 1991. *Cell* 66:23-35
25. Ephrussi A, Dickinson LK, Lehmann R. 1991. *Cell* 66:37-50

26. Nakamura A, Amikura R, Mukai M, Kobayashi S, Lasko PF. 1996. *Science* 274:2075-79
27. Golumbeski GS, Bardsley A, Tax F, Boswell RE. 1991. *Genes Dev* 5:2060-70
28. Wang C, Dickinson LK, Lehmann R. 1994. *Dev. Dyn.* 199:103-15
29. Tirronen M, Lahti V-P, Heino TI, Roos C. 1995. *Mech. Dev.* 52:65-75
30. Hales KH, Meredith JE, Storti RV. 1994. *Dev. Biol.* 165:639-53
31. Theurkauf WE. 1994. *Dev. Biol.* 165:352-60
32. St. Johnston D, Driever W, Berleth T, Riechstein S, Nüsslein-Volhard C. 1989. *Development* 107(Suppl.):13-19
33. Karlin-McGinnes M, Serano TL, Cohen RS. 1996. *Dev. Genet.* 19:238-48
34. Roth S, Neuman-Silberberg FS, Barcelo G, Schüpbach T. 1995. *Cell* 81:967-78
35. González-Reyes A, Elliot H, Johnston DS. 1995. *Nature* 375:654-58
36. Clark IE, Jan LY, Jan YN. 1997. *Development* 124:461-70
37. Pokrywka N-J, Stephenson EC. 1995. *Dev. Biol.* 167:363-70
38. Lane ME, Kalderon D. 1994. *Genes Dev.* 8:2986-95
39. Ruohola H, Bremer KA, Baker D, Swedlow JR, Jan LY, Jan YN. 1991. *Cell* 66:433-49
40. Gillespie DE, Berg CA. 1995. *Genes Dev.* 9:2495-508
41. Clark I, Giniger E, Ruohola-Baker H, Jan LY, Jan YN. 1994. *Curr. Biol.* 4:289-300
42. González-Reyes A, Johnston DS. 1994. *Science* 266:639-41
43. Gavis ER, Curtis D, Lehmann R. 1996. *Dev. Biol.* 176:36-50
44. Zaccai M, Lipshitz HD. 1996. *Dev. Genet.* 19:249-57
45. Zaccai M, Lipshitz HD. 1996. *Zygote* 4:159-66
46. Deleted in proof
47. Lasko PF. 1994. *Molecular Genetics of Drosophila oogenesis*. Austin, TX: Landes
48. Mahajan-Miklos S, Cooley L. 1994. *Cell* 78:291-301
49. Cooley L, Verheyen E, Ayers K. 1992. *Cell* 69:173-84
50. Cant K, Knowles BA, Mooseker MS, Cooley L. 1994. *J. Cell Biol.* 125:369-80
51. Theurkauf WE, Smiley S, Wong ML, Alberts BM. 1992. *Development* 115:923-36
52. Theurkauf WE. 1994. *Science* 265:2093-96
53. Deleted in proof
54. Karr TL, Alberts BM. 1986. *J. Cell Biol.* 102:1494-509
55. Sullivan W, Fogarty P, Theurkauf W. 1993. *Development* 118:1245-54
56. Wang C, Lehmann R. 1991. *Cell* 66:637-47
57. Jongens TA, Hay B, Jan LY, Jan YN. 1992. *Cell* 70:569-84
58. Foe VA, Alberts BM. 1983. *J. Cell Sci.* 61:31-70
59. Raff JW, Whitfield WGF, Glover DM. 1990. *Development* 110:1249-61
60. Dalby B, Glover DM. 1992. *Development* 115:989-97
61. Ding D, Lipshitz HD. 1993. *Zygote* 1:257-71
62. Whitfield WGF, Gonzalez C, Sanchez-Herrero E, Glover DM. 1989. *Nature* 338:337-40
63. Ding D, Parkhurst SM, Halsell SR, Lipshitz HD. 1993. *Mol. Cell. Biol.* 13:3773-81
64. Edgar BA, O'Dell GM, Schubiger G. 1987. *Genes Dev.* 1:1226-37
65. Davis I, Ish-Horowicz D. 1991. *Cell* 67:927-40
66. Gergen JP, Butler BA. 1988. *Genes Dev.* 2:1179-93
67. Tepass U, Speicher SA, Knust E. 1990. *Cell* 61:787-99
68. Baker NE. 1988. *Dev. Biol.* 125:96-108
69. Macdonald PM, Ingham PW, Struhl G. 1986. *Cell* 47:721-34
70. King ML. 1995. See Ref. 1, pp. 137-48
71. Dumont JN. 1972. *J. Morphol.* 136:153-80
72. Gerhart J, Keller R. 1986. *Annu. Rev. Cell Biol.* 2:201-29
73. Gerhart J, Danilchik M, Doniach T, Roberts S, Rowning B, Stewart R. 1989. *Development* 107(Suppl.):37-51
74. Kloc M, Etkin LD. 1995. See Ref. 1, pp. 149-56
75. Smith JL, Wilson JE, Macdonald PM. 1992. *Cell* 70:849-59
76. Ephrussi A, Lehmann R. 1992. *Nature* 358:387-92
77. Wylie CC, Heasman J, Snape A, O'Driscoll M, Holwill S. 1985. *Dev. Biol.* 112:66-72
78. Mosquera L, Forristall C, Zhou Y, King ML. 1993. *Development* 117:377-86
79. Zhou Y, King M-L. 1996. *Development* 122:2947-53
80. Wylie CC, Brown D, Godsave SF, Quarmby J, Heasman J. 1985. *J. Embryol. Exp. Morphol.* 89(Suppl.):1-15
81. Linnen JM, Bailey CP, Weeks DL. 1993. *Gene* 128:181-88

82. Weeks DL, Melton DA. 1987. *Proc. Natl. Acad. Sci. USA* 84:2798-802
83. Hudson JW, Alarcón VB, Elinson RP. 1996. *Dev. Genet.* 19:190-98
84. Otte AP, McGrew LL, Olate J, Nathanson NM, Moon RT. 1992. *Development* 116:141-46
85. Hinkley CS, Martin JF, Leibham D, Perry M. 1992. *Mol. Cell. Biol.* 12:638-49
86. Otte AP, Moon RT. 1992. *Cell* 68:1021-29
87. Kloc M, Reddy BA, Miller M, Eastman E, Etkin L. 1991. *Mol. Reprod. Dev.* 28:341-45
88. Reddy BA, Kloc M, Etkin LD. 1992. *Mech. Dev.* 39:1-8
89. Kloc M, Miller M, Carrasco A, Eastman E, Etkin L. 1989. *Development* 107:899-907
90. Kloc M, Etkin LD. 1995. *Development* 121:287-97
91. Stennard F, Carnac G, Gurdon JB. 1996. *Development* 122:4179-88
92. Zhang J, King M-L. 1996. *Development* 122:4119-29
93. Melton DA. 1987. *Nature* 328:80-82
94. Yisraeli JK, Sokol S, Melton DA. 1990. *Development* 108:289-98
95. Elinson RP, King M-L, Forristall C. 1993. *Dev. Biol.* 160:554-62
96. Pondel MD, King ML. 1988. *Proc. Natl. Acad. Sci. USA* 85:7612-16
97. Kloc M, Spohr G, Etkin LD. 1993. *Science* 262:1712-14
98. Ku M, Melton DA. 1993. *Development* 119:1161-73
99. Zhou Y, King ML. 1997. *Dev. Biol.* 179:173-83
100. Swalla BJ, Jeffery WR. 1996. *Dev. Biol.* 178:23-34
101. Swalla BJ, Jeffery WR. 1995. *Dev. Biol.* 170:353-64
102. Swalla BJ, Jeffery WR. 1996. *Dev. Genet.* 19:258-67
103. Vlahou A, Gonzalez-Rimbau M, Flytzanis CN. 1996. *Development* 122:521-26
104. Steward O, Kleiman R, Banker G. 1995. See Ref. 1, pp. 235-55
105. Van Minnen J. 1994. *Histochem. J.* 26:377-91
106. Garner CC, Tucker RP, Matus A. 1988. *Nature* 336:674-76
107. Tiedge H, Freneau RT, Weinstock PH, Arancio O, Brosius J. 1991. *Proc. Natl. Acad. Sci. USA* 88:2093-97
108. Tiedge H, Chen W, Brosius J. 1993. *J. Neurosci.* 13:2382-90
109. Mayford M, Baranes D, Podsypanina K, Kandel ER. 1996. *Proc. Natl. Acad. Sci. USA* 93:13250-55
110. Furuichi T, Simon-Chazottes D, Fujino I, Yamada N, et al. 1993. *Recept. Channels* 1:11-24
111. Tiedge H, Zhou A, Thorn NA, Brosius J. 1993. *J. Neurosci.* 13:4214-19
112. Litman P, Barg J, Rindzoonki L, Ginzburg I. 1993. *Neuron* 10:627-38
113. Hannan AJ, Schevzov G, Gunning P, Jeffrey PL, Weinberger RP. 1995. *Mol. Cell. Neurosci.* 6:397-411
114. Murphy D, Levy A, Lightman S, Carter D. 1989. *Proc. Natl. Acad. Sci. USA* 86:9002-5
115. Jirikowski GF, Sanna PP, Bloom FE. 1990. *Proc. Natl. Acad. Sci. USA* 87:7400-4
116. Mohr E, Fehr S, Richter D. 1991. *EMBO J.* 10:2419-24
117. Mohr E, Richter D. 1992. *Eur. J. Neurosci.* 9:870-76
118. Ressler KJ, Sullivan SL, Buck LB. 1994. *Cell* 79:1245-55
119. Vassar R, Chao SK, Sitcheran R, Nuñez JM, Vosshall LB, Axel R. 1994. *Cell* 79:981-91
120. Trapp BD, Moench T, Pully M, Barbosa E, Tennekoon G, Griffin J. 1987. *Proc. Natl. Acad. Sci. USA* 84:7773-77
121. Colman DR, Kriebich G, Frey AB, Sabatini DD. 1982. *J. Cell Biol.* 95:598-608
122. Laitala-Leinonen T, Howell ML, Dean GE, Väänänen HK. 1996. *Mol. Biol. Cell* 7:129-42
123. Sundell CL, Singer RH. 1991. *Science* 253:1275-77
124. Lawrence JB, Singer RH. 1986. *Cell* 45:407-15
125. Cheng H, Bjerknes M. 1989. *J. Mol. Biol.* 210:541-49
126. Banerjee U, Renfranz PJ, Pollock JA, Benzer S. 1987. *Cell* 49:281-91
127. Li P, Yang XH, Wasser M, Cai Y, Chia W. 1997. *Cell* 90:437-47
128. Long RM, Singer RH, Meng XH, Gonzalez I, Nasmyth K, Jansen R-P. 1997. *Science* 277:383-87
129. Takizawa P, Sil A, Swedlow JR, Herskowitz I, Vale RD. 1997. *Nature* 389:90-93
130. Daneholt B. 1997. *Cell* 88:585-88
131. Francis-Lang H, Davis I, Ish-Horowicz D. 1996. *EMBO J.* 15:640-49
132. Kobayashi S, Okada M. 1990. *Nucleic Acids Res.* 18:4592
133. Kobayashi S, Okada M. 1989. *Development* 107:733-42
134. Kobayashi S, Amikura R, Okada M. 1993. *Science* 260:1521-24
135. Kobayashi S, Amikura R, Okada M. 1994. *Int. J. Dev. Biol.* 38:193-99

136. Kobayashi S, Amikura R, Nakamura A, Saito H, Okada M. 1995. *Dev. Biol.* 169: 384–86
137. Ding D, Whittaker KL, Lipshitz HD. 1994. *Dev. Biol.* 163:503–15
138. Gottlieb E. 1990. *Curr. Opin. Cell Biol.* 2:1080–86
139. Gavis ER, Lehmann R. 1994. *Nature* 369:315–18
140. Dahanukar A, Wharton RP. 1996. *Genes Dev.* 10:2610–20
141. Smibert CA, Wilson JE, Kerr K, Macdonald PM. 1996. *Genes Dev.* 10:2600–9
142. Halsell SR, Lipshitz HD. 1995. See Ref. 1, pp. 9–39
143. Deleted in proof
144. Cooperstock RL, Lipshitz HD. 1998. *Semin. Cell Dev. Biol.* 8(6):541–49
145. Li MG, McGrail M, Serr M, Hays TS. 1994. *J. Cell Sci.* 126:1475–94
146. McGrail M, Hays TS. 1997. *Development* 124:2409–19
147. Pokrywka N-J, Stephenson EC. 1994. *Dev. Biol.* 166:210–19
148. Suter B, Steward R. 1991. *Cell* 67:917–26
149. Lantz V, Chang JS, Horabin JI, Bopp D, Schedl P. 1994. *Genes Dev.* 8:598–613
150. Pokrywka NJ, Stephenson EC. 1991. *Development* 113:55–66
151. Macdonald PM, Kerr K. 1997. *RNA* 3: 1413–1420
152. Erdélyi M, Michon A-M, Guichet A, Glotzer JB, Ephrussi A. 1995. *Nature* 377:524–27
153. Tetzlaff MT, Jäckle H, Pankratz MJ. 1996. *EMBO J.* 15:1247–54
154. Deshler JO, Highett MI, Schnapp BJ. 1997. *Science* 276:1128–31
155. Knowles RB, Sabry JH, Martone ME, Deerinck TJ, Ellisman MH, et al. 1996. *J. Neurosci.* 16:7812–20
156. Ainger K, Avossa D, Morgan F, Hill SJ, Barry C, et al. 1993. *J. Cell Biol.* 123:431–41
157. Behar L, Marx R, Sadot E, Barg J, Ginzburg I. 1995. *Int. J. Dev. Neurosci.* 13:113–27
158. Litman P, Behar L, Elisha Z, Yisraeli JK, Ginzburg I. 1996. *Dev. Biol.* 176:80–94
159. Glotzer JB, Saffrich R, Glotzer M, Ephrussi A. 1997. *Curr. Biol.* 7:326–37
160. Swan A, Suter B. 1996. *Development* 122:3577–86
161. Kloc M, Etkin LD. 1994. *Science* 265: 1101–3
162. Wang SX, Hazelrigg T. 1994. *Nature* 369:400–3
163. Ferrandon D, Elphick L, Nüsslein-Volhard C, St. Johnston D. 1994. *Cell* 79:1221–32
164. Ferrandon D, Koch I, Westhof E, Nüsslein-Volhard C. 1997. *EMBO J.* 16: 1751–58
165. Walter P, Johnson AE. 1994. *Annu. Rev. Cell Biol.* 10:87–119
166. Macdonald PM, Struhl G. 1988. *Nature* 336:595–98
167. Macdonald PM. 1990. *Development* 110:161–72
168. Kim-Ha J, Webster PJ, Smith JL, Macdonald PM. 1993. *Development* 119: 169–78
169. Lantz V, Schedl P. 1994. *Mol. Cell Biol.* 14:2235–42
170. Mowry KL, Melton DA. 1992. *Science* 255:991–94
171. Kislauskis EH, Zhu X-C, Singer RH. 1994. *J. Cell Biol.* 127:441–51
172. Jackson RJ. 1993. *Cell* 74:9–14
173. Muslimov IA, Santi E, Homel P, Perini S, Higgins D, Tiedge H. 1997. *J. Neurosci.* 17:4722–33
174. Whittaker KL, Lipshitz HD. 1995. See Ref. 1, pp. 41–61
175. Kislauskis EH, Li ZF, Singer RH, Taneja KL. 1993. *J. Cell Biol.* 123:165–72
176. Macdonald PM, Kerr K, Smith JL, Leask A. 1993. *Development* 118:1233–43
177. Macdonald PM, Leask A, Kerr K. 1995. *Proc. Natl. Acad. Sci. USA* 92:10787–91
178. St. Johnston D, Brown NH, Gall JG, Jantsch M. 1992. *Proc. Natl. Acad. Sci. USA* 89:10979–83
179. St. Johnston D, Beuchle D, Nüsslein-Volhard C. 1991. *Cell* 66:51–63
180. Ding D, Lipshitz HD. 1993. *BioEssays* 10:651–58
181. Serano T, Cohen R. 1995. *Development* 121:3809–18
182. Dalby B, Glover DM. 1993. *EMBO J.* 12:1219–27
183. Gautreau D, Cote CA, Mowry KL. 1997. *Development* 124:5013–20
184. Kim-Ha J, Kerr K, Macdonald PM. 1995. *Cell* 81:403–12
185. Gavis ER, Lunsford L, Bergsten SE, Lehmann R. 1996. *Development* 122: 2791–800
186. Webster PJ, Liang L, Berg CA, Lasko P, Macdonald PM. 1997. *Genes Dev.* 11:2510–21
187. Yisraeli JK, Oberman F, Pressman Schwartz S, Havin L, Elisha Z. 1995. See Ref. 1, pp. 157–71
188. Schüpbach T, Wieschaus E. 1986. *Roux's Arch. Dev. Biol.* 195:302–17
189. Frohnhofer HG, Nüsslein-Volhard C. 1987. *Genes Dev.* 1:880–90

190. Rongo C, Gavis E, Lehmann R. 1995. *Development* 121:2737-46
191. Bandziulis R, Swanson MS, Dreyfuss G. 1989. *Genes Dev.* 3:431-37
192. Schüpbach T, Wieschaus E. 1991. *Genetics* 129:1119-36
193. Castrillon DH, Gönczy P, Alexander S, Rawson R, Eberhart CG, et al. 1993. *Genetics* 135:489-505
194. Lasko PF, Ashburner M. 1988. *Nature* 335:611-16
195. Hay B, Jan LY, Jan YN. 1988. *Cell* 55: 577-87
196. Liang L, Diehl-Jones W, Lasko P. 1994. *Development* 120:1201-11
197. Schwartz SP, Aisenthal L, Elisha Z, Oberman F, Yisraeli JK. 1992. *Proc. Natl. Acad. Sci. USA* 89:11895-99
198. Perry-O'Keefe H, Kintner C, Yisraeli J, Melton DA. 1990. In *In situ Hybridization and the Study of Development and Differentiation*, ed. N Harris, D Wilkenson, pp. 115-30. Cambridge: Cambridge Univ. Press
199. Elisha Z, Havin L, Ringel I, Yisraeli JK. 1995. *EMBO J.* 14:5109-14
200. Mowry KL. 1996. *Proc. Natl. Acad. Sci. USA* 93:14608-13
201. Marcey D, Watkins WS, Hazelrigg T. 1991. *EMBO J.* 10:4259-66
202. Macdonald PM, Luk SKS, Kilpatrick M. 1991. *Genes Dev.* 5:2455-66
203. Chao Y-C, Donahue KM, Pokrywka NJ, Stephenson EC. 1991. *Dev. Genet.* 12: 333-41
204. Hegdé J, Stephenson EC. 1993. *Development* 119:457-70
205. Webster P, Suen J, Macdonald P. 1994. *Development* 120:2027-37
206. Lasko PF, Ashburner M. 1990. *Genes Dev.* 4:905-21
207. Hay B, Ackerman L, Barbel S, Jan LY, Jan YN. 1988. *Development* 103:625-40
208. Hay B, Jan LY, Jan YN. 1990. *Development* 109:425-33
209. Yoon C, Kawakami K, Hopkins N. 1997. *Development* 124:3157-66
210. Christerson LB, McKearin DM. 1994. *Genes Dev.* 8:614-28
211. Kelley RL. 1993. *Genes Dev.* 7:948-60
212. Serano TL, Karlin-McGinnes M, Cohen RS. 1995. *Mech. Dev.* 51:183-92
213. Prost E, Derychere F, Roos C, Haenlin M, Pantesco V, Mohier E. 1988. *Genes Dev.* 2:891-900
214. Wilson JE, Connell JE, Schlenker JD, Macdonald PM. 1996. *Dev. Genet.* 19: 199-209
215. Rittenhouse KR, Berg CA. 1995. *Development* 121:3032-33
216. Wilson JE, Connell JE, Macdonald PM. 1996. *Development* 122:1631-39
217. St. Johnston D. 1995. *Cell* 81:161-70
218. Neuman-Silberberg FS, Schupbach T. 1994. *Development* 120:2457-63
219. Driever W, Nüsslein-Volhard C. 1988. *Cell* 54:83-93
220. Driever W, Nüsslein-Volhard C. 1988. *Cell* 54:95-104
221. Struhl G, Struhl K, Macdonald PM. 1989. *Cell* 57:1259-73
222. Driever W, Thoma G, Nüsslein-Volhard C. 1989. *Nature* 340:363-67
223. Driever W, Nüsslein-Volhard C. 1989. *Nature* 337:138-43
224. Driever W, Siegel V, Nüsslein-Volhard C. 1990. *Development* 109:811-20
225. Wharton RP, Struhl G. 1991. *Cell* 67: 955-67
226. Rivera-Pomar R, Niessing D, Schmidt-Ott U, Gehring WJ, Jäckle H. 1996. *Nature* 379:746-49
227. Dubnau J, Struhl G. 1996. *Nature* 379: 694-99
228. Mlodzik M, Fjose A, Gehring WJ. 1985. *EMBO J.* 4:2961-69
229. Macdonald PM, Struhl G. 1986. *Nature* 324:537-45
230. Lehmann R, Nüsslein-Volhard C. 1991. *Development* 112:679-93
231. Gavis ER, Lehmann R. 1992. *Cell* 71: 301-13
232. Hülskamp M, Schröder C, Pfeifle C, Jäckle H, Tautz D. 1989. *Nature* 338: 629-32
233. Irish V, Lehmann R, Akam M. 1989. *Nature* 338:646-48
234. Lehmann R, Nüsslein-Volhard C. 1987. *Dev. Biol.* 119:402-17
235. Tautz D, Lehmann R, Schnürch H, Schuh R, Seifert E, et al. 1987. *Nature* 327:383-89
236. Stanojevic D, Hoey T, Levine M. 1989. *Nature* 341:331-35
237. Lehmann R, Nüsslein-Volhard C. 1987. *Nature* 329:167-70
238. Lehmann R, Nüsslein-Volhard C. 1986. *Cell* 47:141-52
239. Jongens TA, Ackerman LD, Swedlow JR, Jan LY, Jan YN. 1994. *Genes Dev.* 8:2123-36
240. Kobayashi S, Yamada M, Asaoka M, Kitamura T. 1996. *Nature* 380:708-11
241. Thomsen GH, Melton DA. 1993. *Cell* 74:433-41
242. Dale L, Matthews G, Colman A. 1993. *EMBO J.* 12:4471-80
243. Kondaiah P, Sands M, Smith JM, Fields A, Roberts AB, et al. 1990. *J. Biol. Chem.* 265:1089-93

244. Doe CQ, Chu-LaGraff Q, Wright DM, Scott MP. 1991. *Cell* 65:451-64
245. Vaessin H, Grell E, Wolff E, Bier E, Jan LY, Jan YN. 1991. *Cell* 67:941-53
246. Hirata J, Nakagoshi H, Nabeshima Y-I, Matsuzuka F. 1995. *Nature* 377:627-30
247. Knoblich JA, Jan LY, Jan YN. 1995. *Nature* 377:624-27
248. Shen C-P, Jan LY, Jan YN. 1997. *Cell* 90:449-58
249. Jeffery WR, Tomlinson CR, Brodeur RD. 1983. *Dev. Biol.* 99:408-20
250. Macdonald PM. 1992. *Development* 114:221-32
251. Ait-Ahmed O, Thomas-Cavallin M, Rosset R. 1987. *Dev. Biol.* 122:153-62
252. Pomeroy ME, Lawrence JB, Singer RH, Billings-Gagliardi S. 1991. *Dev. Biol.* 143:58-67
253. Trembleau A, Calas A, Fèvre-Montange M. 1990. *Mol. Brain Res.* 8:37-45
254. Perry BA. 1988. *Cell Differ. Dev.* 25:99-108

Chapter 2

Joint action of two RNA degradation pathways controls the timing of maternal transcript elimination at the midblastula transition in *Drosophila melanogaster*

With permission, from Oxford University Press and the European Molecular Biology Organization,

The EMBO Journal, Vol. 18, No.9, pages 2610-2620, 1999

Joint action of two RNA degradation pathways controls the timing of maternal transcript elimination at the midblastula transition in *Drosophila melanogaster*

Arash Bashirullah^{1,2}, Susan R.Halsell^{2,3},
Ramona L.Cooperstock^{1,4}, Malgorzata Kloc⁵,
Angelo Karaiskakis¹, William W.Fisher^{1,2,6},
Weili Fu^{1,7}, Jill K.Hamilton¹,
Laurence D.Etkin⁵ and
Howard D.Lipshitz^{1,2,4,8}

¹Program in Developmental Biology, Research Institute, The Hospital for Sick Children, 555 University Avenue, Toronto, Ontario M5G 1X8, ²Department of Molecular and Medical Genetics, University of Toronto, Toronto, Canada, ³Division of Biology, California Institute of Technology, Pasadena, CA and ⁵Department of Molecular Genetics, University of Texas M.D.Anderson Cancer Center, Houston, TX, USA

³Present address: Department of Cell Biology, Duke University Medical Center, Box 3709, Durham, NC 27710, USA

⁶Present address: Exelixis Pharmaceuticals, Inc., 260 Littlefield Avenue, South San Francisco, CA 94401, USA

⁷Present address: Department of Neuroscience, University of Pennsylvania Medical School, Philadelphia, PA 19104, USA

⁸Corresponding author
e-mail: lipshitz@sickkids.on.ca

A.Bashirullah, S.R.Halsell and R.L.Cooperstock contributed equally to this work

Maternally synthesized RNAs program early embryonic development in many animals. These RNAs are degraded rapidly by the midblastula transition (MBT), allowing genetic control of development to pass to zygotically synthesized transcripts. Here we show that in the early embryo of *Drosophila melanogaster*, there are two independent RNA degradation pathways, either of which is sufficient for transcript elimination. However, only the concerted action of both pathways leads to elimination of transcripts with the correct timing, at the MBT. The first pathway is maternally encoded, is targeted to specific classes of mRNAs through *cis*-acting elements in the 3'-untranslated region and is conserved in *Xenopus laevis*. The second pathway is activated 2 h after fertilization and functions together with the maternal pathway to ensure that transcripts are degraded by the MBT.

Keywords: *Drosophila*/midblastula transition (MBT)/localization/stability/*Xenopus*

Introduction

In animal embryos as diverse as echinoderms, insects, amphibians and mammals, the earliest stages of development are programmed by maternally synthesized RNAs and proteins (reviewed in Davidson, 1986). Subsequent phases of embryogenesis require products encoded by zygotically synthesized transcripts. The transition from maternal to zygotic control of development is referred to as the midblastula transition (MBT) which is defined by the first

developmental processes that require zygotic products. The MBT should not be confused with the onset of zygotic transcription, which initiates earlier. Prior to the MBT, a subset of the maternally synthesized transcripts is degraded. In mammals, maternal transcript degradation is complete by the two-cell stage, while in echinoderms, amphibians and insects it occurs prior to the MBT, when either several hundred cells (echinoderms), several thousand cells (amphibians) or several thousand syncytial nuclei (insects) are present.

Genetic and molecular studies in *Drosophila melanogaster* have demonstrated that a subset of the maternal mRNAs encode proteins controlling the cell cycle, positional specification of cells or the morphogenetic movements that drive gastrulation. These transcripts are eliminated during the syncytial blastoderm stage, shortly after zygotic transcription commences (reviewed in Cooperstock and Lipshitz, 1997; Bashirullah *et al.*, 1998). The subsequent cellularization of the blastoderm is the first developmental process requiring zygotic contributions and thus marks the *Drosophila* MBT (Edgar *et al.*, 1986; Merrill *et al.*, 1988; Sibon *et al.*, 1997).

During early *Drosophila* embryogenesis, from egg-laying until the MBT, there are 13 synchronous syncytial nuclear divisions (Zalokar and Erk, 1976; Foe and Alberts, 1983; Campos-Ortega and Hartenstein, 1998). Subsequently, the nuclei enter interphase of nuclear division cycle 14 and the somatic blastoderm cellularizes by concerted invagination of cell membranes from the periphery. Blastoderm cellularization is followed by the first gastrulation movements and the first zygotically programmed mitosis, mitosis 14, which is no longer synchronous (Foe, 1989). It has been shown that this transition from synchronous maternally driven mitoses to asynchronous zygotically programmed mitoses requires degradation of maternal *string* transcripts (*string* encodes a homolog of the cell cycle regulator, CDC25) (Edgar and O'Farrell, 1989, 1990; Edgar and Datar, 1996).

While turnover of maternal transcripts was first reported more than 20 years ago, little is known of the degradation machinery or of the mechanisms by which specific classes of transcripts are targeted to it. Here we show that two transcript degradation pathways function in the early *Drosophila* embryo. The first, 'maternal', pathway is driven by maternally encoded factors that are recruited by *cis*-acting RNA degradation elements independently of whether the transcript is translationally active or translationally repressed. This maternal degradation apparatus is conserved in *Xenopus* oocytes and early embryos. The second 'zygotic' pathway becomes active 2 h after fertilization. Either pathway acting alone is sufficient to eliminate maternal transcripts; however, the joint action of both pathways is necessary for elimination of transcripts prior to the MBT. This dual degradation system is likely

to coordinate developmental events by ensuring the elimination of maternal transcripts prior to the MBT.

Results

Degradation of maternally synthesized transcripts begins shortly after fertilization in *Drosophila*

We analyzed the dynamics of transcript degradation in the early embryo focusing on three maternally encoded RNAs: *Hsp83*, *string* and *nanos*. *Hsp83* transcripts are particularly abundant, representing 1% of the polyadenylated transcripts in the early embryo (Zimmerman *et al.*, 1983). RNA tissue *in situ* analyses demonstrated that maternal *Hsp83* and *string* transcripts are no longer detectable by late stage 5, after completion of blastoderm cellularization (Figure 1A–F); *nanos* transcripts are undetectable by stage 4 (Figure 1G–I). RNA tissue *in situ* analyses are useful for defining when very low levels of transcripts are reached, but they are not sufficiently quantitative to be used to define the time course of degradation. Consequently, we carried out Northern blot analyses of RNA samples prepared from embryo collections spanning 30 min intervals during the first 5 h after

fertilization. These blots were probed for *Hsp83*, *string*, *nanos* and *rpA1* transcripts. *rpA1* served as an internal control since maternal *rpA1* transcripts are stable beyond the MBT (Riedl and Jacobs-Lorena, 1996) (Figure 1J). Maternal *Hsp83*, *string* and *nanos* transcript levels decrease throughout the pre-MBT stages initiating within the first hour after fertilization (Figure 1K). By the MBT (2.5–3.0 h after fertilization), >96% of the maternal *Hsp83* transcripts loaded into the embryo have disappeared (Figure 1K). The *Hsp83* transcripts present at and after this stage comprise undegraded maternal transcripts in the pole cells and zygotic transcripts. Ninety-five percent of long isoform *string* transcripts (Figure 1J and K; only the long isoform is strictly maternally synthesized and is shown in K, although quantitation was done on each isoform) and >99% of the *nanos* transcripts have been eliminated by the MBT (Figure 1J and K). The remaining *nanos* transcripts represent undegraded maternal transcripts in the pole cells (Figure 1H and I). These results demonstrate that maternal transcript degradation initiates at or shortly after fertilization, and that the vast majority of these transcripts have been eliminated by the MBT.

Maternally encoded products direct transcript degradation, even in unfertilized eggs

We used unfertilized eggs to ask whether maternally encoded products are sufficient to direct transcript degradation in the absence of both fertilization and zygotic transcription. In *Drosophila*, egg activation occurs when the mature oocyte passes from the ovary into the uterus. This process does not require fertilization. Egg activation releases the female pronucleus from meiotic arrest at metaphase I, results in translation of various maternally encoded transcripts deposited in the oocyte, and induces

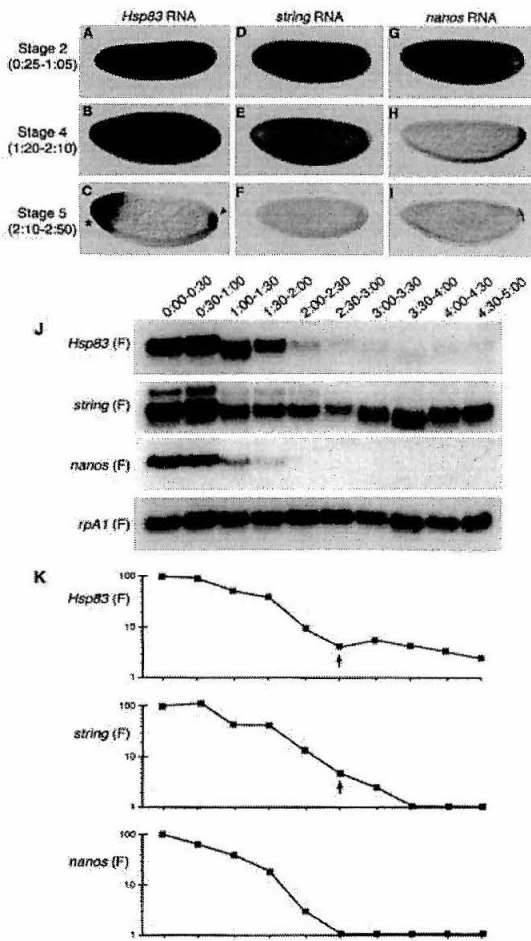


Fig. 1. Degradation of maternal *Hsp83*, *string* and *nanos* transcripts begins at fertilization, and >95% of the transcripts are eliminated by the MBT. Whole-mount *in situ* analysis of transcript distributions in wild-type early embryos are shown in (A–I) while Northern blots and quantitative analysis are shown in (J) and (K). All three species of transcripts are present throughout the embryo at late stage 2 (A, D and G; at about nuclear cycle 8; 25 min–1 h 5 min after fertilization). By stage 4 (nuclear cycle 13, 1 h 20 min–2 h 10 min after fertilization), *nanos* transcripts have been degraded in the somatic region (H) while *Hsp83* and *string* transcripts are still present (B and E). By the cellular blastoderm stage (nuclear cycle 14, 2 h 10 min–2 h 50 min after fertilization), *Hsp83* and *string* transcripts have been degraded throughout the somatic region (C and F) while *Hsp83* transcripts (arrowhead, C) and *nanos* transcripts (I) remain undegraded in the pole cells. The previously reported zygotic expression of *Hsp83* RNA (Ding *et al.*, 1993a) can be seen in the presumptive head region (asterisk). Stages are according to Campos-Ortega and Hartenstein (1998). Embryos are oriented with the anterior to the left and dorsal up. This convention will be followed throughout. (J) Northern blots are shown for *Hsp83*, *string*, *nanos* and *rpA1* transcripts in developing embryos. For quantitation (K), amounts were normalized relative to *rpA1* levels since *rpA1* transcripts are stable. The time points shown in (J) also apply to (K). The ordinate in (K) presents [RNA] plotted on a logarithmic scale. A total of 96% of the maternally encoded *Hsp83* transcripts, 95% of the strictly maternally encoded *string* transcripts ('long isoform', upper band in J) and >99% of the *nanos* transcripts have disappeared by 2.5 h after fertilization (arrows). The *Hsp83* transcripts present after 2.5 h in embryos comprise maternal transcripts present in pole cells and zygotically synthesized transcripts. The larger *string* transcript, which is strictly maternal in origin (Edgar and Datar, 1996), was quantified. Details of the number of repetitions of each Northern blot experiment are given in Materials and methods.

depolymerization of cortical microtubules and cross-linking of the vitelline membrane (Mahowald *et al.*, 1983).

The transcripts which we analyzed, i.e. maternal *Hsp83* (Figure 2A–C), *string* (Figure 2D–F), *nanos* (Figure 2G–I) and *Polar granule component* (*Pgc*; Figure 7G), are degraded in unfertilized eggs. Northern blot analyses (Figure 2J) indicated that 99% of the *Hsp83* transcripts and 90% of the long isoform *string* transcripts have been degraded by 4–5 h after egg activation (Figure 2K), 1–2 h later than in developing embryos (Figure 2J and K). Over 99% of the *nanos* transcripts have been degraded by 3 h after egg activation (Figure 2J and K), 0.5 h later than in developing embryos but >1 h earlier than *Hsp83* and *string* transcripts. *rpA1* transcripts are stable throughout this period (Figure 2J). We conclude that maternally encoded factors are sufficient for degradation of *Hsp83*, *string*, *nanos* and *Pgc* transcripts. A second, superimposed, degradation pathway causes the more rapid elimination of transcripts in embryos than in unfertilized eggs (see below).

Cis-acting elements in the 3'-UTR target transcripts for degradation

To identify *cis*-acting sequences essential for transcript degradation, we focused on the 3'-untranslated regions (3'-UTRs) of *Hsp83* and *nanos* transcripts. If an element targets transcripts for degradation, then absence of this element would be expected to stabilize the transcript. Unfertilized eggs were used for the analysis in order to identify those elements necessary for maternally encoded transcript degradation.

For *Hsp83*, a series of reporter transgenes was constructed that contained a fragment of the *Escherichia coli lacZ* gene and either the full 407 nucleotides of the *Hsp83* 3'-UTR or deleted versions (see Figure 3A for sequence, Figure 3B for transgenic constructs). By this analysis, a region in the 3'-UTR from nucleotide 253 to 349, which we refer to as the *Hsp83* degradation element (HDE), proved necessary for maternally encoded *Hsp83* transcript degradation (Figure 3C–F). Transcripts lacking the HDE (252Δ350) are stable in unfertilized eggs for at least 6 h (Figure 3F). This contrasts with transcripts that include the HDE (endogenous *Hsp83* transcripts or transgenic transcripts that include the HDE) which are fully degraded in unfertilized eggs by 4 h after activation (see Figure 2C, J and K for endogenous transcripts; data not shown for transgenic transcripts). Elimination of either the 5' or the 3' half of the HDE (252Δ301 or 300Δ351) results in incomplete degradation (data not shown; see Figure 3B).

The first 186 nucleotides of the *nanos* 3'-UTR, designated the translation control element (TCE), have also been implicated in control of transcript stability (Dahanukar and Wharton, 1996; Smibert *et al.*, 1996). In unfertilized eggs, this element is shown here to target the maternally encoded degradation machinery to *nanos* transcripts. Transcripts lacking the first 186 nucleotides (ΔTCE) are not degraded by 2–4 h after egg activation (Figure 4C and D) whereas endogenous *nanos* transcripts have completely disappeared (Figure 4A and B).

To study whether the *Hsp83* HDE and the *nanos* TCE are functionally interchangeable, two additional transgenic constructs were made. In one, the HDE was added to a *nanos* transgene lacking the TCE (*nos*[ΔTCE+HDE])

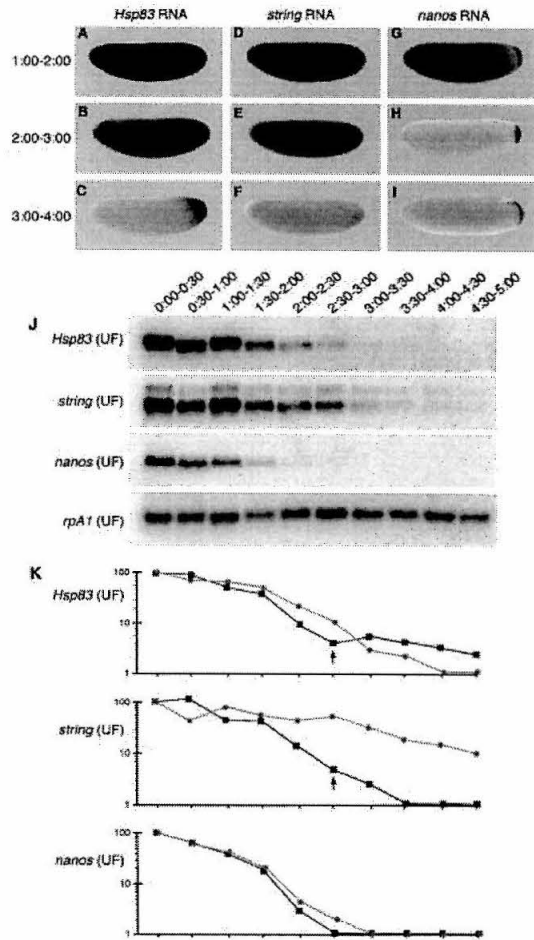


Fig. 2. *Hsp83*, *string* and *nanos* transcripts are degraded in unfertilized eggs. Whole-mount *in situ* analysis of transcript distributions in unfertilized eggs are shown in (A–I) while Northern blots and quantitative analysis are shown in (J) and (K). *Hsp83*, *string* and *nanos* transcripts are present throughout the egg from 0 to 2 h after egg activation (A, D and G). Between 2 and 3 h after egg activation, levels of *Hsp83* and *string* transcripts have decreased (B and E), *nanos* transcripts are no longer detectable outside the posterior polar plasm (H) and *Hsp83* transcripts can be seen to be concentrated in the posterior polar plasm (B). By 3–4 h, all three classes of transcripts are undetectable (C, F and I) except for the posterior-localized *Hsp83* and *nanos* transcripts (C and I). (J) Northern blots are shown for *Hsp83*, *string*, *nanos* and *rpA1* transcripts in unfertilized eggs. *Hsp83* and *string* transcripts (strictly maternal, upper band) reach minimal levels by 4–5 h, whereas *nanos* transcripts have disappeared by 3 h after egg activation. For quantitation (K), amounts were normalized relative to *rpA1* levels since *rpA1* transcripts are stable. The time points shown in (J) also apply to (K). The ordinate in (K) presents [RNA] plotted on a logarithmic scale. In unfertilized eggs, >99% of the *nanos* transcripts, 99% of the *Hsp83* transcripts and 90% of the *string* transcripts (strictly maternal, upper band in J) are degraded. Transcripts from unfertilized eggs are shown in gray (●) while transcripts from embryos (taken from Figure 1) are shown in black (■) for comparison. Details of the number of repetitions of each Northern blot experiment are given in Materials and methods.

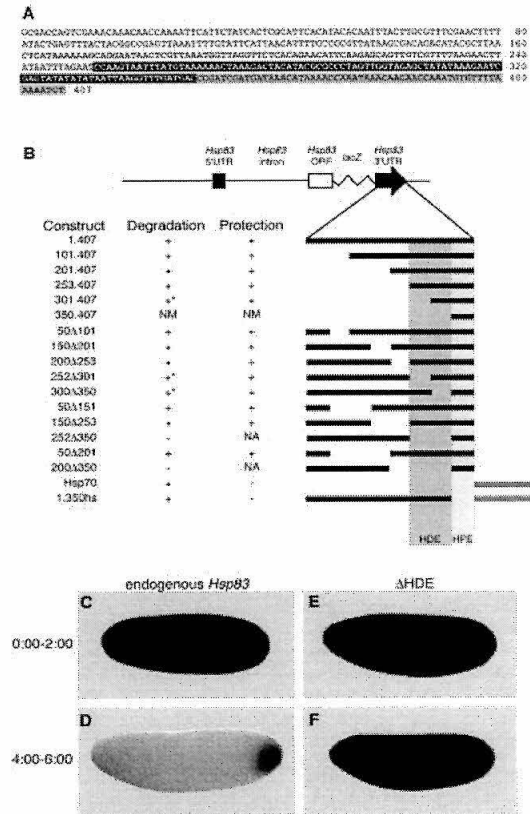


Fig. 3. Mapping of the *Hsp83* degradation (HDE) and protection (HPE) elements. (A) Sequence of the *Hsp83* 3'-UTR with highlighted HDE (black) and HPE (gray). (B) Transcription of the transgenes is under the control of *Hsp83* regulatory sequences fused to a 603 bp *lacZ* tag and followed by the 407 nucleotide *Hsp83* 3'-UTR (1.407) or the *Hsp70* 3'-UTR ('*Hsp70*') (see Materials and methods). 3', 5' and internal deletions within the *Hsp83* 3'-UTR are shown as a diagram. +, degradation or protection occur as in wild-type; ++, degradation incomplete; -, degradation or protection fail; NA, protection cannot be assayed in the absence of degradation; NM, no maternal RNA present in the egg (Halsell, 1995). Black bars represent *Hsp83* 3'-UTR sequences; gray bars represent *Hsp70* 3'-UTR sequences. The HDE which maps from nucleotide 253 to 349 and the HPE which maps from nucleotide 350 to 407 are highlighted. (C and D) Endogenous *Hsp83* transcripts visualized with an antisense *Hsp83* RNA probe. (E and F) Transgenic 252 Δ 350 reporter transcripts visualized with an antisense β -galactosidase RNA probe. The age of eggs or embryos in hours is shown to the left. In contrast to endogenous transcripts (C and D), the 252 Δ 350 transcripts persist throughout the egg until at least 6 h after activation (E and F).

(Figure 4E and F); in the other, the *nanos* TCE was added to an *Hsp83-lacZ* reporter construct lacking the HDE (*Hsp83*[Δ HDE+TCE]) (Figure 4G and H). Addition of the *Hsp83* HDE restores degradation to the otherwise stable *nos*[Δ TCE] transcript (Figure 4E and F) while addition of the *nanos* TCE similarly targets the stable *Hsp83-lacZ*[Δ HDE] transcript for degradation (Figure 4G and H). While our data demonstrate that the HDE and TCE are functionally interchangeable, we have been unable to identify any significant primary sequence or secondary structure conservation between these elements.

These data support a model in which specific *cis*-acting elements recruit a maternally encoded degradation machinery to both the *Hsp83* and *nanos* transcripts.

Relationship between translation and RNA degradation

Our next goal was to study whether translational repression is a prerequisite for transcript degradation. Such a requirement had been postulated for *nanos* transcripts in early embryos since relief of translational repression (by deletion of the TCE) correlated with an increase in transcript stability (Dahanukar and Wharton, 1996; Smibert *et al.*, 1996). Translation of *nanos* in the head region of the embryo causes repression of *bicoid* translation and thus head skeleton defects (Dahanukar and Wharton, 1996; Smibert *et al.*, 1996). The severity of the defect serves as a sensitive readout of the Nanos protein level (Wharton and Struhl, 1991; Gavis and Lehmann, 1994) in the absence of a direct assay using anti-Nanos antibodies, which are no longer available.

We examined the head skeleton of transgenic embryos carrying *nos*[Δ TCE] or *nos*[Δ TCE+HDE] transcripts. As previously reported (Dahanukar and Wharton, 1996; Smibert *et al.*, 1996), *nos*[Δ TCE] transcripts are translated and produce head skeleton defects (Figure 4J). Surprisingly, even though *nos*[Δ TCE+HDE] transcripts are degraded (Figure 4F), they too produce head skeleton defects (Figure 4K). Furthermore, the severity of the head skeleton defects was greater in the case of *nos*[Δ TCE+HDE] than *nos*[Δ TCE]. In five independent *nos*[Δ TCE] transgenic lines, an average of $72 \pm 29\%$ of the embryos exhibited defects and these were restricted to the dorsal bridge. In contrast, all four independent *nos*[Δ TCE+HDE] lines resulted in $100 \pm 0\%$ of the embryos exhibiting severe defects (loss of dorsal bridge, dorsal arms, vertical plates and ventral arms).

Thus, not only are the *nos*[Δ TCE+HDE] transcripts translated, but they are translated at higher levels than the *nos*[Δ TCE] transcripts, perhaps because the HDE includes a translational enhancer. We conclude that translational repression and transcript degradation are not causally linked; even highly translated transcripts are targeted for degradation. Moreover, non-protein-coding transcripts (e.g. *Pgc*) are also degraded in unfertilized eggs (Figure 7G). Together, these data indicate that the transcript degradation machinery acts on transcripts that contain a degradation element independently of whether they are untranslatable, translationally repressed or translated.

Discovery of a second, zygotically encoded or activated degradation pathway

We next addressed why *Hsp83* transcripts are eliminated more rapidly in embryos than in unfertilized eggs. We asked whether embryos contain an additional degradation machinery that acts independently of the HDE, by comparing the stability of transcripts containing or lacking the HDE. Degradation of endogenous *Hsp83* transcripts as well as HDE-containing transgenic transcripts is initiated shortly after fertilization, and minimal transcript levels are reached by 2.5 h (Figure 5A, B and F for endogenous transcripts; transgenic transcripts not shown). In unfertilized eggs, transcripts lacking the HDE are stable for well over 5 h (Figures 3E and F, and 5E).

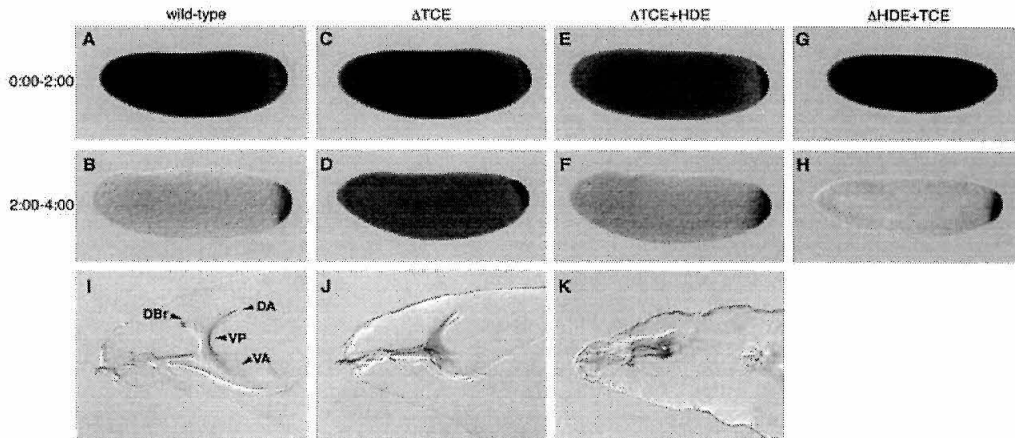


Fig. 4. The *Hsp83* HDE and the *nanos* TCE are interchangeable with respect to maternal transcript degradation, which is independent of translational repression. (A and B) Endogenous *nanos* transcripts are degraded by 2 h after egg deposition. (C and D) Deletion of the *nanos* TCE (*nanos* 3'-UTR nucleotides 1–185) results in transcript stabilization. (E and F) Replacement of the *nanos* TCE with the *Hsp83* HDE (*Hsp83* 3'-UTR nucleotides 253–349) restores transcript degradation. (G and H) Replacement of the *Hsp83* HDE with the *nanos* TCE restores transcript degradation. *nanos*[Δ TCE+HDE] transcripts are not translationally repressed even though they are degraded. Head skeletons are shown from wild-type (I), embryos from *nanos*[Δ TCE] transgenic females (J) and embryos from *nanos*[Δ TCE+HDE] females (K). As previously reported (Dahanukar and Wharton, 1996; Smibert *et al.*, 1996), there is a reduction of the dorsal bridge in *nanos*[Δ TCE] embryos (J). Surprisingly, although *nanos*[Δ TCE+HDE] transcripts are degraded (F), they are not translationally repressed, as evidenced by the severe head skeleton phenotype (K) (note the loss of dorsal bridge, dorsal arms, vertical plate and ventral arms). DBr, dorsal bridge; DA, dorsal arms; VP, vertical plate; VA, ventral arms.

HDE-deleted (252 Δ 350) transcripts are stable throughout the first 2 h of embryogenesis, after which degradation initiates, and 95% of these transcripts are gone by 4 h after fertilization (Figure 5C, D, F and G). Thus, in addition to the maternally encoded degradation machinery, a zygotically synthesized or zygotically triggered degradation machinery is active starting 2 h after fertilization. Furthermore, since transcript degradation occurs at this stage in the absence of the HDE, this 'zygotically' degradation is independent of elements in the 3'-UTR that mediate the maternally encoded degradation. Zygotic transcript degradation occurs for all 3'-UTR reporter constructs listed in Figure 3.

Taken together, our analyses demonstrate that the joint action of both the 'maternal' and the 'zygotically' degradation pathways is needed to eliminate the bulk of maternal transcripts by the onset of the MBT.

Elements in the 3'-UTR protect transcripts from degradation in the pole cells

Certain maternal transcripts fail to degrade in pole cells of developing embryos or in the posterior polar plasm of unfertilized eggs. These include *Hsp83* (Figures 1C and 2C), *nanos* (Figures 1H and I, and 2H and I) and *Pgc* (Figure 7G) (Wang and Lehmann, 1991; Ding *et al.*, 1993a; Nakamura *et al.*, 1996). Our time course analysis shows that 1% of the total maternally loaded *Hsp83* transcripts and <1% of the total maternally loaded *nanos* transcripts remain in the posterior polar plasm of unfertilized eggs (Figure 2K). Two possible mechanisms could lead to the absence of transcript degradation at the posterior: the degradation machinery might be excluded from the posterior polar plasm and thus also from the pole cells. Alternatively, the machinery could be active in

the posterior polar plasm and pole cells, but certain classes of transcripts could be masked from the machinery by components of the polar plasm.

To distinguish between these possibilities, we replaced the *Hsp83* 3'-UTR in our reporter construct with the 3'-UTR from the *Hsp70* transcript (Figure 3B). Transgenic reporter transcripts carrying the *Hsp83* 3'-UTR are degraded normally in the soma but are not degraded in the pole cells (Figure 6A–C), mimicking the distribution of the endogenous *Hsp83* transcripts (Figure 1A–C). The reporter transcripts carrying the *Hsp70* 3'-UTR are taken up into the pole cells when they bud (Figure 6D and E) but are unstable and are degraded by the cellular blastoderm stage (Figure 6F; see figure legend for details). These results demonstrate that the maternally encoded degradation machinery is present throughout the egg and embryo.

To identify 'protection' elements within the *Hsp83* 3'-UTR, we assayed posterior protection of our reporter transcripts in unfertilized eggs (Figure 3B). Sequences sufficient for protection reside within the 3'-most nucleotides of the *Hsp83* 3'-UTR since transgenic RNA produced by the 301.407 construct is protected (Figure 3A and B). Since transgenic RNA carrying only nucleotides 351–407 is unstable during oogenesis (Halsell, 1995), it was not possible to determine whether the 3'-most 57 nucleotides alone are sufficient for protection. However, replacement of nucleotides 351–407 with the *Hsp70* 3'-UTR results in failure of protection (Figure 3B), showing that nucleotides 351–407 are necessary for protection. We refer to nucleotides 351–407 as the *Hsp83* protection element or HPE. Thus elements necessary for degradation versus protection map to distinct regions within the *Hsp83* 3'-UTR.

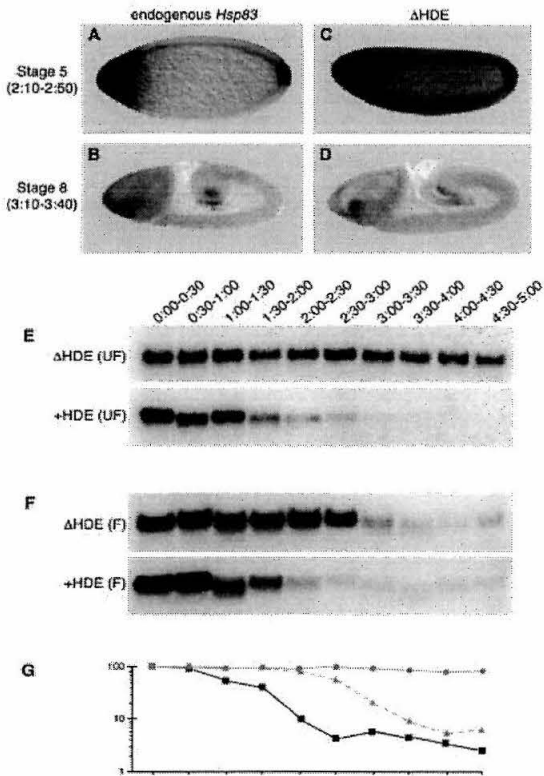


Fig. 5. *Hsp83* transcripts lacking the HDE are degraded in embryos by a zygotically synthesized or activated degradation mechanism. (A and B) Endogenous *Hsp83* transcripts visualized with an antisense *Hsp83* RNA probe. (C and D) Transgenic 252 Δ 350 reporter transcripts visualized with an antisense β -galactosidase RNA probe. The stage of embryos is shown to the left. In contrast to endogenous transcripts (A and B) which are degraded by the MBT and so are absent by stage 5, the 252 Δ 350 transcripts persist beyond stage 5 (C) and are degraded by stage 8 (D). Zygotically synthesized transcripts accumulate in the head region and in the germ band (B and D). Northern blots are shown of unfertilized eggs ('UF' in E) and developing embryos ('F' in F). Quantitation is shown in (G). In unfertilized eggs, transgenic transcripts lacking the HDE (●, solid gray line) are stable, whereas they are degraded starting after 2 h and are gone by 4 h after fertilization in embryos (▲, dashed gray line). Endogenous transcripts in embryos are shown for reference (■, solid black line; taken from Figure 1K). For quantitation, amounts were normalized as in Figures 1 and 2. In embryos, the *Hsp83* transcripts that persist after 2.5 h (black, endogenous) or after 4 h (dashed line, Δ HDE) comprise maternal transcripts present in pole cells and zygotically synthesized transcripts. Details of the number of repetitions of each Northern experiment are given in Materials and methods.

Identification of mutants that fail to undergo maternally encoded RNA degradation

Since our data demonstrated that maternal factors are sufficient for transcript degradation prior to the MBT, we tested a collection of female sterile mutant lines (Schupbach and Wieschaus, 1989) to identify maternal effect mutants that fail to undergo degradation (see Materials and methods for list). Mutants were assayed for *Hsp83* RNA degradation in unfertilized eggs aged well beyond the stage at which transcripts would have disappeared in the wild-type. The presence of protected

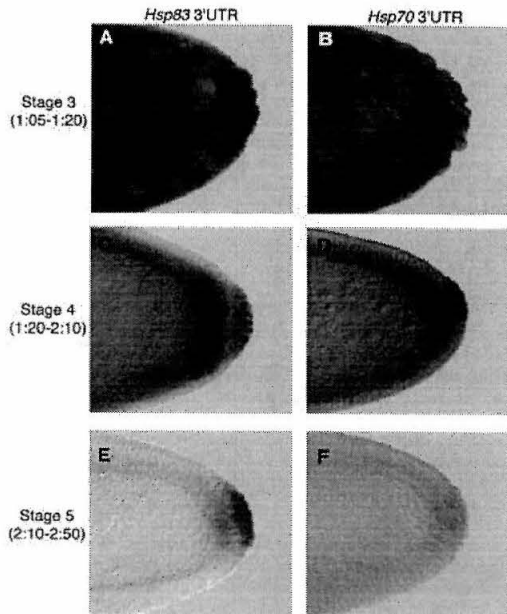


Fig. 6. Degradation activity is present in pole cells but *Hsp83* transcripts are normally protected from it. (A and B) Stage 3 pole cells; (C and D) stage 4 pole cells; (E and F) stage 5 pole cells. (A–C) *Hsp83* 1.407 transgenic transcripts or (D–F) transgenic transcripts that replace the *Hsp83* 3'-UTR with the *Hsp70* 3'-UTR (see Figure 3A), visualized with an antisense β -galactosidase probe. Transcripts that include the *Hsp83* 3'-UTR are protected from degradation in pole cells, while transcripts with the *Hsp70* 3'-UTR are degraded in both the pole cells and the soma by stage 5, indicating that degradation activity is present in pole cells. At stage 5, 82% of the embryos with the *Hsp70* 3'-UTR transgenic RNA had little or no detectable transcript in pole cells ($n = 39$). At stages 6–8, 95% of the embryos with the *Hsp70* 3'-UTR transgenic RNA had little or no detectable transcript in pole cells ($n = 42$). In contrast, 100% of the embryos carrying full-length *Hsp83* 3'-UTR transgenic RNA had high levels of transcript in their pole cells at these stages ($n = 50$).

transcripts at the posterior served as an internal control for the *in situ* hybridizations (if degradation occurs, then protected *Hsp83* transcripts are visible at the posterior). Mutations in two loci, *cortex* and *grauzone*, result in failure of *Hsp83* transcript degradation (Figure 7B and C). Failure of degradation was not specific to *Hsp83* since *nanos* (Figure 7E and F), *Pgc* (Figure 7H and I) and *string* (Figure 7K and L) transcripts also failed to degrade. The *cortex* and *grauzone* mutants exhibit defective egg activation and cytoplasmic polyadenylation of transcripts (Lieberfarb *et al.*, 1996; Page and Orr-Weaver, 1996).

The maternally encoded degradation pathway is conserved in *Xenopus*

Several maternal transcripts are localized during *Xenopus* oogenesis although it is not yet known whether the type of degradation–protection system described here for *Drosophila* functions in their localization (reviewed in Bashirullah *et al.*, 1998). Furthermore, as in *Drosophila*, many maternal transcripts are degraded prior to the *Xenopus* MBT (reviewed in Davidson, 1986). Thus, it was of interest to determine whether *Xenopus* oocytes and early embryos have a maternal RNA degradation

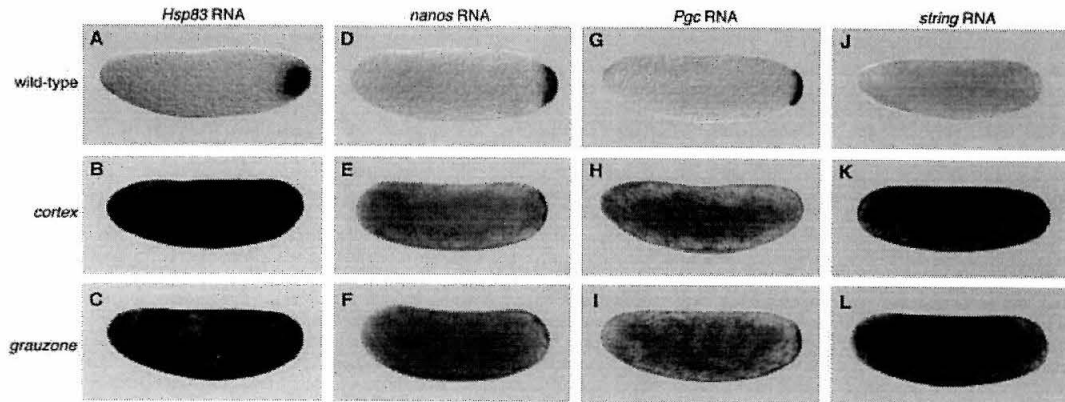


Fig. 7. The *cortex* and *grauzone* mutants result in failure of maternally encoded transcript degradation. Assays were conducted in unfertilized eggs, aged for at least 3 h, from wild-type females (A, D, G and J), *cortex* females (B, E, H and K) or *grauzone* females (C, F, I and L). Degradation of *Hsp83* (A–C), *nanos* (D–F), *Pgc* (G–I) and *string* (J–L) transcripts fails in eggs produced by the mutants. The defects in transcript localization (E, F, H and I) may result from cytoskeletal abnormalities (Lieberfarb et al., 1996; Page and Orr-Weaver, 1996).

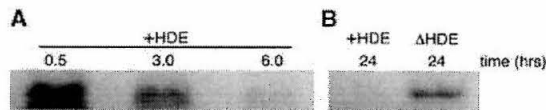


Fig. 8. The maternal transcript degradation pathway is conserved in *Xenopus* and *Drosophila*. (A) *In vitro* synthesized *Drosophila Hsp83* 3'-UTR transcripts (1.407) that carry the HDE ('+HDE') are highly unstable in *Xenopus* oocytes and are almost completely degraded within 6 h of injection. (B) In contrast, *in vitro* synthesized *Drosophila Hsp83* 3'-UTR transcripts that lack the HDE ('ΔHDE'; 252Δ350) are stable and can still be readily detected 24 h after injection.

machinery similar to that identified here in *Drosophila*. We injected *in vitro* synthesized, digoxigenin-labeled transcripts comprising the full-length *Drosophila Hsp83* 3'-UTR into stage 6 *Xenopus* oocytes or recently fertilized embryos. These transcripts are unstable and are degraded rapidly after injection (Figure 8A for oocytes; data not shown for embryos). We then injected *in vitro* transcribed *Drosophila Hsp83* 3'-UTR ΔHDE transcripts into stage 6 oocytes; these transcripts are extremely stable and are still readily detectable 24 h after injection (Figure 8B). We conclude that the *Drosophila* HDE functions as a degradation element in *Xenopus* oocytes and embryos. Thus, *Xenopus* must contain a transcript degradation activity highly related to the *Drosophila* maternal activity and capable of recognizing the *Drosophila* HDE.

Discussion

Passage from maternal to zygotic control of development is thought to depend on the elimination of a subset of maternal transcript classes from the early embryo. For example, degradation of ubiquitous maternal *string* transcripts is necessary to permit zygotically driven, patterned domains of cell division after the MBT (Edgar and Datar, 1996). Here we have shown that the joint action of two RNA degradation pathways controls maternal transcript degradation and its timing in the early *Drosophila* embryo, and that at least one of these pathways (the 'maternal' pathway) is conserved in *Xenopus*.

Two genetic pathways ensure RNA degradation prior to the *Drosophila* MBT

The first degradation pathway is maternally encoded and does not require fertilization or zygotic gene transcription for its function. This 'maternal' pathway begins to function at or shortly after egg activation, and is sufficient for degradation of even abundant maternally loaded transcripts by 4–5 h after egg activation (Figure 9). The second 'zygotic' pathway requires fertilization and becomes active 1.5–2 h after fertilization. Acting alone, the zygotic pathway eliminates transcripts by 4 h after fertilization. Since the zygotic pathway can remove *Hsp83* transcripts in 2 h, while the maternal pathway takes 4–5 h, the zygotic machinery is approximately twice as efficient as the maternal machinery. Under normal circumstances, relatively rare transcripts are degraded almost exclusively by the maternal pathway (e.g. *nanos*). In contrast, more abundant transcripts require the action of both pathways in order to be eliminated by the MBT (e.g. *Hsp83*, *string*). The maternal pathway initiates transcript degradation at or shortly after egg activation, while the zygotic pathway ensures degradation of abundant transcripts prior to the MBT.

Our results predict four classes of maternal RNAs in the early embryo. The first class lacks both maternal and zygotic degradation elements and is stable (e.g. *rpA1*). The second class (if it exists—there are no known examples) would be degraded exclusively by the maternal machinery either because these transcripts lack zygotic degradation elements or because their low abundance enables them to be fully degraded by the maternal machinery prior to activation of the zygotic factors. A third class (if it exists—there are no known examples) would be degraded exclusively by the zygotic machinery, possibly because of a lack of elements that target the maternal factors. The fourth class (e.g. *Hsp83*, *string* and *nanos*) is degraded by the combined action of the maternal and zygotic machinery.

The dual mechanism for transcript degradation discovered here sheds light on two previously reported observations. First, it has been shown that modulation

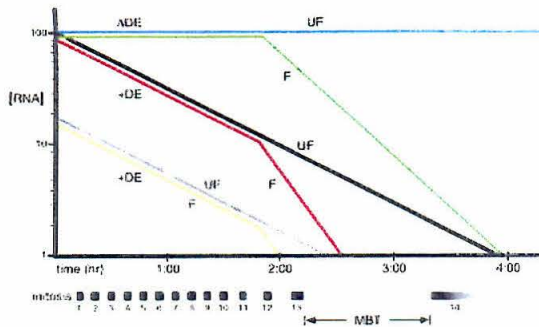


Fig. 9. Maternal and zygotic degradation activities cooperate to eliminate maternal transcripts by the MBT. Below the time scale on the x-axis are shown the maternally driven mitoses (1–13) followed by interphase 14 (the MBT) during which zygotic products take over control of the cell cycle before mitosis 14, the first patterned and asynchronous mitosis. The y-axis represents the [RNA] plotted on a logarithmic scale. In unfertilized eggs, an abundant transcript (e.g. *Hsp83*) lacking a maternal degradation element but carrying a zygotic degradation element is stable (ADE, blue). In contrast, such a transcript is degraded in fertilized, developing embryos by the zygotic degradation apparatus, starting ~2 h after fertilization, such that transcripts are fully degraded by 4 h after fertilization (ADE, green). In the presence of both maternal and zygotic degradation elements, transcript degradation initiates at or shortly after activation of unfertilized eggs and is complete by 4 h after fertilization (+DE, black). In fertilized, developing embryos, transcripts carrying both maternal and zygotic degradation elements initially are degraded solely by the maternal apparatus (<2 h after fertilization) and then cooperatively by both the maternal and zygotic factors (>2 h after fertilization) (+DE, red). Only in this last case do abundant transcripts disappear by the MBT (2.0–2.5 h after fertilization). Rarer transcripts (e.g. *nanos*) are eliminated almost exclusively by the maternal machinery (yellow and grey). ADE, no maternal degradation element; +DE, maternal degradation element present; UF, unfertilized egg; F, developing embryo.

of the nuclear:cytoplasmic ratio affects the timing of disappearance of maternally synthesized *string* transcripts (Yasuda *et al.*, 1991). Changing the nuclear:cytoplasmic ratio would not affect the maternal degradation machinery since it would be pre-loaded into the embryo and its activity/concentration should be independent of that ratio. In contrast, changes in the nuclear:cytoplasmic ratio might be expected to alter the synthesis or local concentration of the zygotic degradation machinery, particularly if activation of this machinery is dependent on zygotic transcription. Thus, altering the nuclear:cytoplasmic ratio would alter the exact timing of *string* transcript disappearance by modulating the zygotic pathway. Secondly, our results explain why α -amanitin injection into embryos prior to nuclear cycle 6 causes a delay in degradation of maternal *string* transcripts (α -amanitin inhibits RNA polymerase II and thus zygotic transcription) (Edgar and Datar, 1996). If production or activation of the zygotic degradation machinery requires zygotic transcription, α -amanitin would be expected to inhibit it while leaving the maternal degradation machinery unaffected. This would result in a delay in *string* degradation since only the maternally encoded degradation apparatus would be functional.

In summary, while previous results suggested that turnover of transcripts at the MBT might be controlled by zygotic products (O'Farrell *et al.*, 1989; Yasuda *et al.*,

1991), we have uncovered a dual maternal–zygotic degradation system that is likely to coordinate developmental events by ensuring the elimination of maternal transcripts prior to the MBT.

Cis-acting elements target transcripts for degradation or for protection

We have shown that the maternal transcript degradation activity is present throughout the embryo and unfertilized egg. Deletion of specific *cis*-acting 3'-UTR sequences results in failure of maternally encoded transcript degradation. These elements do not share any obvious primary sequence or secondary structure, nor do they include any previously defined degradation tags (reviewed in Jacobson and Peltz, 1996). Despite the lack of sequence conservation, our data demonstrate that the degradation elements are interchangeable (the *Hsp83* HDE can substitute for the *nanos* TCE, and vice versa). The *cis*-acting elements defined here are not necessary for targeting transcripts to the zygotic degradation pathway since deletion of these elements has no detectable effect on the zygotic degradation process; in fact, none of our *Hsp83* 3'-UTR deletions abrogates zygotic transcript degradation. There are three plausible explanations for this result: (i) there are redundant 'zygotic' degradation elements in the *Hsp83* 3'-UTR; (ii) such elements reside in another part of the *Hsp83* transcript [given the structure of the reporter transgenes, this could be the 5'-UTR or the first 333 nucleotides of the open reading frame (ORF)]; or (iii) zygotic degradation is not a targeted event but is the default state.

For RNAs such as *rpA1*, which are stable in the early embryo, we do not yet know whether there are specific stabilization elements or whether transcript stability is a default state. Indirect evidence in support of the latter possibility comes from analyses of a transcript instability element in the *flz* 3'-UTR (Riedl and Jacobs-Lorena, 1996). Addition of this element (FIE3) to *rpA1* transcripts destabilizes them, suggesting that for *rpA1* transcripts, stability is either the default state or that instability elements such as FIE3 are dominant to as yet undefined stability elements.

Our data indicate that it is possible to differentially stabilize transcripts carrying degradation tags in different regions of the cytoplasm and/or in different cell types. Specifically, we have shown that the maternal degradation apparatus is active throughout the egg and embryo, but that transcripts such as *Hsp83*, *nanos* and *Pgc* are protected from degradation in the pole plasm and pole cells. We have also been able to map sequences in the *Hsp83* 3'-UTR that are necessary for this protection. The most likely candidate organelles for protecting transcripts in the polar plasm and pole cells are the polar granules themselves. First, one of the RNAs we have studied (*Pgc*) has been shown to be an integral component of the polar granules (Nakamura *et al.*, 1996). Secondly, it has been shown that disruption of the polar granules results in failure of *Hsp83*, *nanos* and *Pgc* transcript protection in the polar plasm and pole cells, while ectopic assembly of polar granules at the anterior of the embryo results in ectopic protection of these transcripts anteriorly (Ephrussi and Lehmann, 1992; Ding *et al.*, 1993a; Nakamura *et al.*, 1996).

Role of transcript degradation and protection in cytoplasmic RNA localization

Differential stabilization of transcripts in specific regions of the cytoplasm represents one of several RNA localization mechanisms (reviewed in Bashirullah *et al.*, 1998). *Hsp83* is the only example of a transcript localized by a degradation–protection mechanism (Ding *et al.*, 1993a; St Johnston, 1995). However, we have shown that *nanos*, *Pgc* and *Hsp83* transcript elimination in the somatic region of the embryo is accomplished by the same RNA degradation machinery. Further, our data suggest that 99% of the *Hsp83* transcripts and >99% of the *nanos* transcripts reside in somatic region. This last result is very similar to the 96% value reported recently for somatic *nanos* transcripts (Bergsten and Gavis, 1999). We speculate that the differences in localization patterns of transcripts that are obviously localized prior to egg activation and those which only appear localized well after egg activation may be largely quantitative.

Relationship of transcript degradation to translation and polyadenylation status

The literature contains numerous examples of a correlation between translational repression of mRNAs and their degradation (reviewed in Jacobson and Peltz, 1996; Cooperstock and Lipshitz, 1997). In the early *Drosophila* embryo, the best studied example is *nanos*: *nanos* transcripts outside of the posterior polar plasm are translationally repressed and are also unstable (Figure 4, and see also Dahanukar and Wharton, 1996; Gavis *et al.*, 1996; Smibert *et al.*, 1996). Deletion or mutation of *cis*-acting elements that mediate translational repression results in transcript stabilization (Dahanukar and Wharton, 1996; Smibert *et al.*, 1996; this study). Despite this correlation, our data demonstrate that there is no obligatory link between translational repression and transcript degradation. Replacing the element from the *nanos* 3'-UTR that mediates translational repression and degradation (the TCE) with the *Hsp83* degradation element (the HDE) is sufficient to allow maternal degradation of *nanos* [Δ TCE+HDE] transcripts. However, at the same time, the presence of severe head defects demonstrates that this transgenic RNA is in fact highly translated. Thus, transcript degradation can be unlinked from translational repression.

There are several examples of a correlation between polyadenylation status and transcript stability (reviewed in Jacobson and Peltz, 1996). In particular, long poly(A) tails are associated with translational activation and transcript stabilization, while short poly(A) tails are associated with translational repression and transcript destabilization. In the *Drosophila* embryo, it has been shown that several classes of maternal transcripts are cytoplasmically polyadenylated after fertilization, correlating with initiation of their translation (Salles *et al.*, 1994). The *cortex* and *grauzone* mutations perturb cytoplasmic polyadenylation (Lieberfarb *et al.*, 1996), but transcript stability was not assayed in those studies. We have shown here that maternal transcripts are stabilized by *cortex* and *grauzone* mutations. The primary cause of the defects in embryos produced by *cortex* and *grauzone* females is unknown; their phenotypes are complex and several aspects of egg activation are abnormal (Lieberfarb *et al.*, 1996; Page and Orr-Weaver, 1996). Thus it is not yet possible to draw firm conclusions

from these mutants regarding a possible link between cytoplasmic polyadenylation status and transcript stability.

Evolutionary conservation of transcript degradation pathways

We have shown that *Xenopus* oocytes and early embryos contain an activity highly related to the maternal transcript degradation activity we have defined in *Drosophila*. Remarkably, the *Drosophila* HDE is recognized by this activity, and *in vitro* synthesized, injected transcripts are degraded rapidly, disappearing within a few hours. Removal of the HDE stabilizes these transcripts for at least 24 h. These results suggest that evolutionarily highly conserved pathways may control transcript degradation and localization throughout metazoa, opening up the possibility of exploiting the particular advantages of different model systems for future mechanistic and functional analysis.

Materials and methods

Drosophila whole-mount RNA *in situ* hybridization

RNA *in situ* hybridization with DNA probes was performed as described previously, with minor modifications (Tautz and Pfeifle, 1989; Ding *et al.*, 1993a,b). Digoxigenin-labeled antisense RNA probes were made using the Megascript RNA transcription kit (Ambion, Inc.) according to the manufacturer's instructions, and included digoxigenin-labeled UTP (Boehringer Mannheim). The RNA probes were subjected to limited alkaline hydrolysis by incubation in an equal volume of 100 mM NaCO₃ pH 10.2 for 1 h at 60°C followed by ethanol precipitation. Pre-hybridization and hybridization were carried out at 55°C for RNA probes and at 48°C for DNA probes, and detection of the probe was as previously described (Tautz and Pfeifle, 1989). After hybridization, eggs or embryos were cleared in 50% glycerol followed by 70% glycerol. For exact staging, nuclei were visualized with 1 µg/ml 4',6-diamidino-2-phenylindole (DAPI) in phosphate-buffered saline (PBS) for 5 min prior to clearing of the embryos. Eggs or embryos were then individually mounted in 70% glycerol and images were captured using a Spot cooled-CCD camera (Diagnostic Instruments, Inc.) mounted on a Zeiss Axioplan microscope. Adobe Photoshop software was used to process the images. For transgenic lines, at least two independently derived lines were analyzed for each construct.

Drosophila RNA extraction and analysis

RNA samples were isolated from staged egg collections by phenol extraction using Trizol (BRL). Equal amounts of total RNA were electrophoresed in 1.2% agarose/formaldehyde/MOPS gels (Sambrook *et al.*, 1989), and transferred onto nylon membranes (Amersham). Filters were pre-hybridized for at least 1 h at 63°C in hybridization buffer containing 0.5 M Na-phosphate/7% SDS. ³²P-labeled random primed DNA probes were added and hybridization was performed overnight at the same temperature. Filters were rinsed twice at 60°C in 30 mM Na-phosphate/0.1% SDS, and exposed to Kodak XAR5 film at -80°C with an intensifying screen. Films were also exposed to a Molecular Dynamics phosphor screen, and quantitation was performed using ImageQuant software. *Hsp83*, *string* and *nanos* transcript levels were normalized to *rpl1* mRNA levels to control for variations in loading. The number of repetitions of each experiment was as follows: *Hsp83* endogenous transcripts, fertilized = 3; *Hsp83* endogenous transcripts, unfertilized = 2; *Hsp83* Δ HDE transcripts, fertilized = 2; *Hsp83* Δ HDE transcripts, unfertilized = 1; *string* transcripts, fertilized = 2; *string* transcripts, unfertilized = 2; *nanos* transcripts, fertilized = 1; *nanos* transcripts, unfertilized = 1.

Construction of transgenes for *Drosophila* germline transformation

Standard protocols were used (Sambrook *et al.*, 1989).

Hsp83-lacZ transgenes. The following approach was taken to generate the series of *lacZ-Hsp83* 3'-UTR constructs that include the 5'-*Hsp83* enhancer sequences and promoter (Figure 3B). Previous reports (Kim-Ha *et al.*, 1993) suggested that a full-length *lacZ* ORF might not

be completely transcribed *in vivo*. Therefore, we inserted the *Hsp83* 3'-UTR fragments downstream of a truncated *lacZ* tag. We accomplished this by constructing pB83Z, a Bluescript subclone that contains all of the *Hsp83* 5' upstream region, the first exon, the intron and the first 111 codons of the ORF fused to 603 bp of *lacZ* sequence (Halsell, 1995). At the 3' end of the *lacZ* sequence are *AatII*, *HindIII* and *KpnI* cloning sites for inserting the *Hsp83* 3'-UTR fragments. The template for the PCR was Eco9, an 8 kb *EcoRI* fragment subcloned in Bluescript that contains the full-length *Hsp83* transcription unit. 5' Fragments of the 3'-UTR were PCR amplified and were flanked with *AatII* and *HindIII* restriction sites, while 3' fragments of the 3'-UTR were flanked with *HindIII* and *KpnI* restriction sites. The position of the *HindIII* restriction site within the amplified fragments allowed us to generate nested 5' deletion constructs, the 1.350hs 3' deletion construct and a series of internal deletions within the 3'-UTR. 3'-UTR constructs with internal deletions (the 'Δ' series) were generated by first subcloning an *AatII*-*HindIII* 5' fragment into pB83Z and subsequently adding a *HindIII*-*KpnI* 3' fragment. After subcloning into pB83Z, a *NotI*-*KpnI* fragment was isolated and subcloned into *NotI*-*KpnI*-digested CaSpeR4 (Thummel and Pirrotta, 1991). As a control, the *Hsp70* 3'-UTR was also cloned independently of any *Hsp83* 3'-UTR sequence (Figure 3A, '*Hsp70*'). The *Hsp70* fragment was generated by PCR from a CaSpeR-hs template (Thummel and Pirrotta, 1991).

nanos-*Hsp83* hybrid transgenes. (i) *nanos*[ΔTCE]: a genomic 3' fragment (*BglIII*-*EcoRI*) containing a *nanos* 3'-UTR lacking the TCE was subcloned into pCaSpeR2 (Thummel and Pirrotta, 1991). Subsequently a genomic 5' fragment (*Bam*HI) extending from the *nanos* cis-regulatory sequences to the end of the ORF was inserted. (ii) *nanos*[ΔTCE + HDE]: a genomic 3' fragment (*BglIII*-*EcoRI*) containing a *nanos* 3'-UTR lacking the TCE was subcloned into pCaSpeR2. The *Hsp83* HDE was PCR amplified incorporating 5'-*Bam*HI and 3'-*BglIII* sites. This fragment was subcloned upstream of the *nanos* 3' fragment. Subsequently a genomic 5' fragment (*Bam*HI) extending from the *nanos* cis-regulatory sequences to the end of the ORF was inserted. (iii) *Hsp83*[ΔHDE + TCE]: the *nanos* TCE was amplified by PCR incorporating *HindIII* sites at the ends, and inserted into *lacZ*-tagged pBS *Hsp83*[ΔHDE] (253Δ350) at the *HindIII* site.

Drosophila germline transformation

Germline transformation was carried out using standard procedures (Rubin and Spradling, 1982). *w*¹¹¹⁸ embryos were co-injected with 500 μg/ml of the *Hsp83*-*lacZ* construct and 100 μg/ml of pHSπ helper plasmid (Steller and Pirrotta, 1985). All transgenic insertions were homozygosed or balanced over *CyO* or *TM3*.

Drosophila stocks and egg collection

Drosophila melanogaster Oregon-R and *w*¹¹¹⁸ stocks are described in Lindsley and Zimm (1992). The following 'class 2' and 'class 3' maternal effect lethal mutants (Schupbach and Wieschaus, 1989) were assayed for transcript degradation in unfertilized eggs: *cell-PK42*, *cell-RH36*, *cortex*, *cribble*, *grauzone*, *luckenhaft*, *syn-H110*, *presto*, *scraps*, *valois*. For collection of unfertilized eggs, males of genotype *T(Y;2)bw^{DRev#11}, cn bw^{DRev#11} mr2/SM6a* were crossed to appropriate females (Reed and Orr-Weaver, 1997). Terminal duplication segregants are male sterile (Reed and Orr-Weaver, 1997).

Drosophila embryo cuticle preparations

For cuticle preparations, wild-type and mutant embryos were dechorionated, devitelinized and mounted as described previously (Raz and Shilo, 1993).

RNA analysis in *Xenopus*

Drosophila Hsp83 full-length 3'-UTR (1.407, see above and Figure 3) was transcribed from a pBluescriptSK subclone using T3 RNA polymerase after linearization at the *KpnI* site. ΔHDE 3'-UTR (252Δ350, see above and Figure 3) was transcribed from a PCR-amplified fragment that included the T3 RNA polymerase promoter at the 5' end of the 3'-UTR sequence. Transcription was carried out in the presence of digoxigenin-11-UTP (Kloc *et al.*, 1996). For oocyte injections, ovaries were surgically removed from anaesthetized *X.laavis* females, stage 6 oocytes were manually defolliculated in calcium-deficient buffer (1× OR2) and were stored, injected and cultured for 0.5, 3, 6 or 24 h in 1× modified Barth's buffer. For embryo injections, recently fertilized eggs were collected, injected and allowed to develop to stage 12 (gastrula stage, ~24 h). For the time course in stage 6 oocytes (Figure 8A), 500 ng of synthetic labeled RNA was injected into the cytoplasm

whereas for comparative analysis of +HDE and ΔHDE 3'-UTRs (Figure 8B), ~100 ng of RNA was injected. Total RNA was prepared from injected oocytes or embryos, separated on a formaldehyde gel and blotted as previously described (Kloc *et al.*, 1989). The blot was blocked for 1.5 h in 2% blocking solution (BMB, Genius kit) and was then incubated for 1.5 h with a 1:5000 dilution of anti-digoxigenin-alkaline phosphatase antibody in 2% blocking buffer. Subsequently blots were washed twice for 15 min each wash in G1 buffer and stained in NBT/BCIP solution. All of the preceding used BMB Genius kit reagents and protocols.

Acknowledgements

We thank C.Thummel for transformation vectors, T.Cutforth and G.Rubin for providing the Eco9 clone and 63B-T2 DNA sequence, B.Reed for the *T(Y;2)bw^{DRev#11}, cn bw^{DRev#11} mr2/SM6a* flies, T.Schupbach for mutant fly lines, C.Smbert for the *nanos* clone, E.Gavis for communicating unpublished results, and R.McInnes, H.Krause, M.Lamka, S.Egan, S.Lewis and C.C.Hui for critical comments on the manuscript. S.R.H. was supported in part by a National Research Service Award (T32GM07616) and graduate fellowships from the Lucille P.Markey Charitable Trust and Howard Hughes Medical Institute. J.K.H. is supported by a Medical Research Council/Pharmaceutical Manufacturers Association of Canada Health Program Fellowship. R.L.C. has been supported in part by a studentship from the Medical Research Council (Canada) and a University of Toronto Open Scholarship. This research has been supported by research grants from the National Institutes of Health, USPHS (GM50221 to L.D.E.), the National Science Foundation (IBN-9418453 to H.D.L.) and the Medical Research Council of Canada (MT13208 and, currently, MT14409, both to H.D.L.).

References

- Bashirullah, A., Cooperstock, R.L. and Lipshitz, H.D. (1998) RNA localization in development. *Annu. Rev. Biochem.*, **67**, 335-394.
- Bergsten, S.E. and Gavis, E.R. (1999) Role for mRNA localization in translational activation but not spatial restriction of *nanos* RNA. *Development*, **126**, 659-669.
- Campos-Ortega, J.A. and Hartenstein, V. (1998) *The Embryonic Development of Drosophila melanogaster*. Springer-Verlag, Heidelberg, Germany.
- Cooperstock, R.L. and Lipshitz, H.D. (1997) Control of mRNA stability and translation during *Drosophila* development. *Semin. Cell Dev. Biol.*, **8**, 541-549.
- Dahanukar, A. and Wharton, R.P. (1996) The Nanos gradient in *Drosophila* embryos is generated by translational regulation. *Genes Dev.*, **10**, 2610-2620.
- Davidson, E.H. (1986) *Gene Activity in Early Development*. Academic Press, Orlando, FL.
- Ding, D., Parkhurst, S.M., Halsell, S.R. and Lipshitz, H.D. (1993a) Dynamic *Hsp83* RNA localization during *Drosophila* oogenesis and embryogenesis. *Mol. Cell. Biol.*, **13**, 3773-3781.
- Ding, D., Parkhurst, S.M. and Lipshitz, H.D. (1993b) Different genetic requirements for anterior RNA localization revealed by the distribution of *Adducin-like* transcripts during *Drosophila* oogenesis. *Proc. Natl. Acad. Sci. USA*, **90**, 2512-2516.
- Edgar, B.A. and O'Farrell, P.H. (1989) Genetic control of cell division patterns in the *Drosophila* embryo. *Cell*, **57**, 177-187.
- Edgar, B.A. and O'Farrell, P.H. (1990) The three postblastoderm cell cycles of *Drosophila* embryogenesis are regulated in G₂ by string. *Cell*, **62**, 469-480.
- Edgar, B.A. and Datar, S.A. (1996) Zygotic degradation of two maternal *Cdc25* mRNAs terminates *Drosophila*'s early cell cycle program. *Genes Dev.*, **10**, 1966-1977.
- Edgar, B.A., Kiehle, C.P. and Schubiger, G. (1986) Cell cycle control by the nucleo-cytoplasmic ratio in early *Drosophila* development. *Cell*, **44**, 365-372.
- Ephrussi, A. and Lehmann, R. (1992) Induction of germ cell formation by *oskar*. *Nature*, **358**, 387-392.
- Foe, V.A. (1989) Mitotic domains reveal early commitment of cells in *Drosophila* embryos. *Development*, **107**, 1-23.
- Foe, V.A. and Alberts, B.M. (1983) Studies of nuclear and cytoplasmic behaviour during the five mitotic cycles that precede gastrulation in *Drosophila* embryogenesis. *J. Cell Sci.*, **61**, 31-70.
- Gavis, E.R. and Lehmann, R. (1994) Translational regulation of *nanos* by RNA localization. *Nature*, **369**, 315-318.
- Gavis, E.R., Lunsford, L., Bergsten, S.E. and Lehmann, R. (1996) A

- conserved 90 nucleotide element mediates translational repression of *nanos* RNA. *Development*, **122**, 2791–2800.
- Halsell, S.R. (1995) *Expression and Localization of Hsp83 RNA in the Early Drosophila Embryo*. Ph.D. Thesis, Division of Biology, California Institute of Technology, Pasadena, CA.
- Jacobson, A. and Peltz, S.W. (1996) Interrelationships of the pathways of mRNA decay and translation in eukaryotic cells. *Annu. Rev. Biochem.*, **65**, 693–739.
- Kim-Ha, J., Webster, P.J., Smith, J.L. and Macdonald, P.M. (1993) Multiple RNA regulatory elements mediate distinct steps in localization of *oskar* mRNA. *Development*, **119**, 169–178.
- Kloc, M., Larabell, C. and Etkin, L.D. (1996) Elaboration of the messenger transport organizer pathway for localization of RNA to the vegetal cortex of *Xenopus* oocytes. *Dev. Biol.*, **180**, 119–130.
- Kloc, M., Miller, M., Carrasco, A., Eastman, E. and Etkin, L. (1989) The maternal store of the *xlgr7* mRNA in full-grown oocyte is not required for normal development in *Xenopus*. *Development*, **107**, 899–907.
- Lieberfarb, M.E., Chu, T., Wreden, C., Theurkauf, W., Gergen, J.P. and Strickland, S. (1996) Mutations that perturb poly(A)-dependent maternal mRNA activation block the initiation of development. *Development*, **122**, 579–588.
- Lindsley, D.L. and Zimm, G. (1992) *The Genome of Drosophila melanogaster*. Academic Press, San Diego, CA.
- Mahowald, A.P., Goralski, T.J. and Caulton, J.H. (1983) *In vitro* activation of *Drosophila* eggs. *Dev. Biol.*, **98**, 437–445.
- Merrill, P.T., Sweeton, D. and Wieschaus, E. (1988) Requirements for autosomal gene activity during precellular stages of *Drosophila melanogaster*. *Development*, **104**, 495–509.
- Nakamura, A., Amikura, R., Mukai, M., Kobayashi, S. and Lasko, P.F. (1996) Requirement for a noncoding RNA in *Drosophila* polar granules for germ cell establishment. *Science*, **274**, 2075–2079.
- O'Farrell, P.H., Edgar, B.A., Lakich, D. and Lehner, C.F. (1989) Directing cell division during development. *Science*, **246**, 635–640.
- Page, A.W. and Orr-Weaver, T.L. (1996) The *Drosophila* genes *grauzone* and *cortex* are necessary for proper female meiosis. *J. Cell Sci.*, **109**, 1707–1715.
- Raz, E. and Shilo, B.-Z. (1993) Establishment of ventral cell fates in the *Drosophila* embryonic ectoderm requires DER, the EGF receptor homolog. *Genes Dev.*, **7**, 1937–1948.
- Reed, B. and Orr-Weaver, T. (1997) The *Drosophila* gene *morula* inhibits mitotic functions in the endo cell cycle and the mitotic cell cycle. *Development*, **124**, 3543–3553.
- Riedl, A. and Jacobs-Lorena, M. (1996) Determinants of *Drosophila fushi tarazu* mRNA instability. *Mol. Cell Biol.*, **16**, 3047–3053.
- Rubin, G.M. and Spradling, A.C. (1982) Genetic transformation of *Drosophila* with transposable elements. *Science*, **218**, 348–353.
- Salles, F.J., Lieberfarb, M.E., Wreden, C., Gergen, J.P. and Strickland, S. (1994) Coordinate initiation of *Drosophila* development by regulated polyadenylation of maternal messenger RNAs. *Science*, **266**, 1996–1999.
- Sambrook, J., Fritsch, E.F. and Maniatis, T. (1989) *Molecular Cloning: A Laboratory Manual*. Cold Spring Harbor Laboratory Press, Cold Spring Harbor, NY.
- Schupbach, T. and Wieschaus, E. (1989) Female sterile mutations on the second chromosome of *Drosophila melanogaster*. I. Maternal effect mutations. *Genetics*, **121**, 101–117.
- Sibon, O.C.M., Stevenson, V.A. and Theurkauf, W.E. (1997) DNA-replication checkpoint control at the *Drosophila* midblastula transition. *Nature*, **388**, 93–97.
- Smibert, C.A., Wilson, J.E., Kerr, K. and Macdonald, P.M. (1996) Smaug protein represses translation of unlocalized *nanos* mRNA in the *Drosophila* embryo. *Genes Dev.*, **10**, 2600–2609.
- St Johnston, D. (1995) The intracellular localization of messenger RNAs. *Cell*, **81**, 161–170.
- Steller, H. and Pirrotta, V. (1985) A transposable P vector that confers G418 resistance to *Drosophila* larvae. *EMBO J.*, **4**, 167–171.
- Tautz, D. and Pfeifle, C. (1989) A non-radioactive *in situ* hybridization method for the localization of specific RNAs in *Drosophila* embryos reveals translational control of the segmentation gene *hunchback*. *Chromosoma*, **98**, 81–85.
- Thummel, C.S. and Pirrotta, V. (1991) New pCaSpeR P element vectors. *Drosophila Information Newsl.*, **2**, 19.
- Wang, C. and Lehmann, R. (1991) *Nanos* is the localized posterior determinant in *Drosophila*. *Cell*, **66**, 637–647.
- Wharton, R.P. and Struhl, G. (1991) RNA regulatory elements mediate control of *Drosophila* body pattern by the posterior morphogen *nanos*. *Cell*, **67**, 955–967.
- Yasuda, G.K., Baker, J. and Schubiger, G. (1991) Temporal regulation of gene expression in the blastoderm *Drosophila* embryo. *Genes Dev.*, **5**, 1800–1812.
- Zalokar, M. and Erk, I. (1976) Division and migration of nuclei during early embryogenesis of *Drosophila melanogaster*. *J. Microsc. Biol. Cell*, **25**, 97–106.
- Zimmerman, J.L., Petri, W. and Meselson, M. (1983) Accumulation of a specific subset of *D.melanogaster* heat shock mRNAs in normal development without heat shock. *Cell*, **32**, 1161–1170.

Received December 22, 1998; revised and accepted March 5, 1999

Appendix 1

Mammalian NUMB is an evolutionary conserved signaling adapter protein that specifies cell fate

With permission, from Current Biology, Ltd.,
Current Biology, Vol. 6, pages 1134-1145, 1996

Mammalian NUMB is an evolutionarily conserved signaling adapter protein that specifies cell fate

Joseph M. Verdi*, Rosemarie Schmandt*, Arash Bashirullah^{†‡}, Sara Jacob*, Ralph Salvino*, Constance G. Craig*, Amgen EST Program[§], Howard D. Lipshitz^{†#} and C. Jane McGlade*

Background: *Drosophila numb* was originally described as a mutation affecting binary divisions in the sensory organ precursor (SOP) lineage. The *numb* gene was subsequently shown to encode an asymmetrically localized protein which is required for binary cell-fate decisions during peripheral nervous system development. Part of the *Drosophila* NUMB protein exhibits homology to the SHC phosphotyrosine-binding (PTB) domain, suggesting a potential link to tyrosine-kinase signal transduction.

Results: A widely expressed mammalian homologue of *Drosophila numb* (*dnumb*) has been cloned from rat and is referred to here as mammalian *Numb* (*mNumb*). The mNUMB protein has a similar overall structure to dNUMB and 67% sequence similarity. Misexpression of *mNumb* in *Drosophila* during sensory nervous system precursor cell division causes identical cell fate transformations to those produced by ectopic dNUMB expression. *In vitro*, the mNUMB PTB domain binds phosphotyrosine-containing proteins, and SH3 domains of SRC-family tyrosine kinases bind to mNUMB presumably through interactions with proline-rich regions in the carboxyl terminus. Overexpression of full-length mNUMB in the multipotential neural crest stem cell line MONC-1 dramatically biases its differentiation towards neurons, whereas overexpression of the mNUMB PTB domain biases its differentiation away from neuronal fates.

Conclusions: Our results demonstrate that mNUMB is an evolutionarily conserved functional homologue of dNUMB, and establish a link to tyrosine-kinase-mediated signal transduction pathways. Furthermore, our results suggest that mNUMB and dNUMB are new members of a family of signaling adapter molecules that mediate conserved cell-fate decisions during development.

Introduction

Many cytoplasmic signaling molecules that are targets of tyrosine kinases contain one or more SH2 (Src homology 2) domains, which bind with high affinity to specific tyrosine-phosphorylated sequences [1,2]. Signaling enzymes often couple directly to receptor tyrosine kinases through their SH2 domains by binding to receptor autophosphorylation sites. In addition, a number of other conserved protein modules are found either alone or in combination with SH2 domains in cytoplasmic signaling proteins. These include SH3 and WW domains, which bind to proline-based peptide sequences [3,4], and PH (pleckstrin homology) domains, which may interact with protein targets or with phosphoinositides [5–7]. A family of molecules composed solely of these conserved domains — for example, SHC, NCK, CRK and GRB-2 — and which exhibit no enzymatic activity have been termed adapters, representing an alternative mechanism by which cytoplasmic signaling molecules can be coupled to activated receptors. Many signaling adapters have been conserved

throughout evolution; for example, *Drosophila* homologues of SHC (*dshc*), GRB-2 (*drk*) and NCK (*dck*) have been identified [8–11]. Genetic experiments have revealed the importance of these molecules in development: DRK is required to couple the SEVENLESS receptor tyrosine kinase to RAS for normal development of the *Drosophila* eye [9,10]; and mutations in the *dck* gene lead to a defect in axonal path-finding [11].

The PTB domain was described recently as an alternative phosphotyrosine-binding domain. The function of this domain was first demonstrated in the adapter molecule SHC [12–14], and subsequently in the IRS-1 molecule [15]. The SHC PTB domain has been shown to recognize phosphotyrosine in a specific sequence motif, NPXpY ([16,17]; single-letter amino-acid code, where X indicates any amino acid), found in several tyrosine kinase receptors and cytoplasmic proteins. A number of molecules containing potential PTB domains have been identified by sequence homology, including the SHC-related protein

Addresses: *AMGEN Institute, Ontario Cancer Institute, and Department of Medical Biophysics, University of Toronto, Toronto M5G 2C1, Canada. [†]Program in Developmental Biology, Division of Endocrinology and Department of Genetics, Research Institute, The Hospital for Sick Children, Toronto, Canada M5G 1X8. [‡]Department of Biology, California Institute of Technology, Pasadena, California 91125, USA. [§]c/o Sid Suggs, Program Leader, Amgen, Thousand Oaks, California 91320, USA. [#]Department of Molecular and Medical Genetics, University of Toronto, Toronto M5G 1X8, Canada.

Correspondence: Jane McGlade
E-mail: jmcglade@amgen.com

Received: 24 May 1996
Revised: 8 July 1996
Accepted: 18 July 1996

Current Biology 1996, Vol 6 No 9:1134–1145

© Current Biology Ltd ISSN 0960-9822

SCK, FE65, X11, *Drosophila* DISABLED and *Drosophila* NUMB (dNUMB) [18]. To date, the SHC, IRS-1, and the recently identified SHC-C [19] PTB domains have been shown to bind to tyrosine-phosphorylated proteins.

Drosophila numb was originally described as a mutation affecting the binary division of the sensory organ precursor (SOP) lineage [20]. The *numb* gene was subsequently shown to encode an asymmetrically localized protein which is required for a binary cell-fate decision during peripheral nervous system development [21,22]. *Drosophila* NUMB protein is expressed in the SOP, and during cell division dNUMB is partitioned asymmetrically into the IIb daughter cell and excluded from the IIa daughter cell [21,23]. The IIa cell then divides to produce a hair and socket, while the IIb daughter divides to give a neuron and sheath. Loss of dNUMB function in this lineage results in the overproduction of hair and sockets at the expense of neurons and sheath cells [20]. Reciprocally, ectopic expression of dNUMB early in the lineage leads to an increase in sheath and neuron cells at the expense of hair and socket cells, whereas late expression converts both progeny of the IIa cell into hair cells.

Part of the dNUMB protein exhibits strong homology to the SHC PTB domain [18], suggesting a functional link to tyrosine-kinase signal transduction. Here, we describe the cloning and characterization of a mammalian *Numb* gene (*mNumb*). Furthermore, we establish that the PTB domain of mNUMB binds to phosphotyrosine-containing proteins, suggesting that mNUMB functions as a signaling adapter molecule. We show that the cell-fate transformations caused by misexpression of mNUMB during development of the *Drosophila* peripheral nervous system are identical to those produced by its *Drosophila* counterpart. Finally, we demonstrate that mNUMB biases the lineage determination of multipotent neural crest stem cells toward a neuronal phenotype, establishing a link between tyrosine-kinase signal transduction and cell-fate decisions.

Results

Cloning of a mammalian *Numb* gene

In a search of expressed sequence tag (EST) libraries for novel PTB-containing molecules, one sequence was identified which contained a potential PTB domain and also showed high sequence similarity to the *Drosophila numb* gene. This DNA was used to screen an immortalized rat neural crest cDNA library to obtain a full-length cDNA. Two cDNAs were isolated which coded for a complete open reading frame of 603 amino acids (Fig. 1a). In an *in vitro* transcription/translation system, a 66 kDa protein was produced from the *mNumb* cDNA, which is consistent with the predicted molecular weight of the product of this open reading frame (see Fig. 3b). The sequence of the encoded protein is 67 % similar to that of dNUMB (Fig. 1b), with the highest sequence homology in the putative PTB

domain, where the two proteins are 70 % identical. A comparison of SHC and NUMB PTB domains shows that amino acids critical for the binding of the SHC PTB domain to tyrosine-phosphorylated substrates are conserved in the mNUMB protein [24–26] (Fig. 1c). This suggests that mNUMB may bind tyrosine-phosphorylated targets, and may play a role in a tyrosine-kinase-mediated signaling pathway. Examination of the mNUMB sequence also revealed that the carboxy-terminal half of the protein, which shows much lower homology to dNUMB, contains three potential SH3 binding sites. As for the *Drosophila* protein, no obvious catalytic domains can be identified in the mNumb sequence, suggesting that it may be a member of a group of signaling adapter molecules which include SHC, GRB-2, and NCK and their *Drosophila* homologues dSHC, DRK and DCK [8,9,11].

Expression pattern of *mNumb*

The expression pattern of *mNumb* mRNA was examined by northern-blot analysis. The EST clone g116, which includes the amino-terminal 250 codons of *mNumb*, was used to probe a northern blot of poly(A)⁺ RNA isolated from adult rat tissues. A strongly hybridizing band of approximately 4.4 kb and a weaker band of approximately 4 kb were detected in all tissues with the exception of skeletal muscle (Fig. 2). In addition, a similarly sized message was observed in multiple human cell lines, indicating that *mNumb* mRNA is widely expressed in both rodents and man (data not shown).

In order to examine the distribution of the mNUMB protein, a peptide corresponding to the carboxy-terminal 15 amino acids of mNUMB (Nb-C peptide) was used to generate polyclonal antiserum in rabbits (anti-Nb-C). Anti-Nb-C antiserum immunoprecipitated three proteins, a doublet of 66 kDa proteins and a protein of 68 kDa (Fig. 3a). *In vitro* transcription/translation of the *mNumb* cDNA produced a 66 kDa protein doublet, which was recognized by the Nb-C antiserum (Fig. 3b). The 66 kDa protein doublet immunoprecipitated from R2 lysates co-migrated with the *in vitro* translated proteins, suggesting that these are the products of the *mNumb* gene *in vivo*. The observed doublet may be due to phosphorylation of mNUMB both *in vitro* and *in vivo*, as treatment of anti-Nb-C immunoprecipitates with potato acid phosphatase collapsed this doublet into a single, faster-migrating band (data not shown). The 68 kDa species is likely to be the product of an alternatively spliced message (J.V. and J.M., unpublished data). Following cell fractionation, p66 and p68 were found primarily in the soluble cytoplasmic fraction, but were also detected in the particulate membrane fraction (data not shown). As shown in Figure 3c, the expression of mNUMB protein was not distributed evenly in adult tissues. Highest expression was evident in brain, liver and lung tissues, a pattern of expression that was consistent with, but more restricted than, the pattern of mRNA expression.

Figure 1 (facing page)

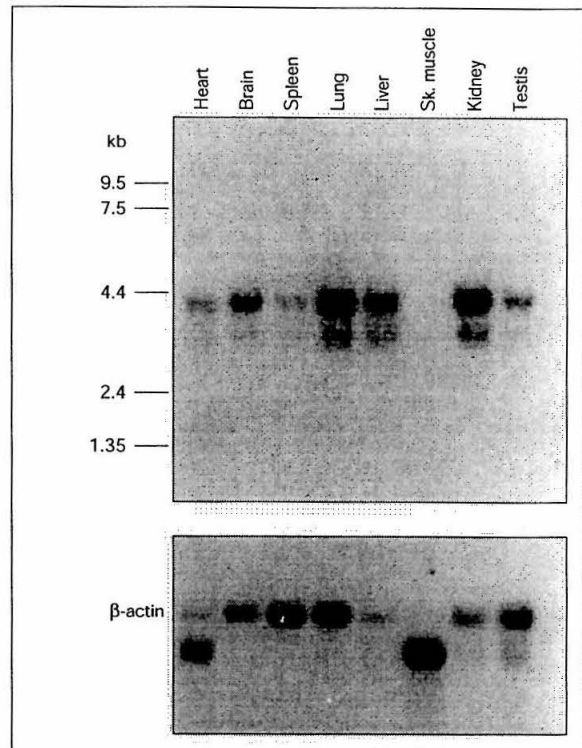
(a) Sequence of *mNumb*. The nucleotide sequence of the *mNumb* cDNA and its translation product are shown. The PTB domain is boxed, and putative SH3-binding sites are underlined. (b) The amino-acid sequence of mNUMB and dNUMB were compared using the GCG GAP program. (c) A multiple sequence alignment of the PTB domains of *Drosophila* (d) and mammalian (m) homologues of SHC and NUMB. Arrowheads indicate the positions of conserved amino acids important for phosphotyrosine binding [24–26].

Consistent with the western-blot analysis, immunohistochemical staining of rat and mouse embryonic tissues with anti-Nb-C antiserum revealed that mNUMB was expressed widely (Fig. 3d–g). Tissue anti-Nb-C immunoreactivity was specific for mNUMB, in so far as preincubation of the antibody with the immunizing peptide prior to staining tissues essentially abolished all observed staining (Fig. 3e). The strongest expression was observed in the nervous system, but was also detectable in non-neural tissue such as the branchial arches, lung, heart and liver (Fig. 3f). In the nervous system, mNUMB expression was especially prominent in the ventricular zones of neuroepithelial tissue (neurogenic regions) (Fig. 3d) and in developing neuronal ganglia (Fig. 3g). The sensory neuron pools, including the dorsal root ganglia (Fig. 3g) and the trigeminal ganglia (Fig. 3d) consistently showed the most intense staining. In two-day-old primary rat neural crest cell cultures, a subpopulation of cells was found to label intensely with anti-Nb-C. Furthermore, double-labeling of these cells with anti- β -3-tubulin indicated that, at least in this model, mNUMB was expressed specifically in cells fated to the neuronal lineage. Surprisingly, it was also evident in these neural crest cell cultures that mNUMB was not distributed asymmetrically in crescents, as has been reported previously in *Drosophila*, but rather the anti-Nb-C immunostaining appeared to be cytoplasmic (Fig. 3i).

Misexpression of mNUMB in *Drosophila*

We misexpressed mNUMB in *Drosophila* sensory organ precursor cells in order to assay whether this would cause the same cell-fate transformations as those observed upon overexpression of dNUMB. Previous analyses of the effects of overexpression of the *Drosophila numb* gene by Rhyu *et al.* [21] revealed a role for dNUMB at two successive cell divisions during peripheral nervous system development. During the first division of the SOP, dNUMB specifies the IIb fate (neuron and sheath precursor) *versus* the IIa fate (hair and socket precursor). During the subsequent division of the IIa cell, dNUMB specifies hair *versus* socket fate. Early misexpression of dNUMB causes both daughters of the SOP to adopt the IIb fate resulting in excess neurons and sheath cells and the absence of hair (microchaete) and socket cells [21]. Late misexpression of dNUMB results in twinning of hairs as a result of transformation of the socket cell into a hair cell [21].

Misexpression of mNUMB during the development of the *Drosophila* notum and the wings caused identical cell-fate

Figure 2

Tissue distribution of *mNumb* mRNA in adult rat tissues. Northern blot containing 2 μ g of poly(A)⁺ mRNA isolated from a variety of rat tissues was analyzed for *mNumb* mRNA expression. Expression of a 4.4 kb transcript is noted in all lanes except skeletal muscle.

transformations to those produced by ectopic expression of dNUMB. When misexpressed in the developing notum under heat-shock control prior to SOP cell division (10–14 hours after puparium formation; APF), mNUMB had no effect on subsequent cell-fate choice and the adult notum appeared wild-type (data not shown; see Fig. 4a for wild-type). Strikingly, however, in 100% of the flies, misexpression of mNUMB under heat-shock control at the time of the first division of the SOPs (14–18 hours APF) resulted in balding of the notum because of loss of microchaetes and associated sockets (Fig. 4b). Similarly, misexpression of mNUMB specifically at the presumptive dorsoventral margin of third instar larval wing disks under GAL4-UAS control (using the C96 line; [27]) caused complete loss of the marginal hairs in the wings (Fig. 5c,d). Misexpression of mNUMB in the notum 18–22 hours APF resulted in partial balding and also twinning of microchaetes. The latter phenotype occurred as a result of transformation of socket cells into hair cells at the division of the IIa cells (Fig. 4c). Misexpression of mNUMB under

heat-shock control in the developing wing 14–18 hours APF caused twinning of the marginal hairs in 100 % of the wings (Fig. 5e,f). Misexpression after this division (22–26 hours APF in the notum, and 18–22 or 22–26 hours APF in the wing) had no effect (data not shown). Thus, *mNUMB* produces identical cell-fate transformations to those induced by misexpression of *Drosophila numb*, and these effects are stage-specific relative to the cell division program of the SOPs.

The mNUMB PTB domain binds phosphotyrosine-containing proteins

Having shown that mNUMB is a functional homologue of dNUMB, we investigated the molecular mechanism of action of mNUMB and its role in mammalian development. To date, although a number of molecules containing PTB domains have been identified, only the SHC, SHC-C and IRS-1 PTB domains have been shown to bind tyrosine phosphorylated proteins. Therefore, we sought to

Figure 3

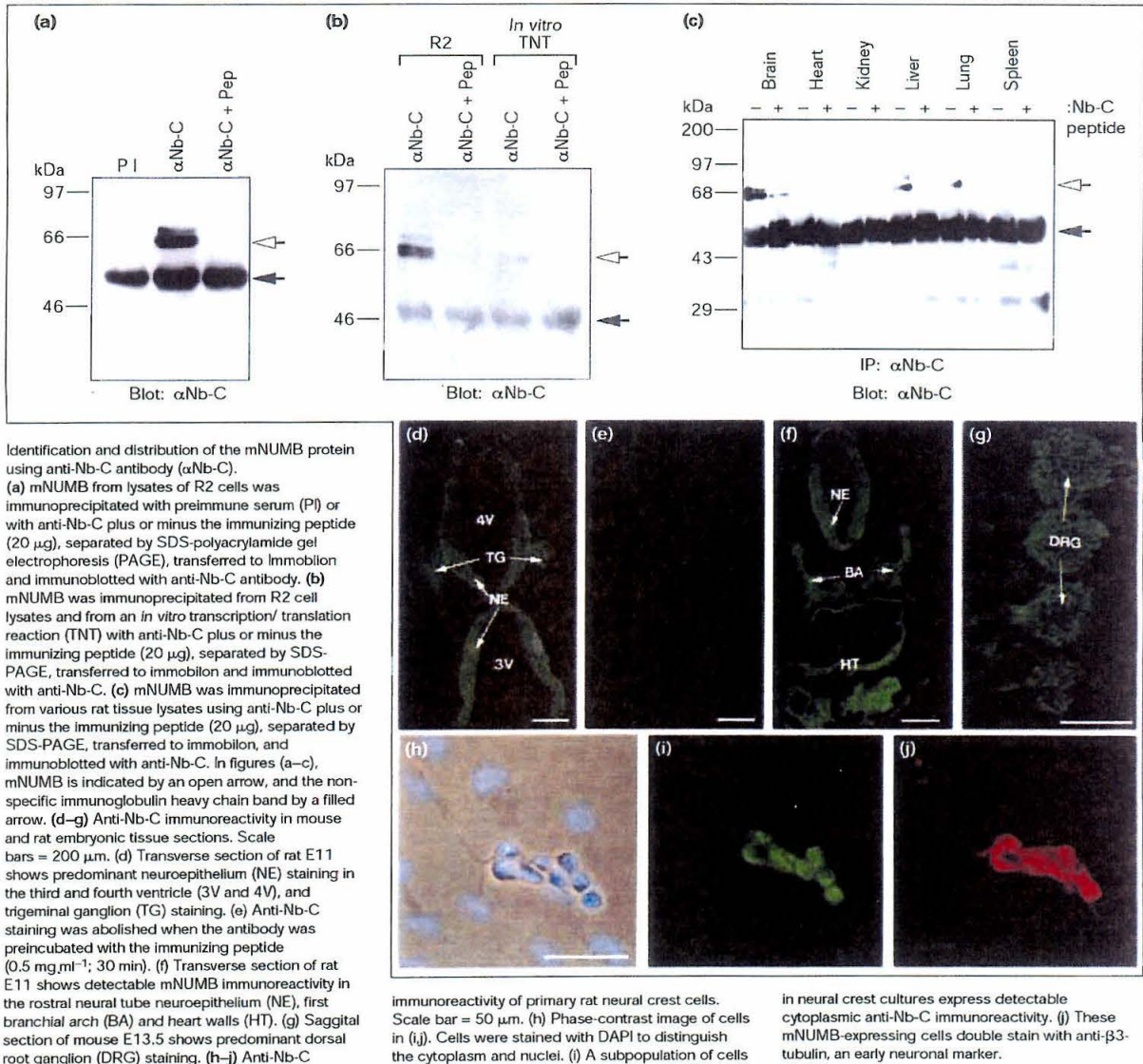
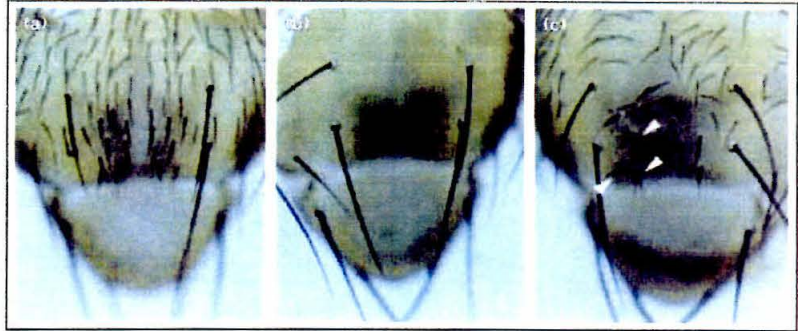


Figure 4

Misexpression of mNUMB during SOP development in the *Drosophila* notum causes cell-fate transformations. (a) Wild-type notum. (b) P[hs-mNumb] notum heat-shocked 14–18 h after puparium formation. Note the absence of microchaetes. (c) P[hs-mNumb] notum heat-shocked 18–22 h after puparium formation. Note the twinning of microchaetes (arrowheads).



establish whether the potential mNUMB PTB domain, located between amino acids 27 and 174, could indeed bind tyrosine-phosphorylated proteins. Amino acids 1–183 were expressed as a glutathione S-transferase (GST) fusion protein in bacteria, purified and immobilized using glutathione sepharose. The immobilized fusion protein was incubated with cell lysates in order to assess its capacity to associate with tyrosine-phosphorylated proteins. Figure 6a shows an anti-phosphotyrosine blot of proteins which bound to the GST–mNUMB-PTB protein or to GST–SHC-PTB in either a *v-src*-transformed cell line

(S7a) or its parental line R2. The GST–mNUMB-PTB protein associated with a set of tyrosine-phosphorylated proteins that were similar in molecular weight to those that associated with the SHC PTB domain. GST alone (Fig. 6a) or a GST-fusion protein containing mNUMB amino acids 184–603 (data not shown) did not associate with these proteins. These data demonstrate that amino acids 1–183 of mNUMB function as phosphotyrosine-binding domain. Both the mNUMB PTB domain and the SHC PTB domain associated with two proteins of 90 kDa and 97 kDa in A431 cells stimulated with epidermal

Figure 5

Misexpression of mNUMB during SOP development in the *Drosophila* wing margin causes cell-fate transformations. (a,b) Wild-type wing. (c,d) Expression of mNUMB at the dorso-ventral margin of P[UAS-mNumb] transgenic larval wing imaginal disks results in loss of the marginal hairs. (e,f) Heat-shock-induced expression of mNUMB in P[hs-mnumb] transgenic flies throughout the developing wing 14–18 h after puparium formation results in twinning of the marginal hairs.

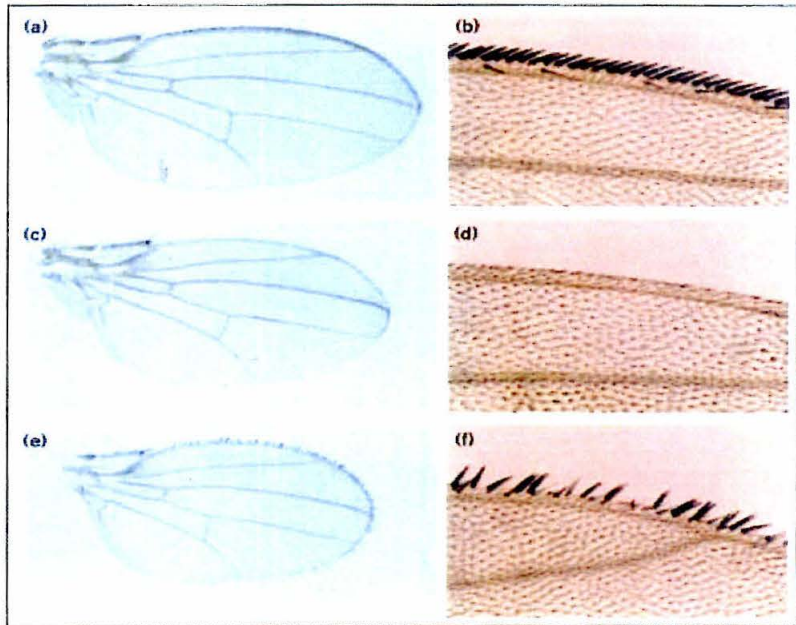
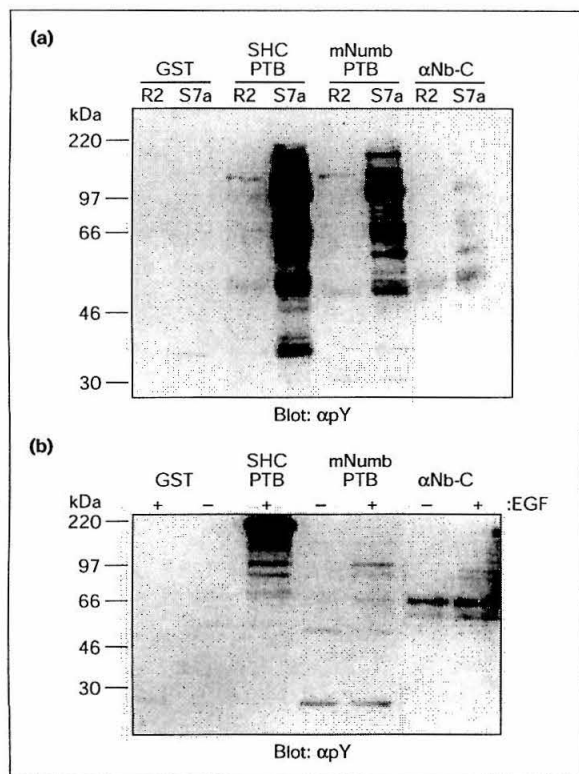


Figure 6



Association of phosphorylated proteins with the mNUMB PTB domain. Purified, immobilized GST, GST-SHC(1-209)PTB or GST-mNUMB(1-187)PTB fusion proteins were incubated with protein lysates from (a) R2 or S7a (*v-src*) cells, or (b) unstimulated (-) or EGF-stimulated (+) A431 cells. mNUMB was also immunoprecipitated from cell lysates with anti-Nb-C antibody. Protein complexes were separated by SDS-PAGE, transferred to Immobilon and immunoblotted with anti-phosphotyrosine antibody (α pY).

growth factor (EGF) (Fig. 6b). Unlike the PTB domain of SHC, however, the mNUMB PTB domain did not associate with the autophosphorylated EGF receptor (Fig. 6b). Therefore, the mNUMB PTB and the SHC PTB domains may share some cytoplasmic targets, but the mNUMB PTB does not recognize similar receptor autophosphorylation sites. *In vivo*, [32 P]orthophosphate labeling of R2 cells has shown that mNUMB is a phosphoprotein (J.M., unpublished data). However, immunoprecipitated mNUMB was not detected by western blotting with anti-phosphotyrosine antibodies (Fig. 6a,b), suggesting that mNUMB may be a substrate for serine/threonine kinases.

mNUMB associates with SH3 domains *in vitro*

The carboxy-terminal domain of mammalian mNUMB contains several proline-rich regions with sequences that

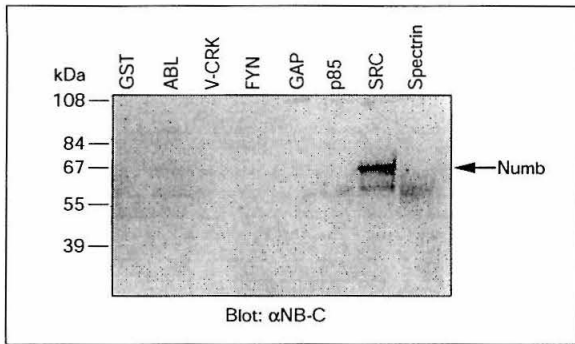
match the minimal consensus motif for potential SH3 binding (PXXP) (Fig. 1a). To test whether mNUMB associates with SH3 domains *in vitro*, a series of GST-SH3 domain fusion proteins was incubated with protein lysates from R2 fibroblasts. The resulting protein complexes were separated by SDS-polyacrylamide gel electrophoresis (PAGE) and immunoblotted with anti-Nb-C antiserum (Fig. 7). Of the different SH3 domains tested, only the SRC SH3 domain seemed to interact with mNUMB *in vitro*. With longer exposures, weaker interactions with ABL and FYN SH3 domains could be detected, suggesting that, of those tested, mNUMB associated preferentially with SH3 domains of Src family kinases. Consistent with this observation, we have found that tyrosine kinase activity is present in protein complexes precipitated with GST-mNUMB(183-603), which contains these proline-rich sequences (S.J. and R.S., unpublished data). The tyrosine kinase present in these *in vivo* protein complexes has not been identified, but is not SRC itself as immunoblotting with anti-SRC antibodies was negative.

mNUMB overexpression influences cell-fate decisions in mammalian neural crest cell lines

If the biological functions of mNUMB are similar to that of its *Drosophila* counterpart, as suggested by the phenotype caused by misexpression in *Drosophila*, then one might expect that overexpression of mNUMB would lead to an increase in the number of neurons formed from mammalian cells with neurogenic potential. Furthermore, suppression of mNUMB function should lead to a decrease in neuron formation. In order to test this hypothesis, mNUMB was overexpressed in the mouse embryonic carcinoma line P19 and in the mouse neural crest stem cell MONC-1.

When pooled stable transformants of P19 cells overexpressing mNUMB were induced to differentiate (using retinoic acid) and stained for neurofilaments on day 6, 31.5 \pm 3.6 % of the total cells stained for the neuronal marker ($n = 3$ independent experiments; Table 1). This represents a greater than 50 % increase over the proportion of control P19 cells that stained positively for neurofilament (Table 1). In an attempt to suppress mNUMB function, a truncated form of mNUMB containing only the PTB domain was used. This construct could potentially act as a dominant negative by uncoupling the PTB domain target from the tyrosine kinase or other downstream targets associated with the proline-rich carboxy-terminal region. P19 cells expressing the mNUMB-PTB protein showed a 23 % reduction in the percentage of neurofilament positive cells over control, a decrease from 20.2 \pm 1.5 % to 15.7 \pm 2.5 %. This was a significant decrease, as more than 15 000 cells were counted per experiment, and similar results were obtained in all three independent experiments.

Drosophila NUMB is necessary for two binary choices in the development of neurons from the SOP: first, it confers

Figure 7


Binding of mNUMB to SH3 domains *in vitro*. Purified, immobilized GST or GST-SH3 (ABL, v-CRK, FYN, GAP, p85, SRC or Spectrin) were incubated with protein lysates of R2 cells. Protein complexes were separated by SDS-PAGE, transferred to Immobilon and immunoblotted with anti-Nb-C antibody.

the IIb fate on one of the daughter cells of the SOP; and second, it specifies hair cell fate in one of the progeny of the IIa cell. To investigate whether mNUMB was involved in early lineage restriction during mammalian nervous system cell-fate determination, the gene was overexpressed in MONC-1 cells. These neural crest stem cells have the potential to form smooth muscle, neurons and glia in culture [28]. Retroviruses designed to express full-length p66 mNUMB, the mNUMB PTB domain alone or the bleomycin resistance gene alone were used to infect MONC-1 cells, which were then plated at clonal density and induced to differentiate by the addition of serum and forskolin. Of the clones containing the bleomycin gene, 79 % contained at least one neuron after 48 hours (50 of 63 clones; Table 2 and Fig. 8). Strikingly,

Table 2
Clonal analysis of differentiated MONC-1 cells.

	Number of clones examined	Neurons only	Neurons/ smooth muscle	Neurons/smooth muscle/glia	Smooth muscle/glia	Smooth muscle only
Experiment 1						
MONC-1 Bleo	28	0 % (0)	43 % (12)	36 % (10)	14 % (4)	7 % (2)
MONC-1 NUMB	43	30 % (13)	49 % (21)	21 % (9)	0 % (0)	0 % (0)
MONC-1 PTB	22	0 % (0)	10 % (2)	0 % (0)	23 % (5)	68 % (15)
Experiment 2						
MONC-1 Bleo	35	0 % (0)	43 % (15)	37 % (13)	14 % (5)	5 % (2)
MONC-1 NUMB	38	36 % (14)	21 % (8)	34 % (13)	8 % (3)	0 % (0)
MONC-1 PTB	32	0 % (0)	6 % (2)	15 % (5)	28 % (9)	50 % (16)

Clonal analysis of MONC-1 cells overexpressing full-length mNUMB, mNUMB PTB or the bleomycin resistance gene (Bleo). Clones were stained for neurofilament and smooth muscle actin and scored accordingly. Staining of only one cell per clone was sufficient to

Table 1
Neuronal differentiation of cells overexpressing mNUMB.

Cell line	% Neurofilament-staining cells		
	Experiment 1	Experiment 2	Experiment 3
P19-Bleo	20.9	18.4	21.2
P19-NUMB	32.6	34.4	27.5
p19-PTB	16.9	12.8	17.4

Presented are the percentages of neurofilament-positive p19 cells after differentiation, induced by retinoic acid, at day 6. Each experiment originates from pooled stable transformants from independent retroviral infections of p19 cells. Note that, in each experiment, stripes of cells were counted from triplicate plates – in excess of 15 000 cells were counted in each experiment.

96 % of the clones (78/81) overexpressing mNUMB had at least one neuron, and 33 % (27/81) of the clones contained only neurons (Fig. 8 and Table 2). In contrast, in clones expressing the mNUMB PTB domain, only 22 % (12/54) produced at least one neuron after 48 hours and no clones of only neurons were observed. Remarkably, of the 42 remaining clones, 31 contained only smooth muscle and the others were mixed clones of smooth muscle and cells that stained with GFAP (glial fibrillary acidic protein). To establish that this phenomenon was not a result of an effect on neuronal survival in the clones expressing the mNUMB PTB domain, 6 hour serial observations of these differentiating MONC-1 cells were undertaken. Cohorts of 30 identified clones were followed for 48 hours. It was observed that the neuronal cells (four cells in three clones) survived the 48 hours of the experiment, indicating that mNUMB does not alter neuronal cell survival but may function to bias the determination of neurogenic precursors into a neuronal phenotype.

categorize the clone. The total number of clones in two independent experiments stemming from independent infections is presented in column 1. The other columns show the percentage of clones in each category, and the total number of clones is in parentheses.

Figure 8



Overexpression of mNUMB leads to an increase in neurogenic capacity. Presented are immunomicrographs of MONC-1 cells expressing (a) full-length mNUMB (NUMB), (b) a bleomycin resistance gene (BLEO) or (c) the PTB domain of mNUMB (PTB). Cultures were first stained for neurofilament

(NF; red) and smooth muscle actin (SMA; green). Note only NF-positive cells in mNUMB-overexpressing clone and SMA in PTB-containing clone. Bleo controls stained for both NF and SMA.

Discussion

In a search for novel PTB-containing molecules, we have cloned a mammalian homologue of *Drosophila numb* by screening a neural crest cDNA expression library with a human EST. The cDNA encodes a 66 kDa protein which is closely related to the *Drosophila* protein. The mammalian and *Drosophila* proteins share a high degree of homology in the amino-terminal 200 amino acids, and we have shown that this region contains a functional PTB domain. The carboxy-terminal region of mNUMB contains several potential SH3 binding sites. We propose, therefore, that NUMB is a component of a tyrosine-kinase-mediated signal transduction pathway. We have established that this mammalian gene (*mNumb*) is the functional homologue of *Drosophila numb*, and have demonstrated that mNUMB functions as a neuronal cell-fate determinant. On the basis of the wide tissue distribution of mNUMB, we suggest it may play a role in cell-fate decisions outside of the nervous system.

mNUMB and dNUMB fulfil analogous roles in neuronal cell-fate choice

The biological role of mNUMB in mammals parallels that exerted by dNUMB during nervous system development. In *Drosophila*, dNUMB has been shown to be required for cell-fate determination at two successive divisions during sensory nervous system development. Remarkably, mNUMB, expressed under either heat-shock promoter or GAL4-UAS control, directed identical cell-fate transformations to those produced by overexpression of dNUMB. We conclude that mNUMB is a functional homologue of dNUMB.

By analogy with the role NUMB plays in biasing the cell-fate determination of IIa and IIb daughter cells in *Drosophila*, the overexpression of mNUMB in multipotential MONC-1 cells results in a strong biasing of the fate

choices of these cells towards neurons. Reciprocally, suppression of mNUMB function biases MONC-1 cells against neuronal lineages. This functional conservation has been seen in other signal-transducing pathways involved in *Drosophila* and mammalian neural development. For example, NOTCH function in neuronal cell-fate decisions is conserved between *Drosophila* and mouse [29,30].

In MONC-1 cells, suppression of mNUMB function leads to a dramatic increase in clones of only smooth muscle. This should not be taken as evidence, however, that neural crest development involves a binary choice between neurogenic potential and myogenic potential. We suggest that mNUMB strongly biases neuronal formation, and that suppression of mNUMB function forces cells with neurogenic potential away from neuronal lineages. In our present culture system, MONC-1 cells give rise to smooth muscle; hence, a bias away from neuronal formation leads to smooth muscle determination. MONC-1 cells expressing the PTB domain or overexpressing full-length mNUMB have never been observed to differentiate in standard medium. Differentiation is only observed when the instructive or inducing factors are supplied through addition of serum. Thus, the bias toward or away from a given lineage is more likely to be the result of a change in the balance of competing signal transduction pathways resulting from the overexpression of mNUMB or the suppression of mNUMB function.

mNUMB is an evolutionarily conserved signaling adapter

In order to understand the molecular mechanism by which mNUMB exerts its effects, it is necessary to analyze the signal transduction pathway in which mNUMB participates. The structure of mNUMB suggests that it is a member of a family of adapter molecules which includes SHC, GRB-2 and NCK. The evolutionarily conserved biological role of these molecules is shown by their functional conservation in invertebrates and

mammals, exemplified by our demonstration that mNUMB and dNUMB can direct identical cell-fate choices when misexpressed in *Drosophila*. The sequence similarity between the *Drosophila* and mammalian NUMB proteins is most striking in the PTB domain (70 % identity), suggesting that this domain plays a critical role in the biological activity of the protein. We have shown that the mNUMB PTB domain binds to tyrosine-phosphorylated proteins *in vitro*, suggesting that both *Drosophila* and mammalian NUMB are involved in tyrosine-kinase signal transduction. It is interesting to note that another PTB-containing adapter molecule, SHC, and its *Drosophila* homologue, dSHC, have been shown to bind activated growth factor receptors through their PTB domains and to recognize a similar binding motif. We expect that the targets of the *Drosophila* and mammalian NUMB PTB domain will also be evolutionarily conserved. This is suggested by the ability of mNUMB to signal when misexpressed in *Drosophila*, which may result from conservation of a specific PTB-binding site on an upstream or downstream target molecule. A yeast two-hybrid screen for sequences encoding proteins that interact with mNUMB has identified *seven in absentia (sina)* [31] from a *Drosophila* library and a *sina*-like cDNA from a rat brain library, supporting this hypothesis (R.S., S.J., J.V. and J.M., unpublished data).

The binding specificity of the mNUMB PTB domain remains to be determined. On the basis of our observation that mNUMB PTB domain does not interact with the activated EGF receptor, it is likely that it recognizes and binds with high affinity a sequence motif different from the SHC PTB domain. The core sequence recognized by SHC and IRS-1 PTB domains is the motif NPXPY, which is predicted to form a tight β -turn structure [17,32,33]. Studies comparing the binding specificities of the SHC and IRS-1 PTB domains have revealed that amino acids outside of this motif, in particular the -5 position relative to the phosphotyrosine, appear to be important for binding specificity and affinity [17,15]. It is also possible that the mNUMB PTB domain could have targets which are not phosphorylated on tyrosine, as both SHC and the PTB domain of FE65 have been reported to interact with specific target molecules in a tyrosine-independent manner [34,35].

Outside of the PTB domain, the amino-acid sequence of *Drosophila* and mammalian NUMB proteins is much less conserved. We have identified several potential SH3 binding sites in this region of mNUMB, and have shown that SH3 domains bind to mNUMB *in vitro*. The dNUMB protein also has several minimal SH3-binding motifs (PXXP), and therefore this region may also be functionally conserved. In this respect, the overall structure of NUMB is similar to that of SHC: it possesses an amino-terminal PTB domain followed by a proline-rich region which contains potential SH3 binding sites [12,36].

The NUMB signaling pathway

It will be necessary to identify proteins that interact with mNUMB in order to define the signal transduction pathway regulating cell-fate decisions. The PTB domain may couple NUMB to a receptor tyrosine kinase, or to another type of cell-surface receptor responsible for initiating the instructive signal. That interaction could also be responsible for directing the asymmetric membrane localization of NUMB which has been reported in *Drosophila* [21,22,37]. To date, we have been unable to observe asymmetric localization of mNUMB by immunohistochemical staining of either tissue culture cells or rat embryo sections, even in circumstances where dividing cells can be visualized. This result may suggest that mammalian and *Drosophila* NUMB proteins are mechanistically distinct in the way in which they localize within the cell. Alternatively, given the functional conservation between dNUMB and mNUMB, our inability to observe this phenomenon could be a result of the recognition of multiple isoforms of mNUMB by our anti-Nb-C antibody. The generation of isoform-specific reagents should aid further studies to establish isoform-specific expression patterns and subcellular distributions.

Recent work of Shah *et al.* [38] demonstrates that, in primary crest stem cell cultures, bone morphogenic protein-2 (BMP-2) forces the majority of stem cells into a neuronal phenotype whereas TGF β directs cells to a smooth muscle fate. BMP-2 receptors signal *via* intrinsic serine and threonine kinase activity [39,40]. In preliminary experiments, we have found that a protein with serine/threonine kinase activity is associated with the mNUMB PTB domain (R.S., unpublished data). We speculate that mNUMB could act in the BMP-2 pathway or a similar parallel pathway. Although we have chosen to examine the role of mNUMB in neuronal determination, the expression pattern of mNUMB suggests that it may play a role in cell-fate decisions outside of the nervous system.

Materials and methods

cDNA cloning

A scan of EST databases identified an 850 base-pair EST from a colon carcinoma cell line. This fragment was random primed and used to screen a rat neural crest library made from NCM-1 cells which have been described previously [41]. Nine positive clones were purified and two which contained 3.5 kb inserts were sequenced. Both clones contained a complete open reading frame of approximately 2.5 kb with high sequence similarity to *Drosophila numb*.

Northern-blot analysis

An 850 base-pair human EST cDNA corresponding to nucleotides 205–1077 of the mNUMB-encoding cDNA was radiolabelled by random hexamer priming and used to probe a series of northern blots containing 2 μ g of poly(A)⁺ RNA isolated from a variety of rat tissues (Clontech). Blots were hybridized overnight at 42 °C in 50 % formamide, 4 \times SSPE, 1 % SDS, 0.5 % skim milk powder, 10 % dextran sulphate and 10 mg ml⁻¹ salmon sperm DNA. Blots were washed twice for 10 min at room temperature in 2 \times SSC, 0.1 % SDS, twice at 65 °C in 0.1 \times SSC, 0.1 % SDS, and then exposed to film. The blots were also probed with radiolabelled β -actin cDNA (Clontech) as an indicator of RNA loading.

Cell culture

Rat fibroblasts (R2), R2 transformed by wild-type *v-src* (S7a) [42], and human A431 cells were cultured in Dulbecco's modified Eagle's Medium (DMEM) containing 10% fetal bovine serum (FBS) and 1% glutamine at 37 °C unless otherwise indicated. P19 cells were cultured according to the methods of Rudnicki and McBurney [43]. In order to differentiate the P19 cells, cells were seeded at 100 000 cells per non-tissue culture Petri plate and allowed to aggregate with 1 μ M retinoic acid for 4 days. The cells were collected, trypsinized and plated back onto 60 mm Nunc plates in the absence of retinoic acid. Cultures were fixed two days later and stained for neural filament, or 6 days later and stained with GFAP. MONC-1 cells were cultured according to the methods of Sommers [28]. For analysis, transformants expressing NUMB or the NUMB PTB domain were plated at clonal density and allowed to reach sizes of 2–4 cells per clone. Differentiation was induced by the addition of 10% FBS and 5 μ M forskolin to the standard media. Neural (NF staining) and smooth muscle differentiation (smooth muscle actin staining) occurred within 36 h and glial differentiation (GFAP staining) within 1–3 days. Primary cultures of rat neural crest cells were prepared from day-11.5 rat embryos and cultured essentially as described [28].

Production and analysis of transgenic *Drosophila* strains

The complete rat open reading frame encoding rat NUMB from the *mNumb* cDNA (nucleotides 196–2007) was inserted directionally into *EcoRI*–*SalI*-digested pCaSpeR-hs [44] and *EcoRI*–*XhoI*-digested pUAST [45]. DNA-mediated transformation was according to standard methods [46]. Two transgenic lines were analyzed: P[hs-mNumb] and P[UAS-mNumb]. For analysis of the effects of ubiquitous expression of mNUMB, staged P[hs-mNumb] prepupae were collected over 4 h intervals and aged for an additional 12–20 h at 25 °C. Heat shock was according to Rhyu *et al.* [21]. For analysis of localized expression of mNUMB, P[UAS-mNumb] flies were crossed to the GAL4 enhancer trap line C96 [27]. Wings and notums were dissected from adult flies, mounted in GMM [47], analyzed and photographed using a Zeiss Axioplan microscope or a Leica M10 stereo dissecting microscope. Images were processed with Adobe Photoshop V. 3.0 software.

Antibodies

The polyclonal antibody (anti-Nb-C) was raised in rabbits to the peptide sequence TNPFSSDAQKAFIEEL, which corresponds to 14 amino-acid residues at the carboxyl terminus of mNUMB; an amino cysteine was added to facilitate conjugation to keyhole limpet haemocyanin. Anti-Nb-C was used at a dilution of 1:200 in immunoblots and 1:100 for immunoprecipitations. Anti-phosphotyrosine antibody RC20H (Transduction Laboratories) was used at a dilution of 1:2500 in immunoblots. Anti- β -3 tubulin monoclonal antibody (Accurate Chemical and Scientific) was used at 1:500 for immunohistochemistry.

Protein lysates, immunoprecipitation and western blotting

Cell monolayers were lysed in 150 mM NaCl, 50 mM Tris-HCl pH 7.5, 1% Triton X-100, 1 mM Na₃VO₄, with Pefabloc (Boehringer Mannheim), aprotinin and leupeptin at 10 μ g ml⁻¹. Rat tissue lysates were made by homogenizing the tissue with a polytron, followed by clarification by centrifugation at 12 000 \times g for 15 min at 4 °C. A protein assay was performed using a BCA kit (Pierce) according to manufacturers instructions. TNT-coupled Reticulocyte Lysate Systems from Promega was used to translate the *mNumb* cDNA cloned into pBSK *in vitro*, as described in the protocol. For immunoprecipitation, clarified lysates from a confluent 10 cm tissue culture plate, or tissue lysate containing 500 μ g of total protein, were incubated with protein A-Sepharose and 10 μ l of the polyclonal peptide sera at 4 °C for 60 min, and washed three times with lysis buffer. For western blotting, samples were separated by SDS-PAGE, transferred to Immobilon-P (Millipore) with a semidry transfer apparatus, and immunoblotted as described previously. Primary antibodies were used at a 1:200 dilution in Tris-buffered saline (TBS-T; 20 mM Tris-HCl, pH 7.5, 150 mM NaCl and 0.05% Tween 20) containing 5% Carnation skim milk powder, or 0.01 M Tris, pH 7.5, 0.1 M NaCl, 0.1% Tween 20 containing 1% bovine serum albumin (RC20 antibodies) and developed using ECL (Amersham).

GST-fusion proteins

Bacteria expressing GST-fusion proteins were induced with IPTG and lysed by sonication in lysis buffer. GST-fusion proteins were purified using glutathione sepharose (Pharmacia). Fusion proteins immobilized on glutathione sepharose were quantitated, and 1 μ g of fusion protein was incubated with cell lysates (prepared as described above) at 4 °C for 90 min. The protein complexes were then washed in lysis buffer three times, the samples were then separated on SDS-PAGE, transferred to Immobilon-P (Millipore) and immunoblotted.

Generation of virus and retroviral infection of cell lines

BOSC23 cells [48] were maintained in GPT selection medium until they were split and plated at a density of 2 000 000 cells per 60 mm dish in DMEM plus 10% FBS. Calcium chloride transfection was used to introduce pBABE [49] constructs into BOSC23 packing line. 10 μ g of precipitate per plate was added to the cells for 10 h in the presence of 25 μ M chloroquin. The cells were then washed with medium, 2 ml of either P19 medium or standard medium were added, and virus collected for the next 48 h. Stable P19 and MONC-1 lines overexpressing the full-length mNUMB or the PTB domain of mNUMB were generated by retroviral infection. Briefly, cells were incubated for a period of 4 h with a viral supernatant containing 4 mg ml⁻¹ polybrene obtained from the transient transfection of BOSC23 cells with either pBABE-NUMB or pBABE-PTB retroviral constructs. The cells were allowed to recover for 12 h prior to the addition of 100 mg ml⁻¹ (P19) or 25 mg ml⁻¹ (MONC-1) bleomycin for 5 days. The cells were then split onto fresh 35 mm dishes and expanded in the presence of 25 mg ml⁻¹ bleomycin or 10 mg ml⁻¹ MONC-1. Cells were either stained with a polyclonal anti-HA antibody or analyzed by PCR using HA and *mNumb*-specific primers to confirm expression of the transgene before use.

Immunohistochemistry

Primary neural crest cell cultures and 14 μ m sections of either mouse E13.5 or rat E11 embryos were fixed with cold acetone/methanol and stained with affinity-purified anti-Nb-C (5 μ g ml⁻¹) overnight at 4 °C. Anti-Nb-C staining was detected with a donkey-anti-rabbit-biotin label (1:100, Jackson) and streptavidin conjugated to CY2 (1:50, Amersham). Neuronal cells were identified with a monoclonal anti- β -3-tubulin and detected with goat-anti-mouse conjugated to Texas Red (1:100, Jackson). Cells were counter stained with DAPI (1 μ g ml⁻¹) to identify nuclei. Photographs were taken on inverted fluorescence microscope.

Cells used in the mNUMB overexpression experiments were fixed in 4% formaldehyde in HBSS. Cells were blocked using 0.1% NP-40 and 1% goat serum for 20 min at room temperature. Primary antibody was incubated in blocking solution overnight at 4 °C. The primary antibodies used were mouse monoclonal anti-smooth muscle actin (1:500 Sigma), mouse monoclonal anti-neurofilament (1:400 Sigma), mouse monoclonal anti-GFAP (1:25 Sigma), rabbit polyclonal anti-neurofilament, (1:1000 Chemicon) and rabbit polyclonal anti-GFAP (1:200 Chemicon). Double labeling of P19 cells was performed using the mouse monoclonal GFAP and rabbit anti-neurofilament. For categorizing MONC-1 clones, the cells were stained using Rabbit NF and mouse SMA and GFAP. Although the two monoclonals were both IgGs, the striking differences in morphology were used to discriminate the two cell types. The secondary antibodies conjugated to either fluorophore or phycoerythrin were used at a dilution of 1:250 (Biosource International). Prior to photography, cells were counter-stained with 1 μ g ml⁻¹ DAPI to help in visualization of the nuclei. Images were processed with Adobe Photoshop V. 3.0 software.

Acknowledgements

The authors wish to thank Martin Bissessar and Margaret Henry for technical assistance, Andrew Hessel for time and expertise in doing database searches and sequence alignments, Mike Bass for generating the PTB domain profile, David Anderson for the MONC-1 cell line, Dave Grosshans for DNA sequencing, Bill Fisher and Angelo Karaiskakis for carrying out the *Drosophila* P-element mediated transformation, and Gabrielle Boulianne for kindly providing us with GAL4 enhancer trap line C96. This work was funded in part by a grant from the Medical Research Council of Canada (to J.M.). R. Schmandt is supported by a fellowship from the MRC.

References

- Sonyang Z, Shoelson S, Chaudhuri M, Gish G, Pawson T, Haser WG, et al.: SH2 domains recognize specific phosphopeptide sequences. *Cell* 1993, 72:767–778.
- Pawson T: Protein modules and signalling networks. *Nature* 1995, 373:573–579.
- Pawson T, Gish GD: SH2 and SH3 domains: from structure to function. *Cell* 1992, 71:359–362.
- Chen H, Sudol M: The WW domain of Yes associated protein binds a proline-rich ligand that differs from the consensus established for Src. *Proc Natl Acad Sci USA* 1995, 92:7819–7823.
- Harlan JE, Jajduk PJ, Yoon HS, Fesik SW: Pleckstrin homology domains bind to phosphatidylinositol-4,5-bisphosphate. *Nature* 1994, 371:168–170.
- Pitcher JA, Touhara K, Payne ES, Lefkowitz RJ: Pleckstrin homology domain-mediated membrane association and activation of the beta-adrenergic-receptor kinase requires coordinate interaction with γ subunits and lipid. *J Biol Chem* 1995, 270:11707–11710.
- Ferguson KM, Lemmon MA, Schlessinger J, Sigler PB: Structure of the high-affinity complex of inositol triphosphate with a phospholipase-C pleckstrin homology domain. *Cell* 1995, 83:1037–1046.
- Lai VK-M, Olivier JP, Gish GD, Henkemeyer M, McGlade J, Pawson T: A *Drosophila shc* gene product is implicated in signaling by the DER receptor tyrosine kinase. *Mol Cell Biol* 1995, 9:4810–4819.
- Olivier JP, Raabe T, Henkemeyer M, Dickson B, Mamamalu G, Margolis J, et al.: A *Drosophila* SH2–SH3 adaptor protein implicated in coupling the sevenless tyrosine kinase to an activator of Ras guanine nucleotide exchange, SOS. *Cell* 1993, 73:179–191.
- Simon MA, Dodson GS, Rubin GM: An SH3–SH2–SH3 protein is required for p21Ras1 activation and binds to the sevenless and Sos proteins *in vitro*. *Cell* 1993, 73:169–177.
- Garrity PA, Rao Y, Salecker I, McGlade J, Pawson T, Zipursky SL: *Drosophila* photoreceptor axon guidance and targeting requires the deadlocks SH2/SH3 adaptor protein. *Cell* 1996, 85:639–650.
- Pellicci G, Lanfranconi L, Grignani F, McGlade J, Cavallo F, Fornì G, et al.: A novel transforming protein (SHC) with an SH2 domain is implicated in mitogenic signal transduction. *Cell* 1992, 70:93–104.
- Kavanaugh WM, Williams LT: An alternative to SH2 domains for SH2 binding. *Science* 1994, 266:1862–1865.
- Blaikie P, Immanuel D, Wu J, Li N, Yajnik V, Margolis B: A region in Shc distinct from the SH2 domain can bind tyrosine phosphorylated growth factor receptors. *J Biol Chem* 1994, 269:32031–32034.
- Wolf G, Trub T, Ottinger E, Groninga I, Lynch A, White MF: PTB domains of IRS-1 and SHC have distinct but overlapping binding specificities. *J Biol Chem* 1995, 270:27407–27410.
- Kavanaugh WM, Turck CW, Williams LT: PTB domain binding to signaling proteins through a sequence motif phosphotyrosine. *Science* 1995, 268:1177–1179.
- van der Geer P, Wiley S, Lai VK-M, Olivier JP, Gish G, Stephens D, et al.: A conserved amino terminal SHC domain binds to phosphotyrosine motifs in activated receptors and phosphopeptides. *Curr Biol* 1995, 5:404–412.
- Bork P, Margolis B: A phosphotyrosine interaction domain. *Cell* 1995, 80:693–694.
- O'Bryan JP, Zhou SY, Cantley L, Der CJ, Pawson T: A mammalian adapter protein with conserved SRC homology-2 and phosphotyrosine-binding domains is related to SHC and is specifically expressed in the brain. *Proc Natl Acad Sci USA* 1996, 93:2729–2734.
- Uemura T, Shepherd S, Ackerman L, Jan LY, Jan YN: *numb*, a gene required in determination of cell fate during sensory organ formation in *Drosophila* embryos. *Cell* 1989, 58:349–360.
- Rhyu MS, Jan LY, Jan YN: Asymmetric distribution of numb protein during division of the sensory organ precursor cell confers distinct fates to daughter cells. *Cell* 1994, 76:477–491.
- Spana EP, Kocyzyński C, Goodman CS, Doe CQ: Asymmetric localization of numb autonomously determines sibling neuron identity in the *Drosophila* CNS. *Development* 1995, 121:3489–3494.
- Knoblich JA, Jan LY, Jan YN: Localization of numb and prospero reveals a novel mechanism for asymmetric protein segregation during mitosis. *Nature* 1995, 377:624–627.
- Zhou M-M, Ravichandran S, Olejniczak ET, Petros AM, Meadows RP, Sattler M, et al.: Structure and ligand recognition of the phosphotyrosine binding domain of SHC. *Nature* 1995, 378:584–592.
- van der Geer P, Wiley S, Gish G, Lai VK-M, Stephens R, White MF, et al.: Identification of residues that control specific binding of the SHC phosphotyrosine-binding domain to phosphorylation sites. *Proc Natl Acad Sci USA* 1996, 93:963–968.
- Yanik V, Blaikie P, Bork P, Margolis B: Identification of residues within the SHC phosphotyrosine binding/phosphotyrosine interaction domain crucial for phosphopeptide interaction. *J Biol Chem* 1996, 271:1813–1816.
- Gustafson K, Boulianne GL: Distinct expression patterns detected within individual tissues by the GAL4 enhancer trap technique. *Genome* 1996, 39:174–182.
- Sommer L, Shaw N, Rao M, Anderson DJ: The cellular function of MASH1 in autonomic neurogenesis. *Neuron* 1995, 15:1245–1258.
- Fortini ME, Rebay I, Caron LA, Artavanis-Tsakonis S: An activated Notch receptor blocks cell-fate commitment in the developing *Drosophila* eye. *Nature* 1993, 365:555–557.
- Nye JS, Kopan R, Axel R: An activated Notch suppresses neurogenesis and myogenesis but not gliogenesis in mammalian cells. *Development* 1994, 120:2421–2430.
- Carthew RW, Rubin GM: *seven in absentia*, a gene required for specification of R7 cell fate in the *Drosophila* eye. *Cell* 1990, 63:561–577.
- Sonyang Z, Margolis B, Chaudhuri M, Shoelson SE, Cantley LC: The phosphotyrosine interaction domain of SHC recognizes tyrosine phosphorylated NPXY motif. *J Biol Chem* 1995, 270:14683–14686.
- Trub T, Choi WE, Ottinger E, Chen YJ, Weiss M, Shoelson SE: Specificity of the PTB domain of SHC for beta-turn-forming pentapeptide motifs amino terminal to the phosphotyrosine. *J Biol Chem* 1995, 270:18205–18208.
- Fiore F, Zambrano N, Minopoli G, Donini V, Dullio A, Russo T: Regions of the FE65 protein homologous to the phosphotyrosine binding domain of SHC bind the intracellular domain of the Alzheimer's amyloid precursor protein. *J Biol Chem* 1995, 270:30853–30856.
- Charest A, Wagner J, Jacob S, McGlade CJ, Tremblay ML: Phosphotyrosine-independent binding of SHC to the NPHL sequence of MPTP-PEST. *J Biol Chem* 1996, 271:8424–8429.
- Weng Z, Thomas SM, Rickles J, Taylor JA, Brauer AW, Seidel-Duncan C, et al.: Identification of Src, Fyn, and Lyn SH3 binding proteins: implications for functions of SH3 domains. *Mol Cell Biol* 1994, 14:4509–4521.
- Doe CQ, Spana EP: A collection of cortical crescents: asymmetric protein localization in CNS precursor cells. *Neuron* 1995, 15:991–995.
- Shah NM, Groves AK, Anderson DJ: Alternative neural crest cell fates are instructively promoted by TGF β superfamily members. *Cell* 1996, 85:331–343.
- Liu F, Ventura F, Doody J, Massague J: Human type II receptor for bone morphogenic proteins (BMPs): extension of the two-kinase receptor model to the BMPs. *Mol Cell Biol* 1995, 15:3479–3486.
- Attisano I, Wrana J, Cheifetz S, Massague J: Novel activin receptors: distinct genes and alternative splicing generate a repertoire of serine/threonine kinase receptors. *Cell* 1992, 68:97–108.
- Lo L-C, Birren JB, Anderson DJ: V-myc immortalization of early rat 11 neural crest cells yields a clonal cell line which generates both glial and adrenergic cells. *Dev Biol* 1991, 145:139–153.
- Brooks-Wilson AR, Ball E, Pawson T: The myristylation signal of p60^{src} functionally complements the N-terminal fps-specific region of p130^{cas}. *Mol Cell Biol* 1989, 9:2214–2219.
- Rudnicki MA, McBurney MA: Cell culture methods and induction of differentiation of embryonal carcinoma lines. In *Teratocarcinomas and Embryonal Stem Cells, a Practical Approach*. Oxford: IRL Press; 1987:19–50.
- Thummel CS, Pirrotta V: New pCaSpeR P element vectors. *Drosophila Information Newsletter* 1991, 2:19.
- Brand AH, Manoukian AS, Perrimon N: Ectopic expression in *Drosophila*. In *Drosophila melanogaster: Practical Uses in Cell and Molecular Biology, Methods in Cell Biology*. San Diego: Academic Press; 1994, 44:635–654.
- Spradling AC: P element-mediated transformation. In *Drosophila: A Practical Approach*. Edited by Roberts DB. Oxford: IRL Press; 1986:175–197.
- Lawrence PA, Johnston P, Morata G: Methods of marking cells. In *Drosophila: A Practical Approach*. Edited by Roberts DB. Oxford: IRL Press; 1986:229–242.
- Pear WS, Nolan GP, Scott ML, Baltimore D: Production of high titer helper-free retroviruses by transient transfection. *Proc Natl Acad Sci USA* 1993, 90:8392–8396.
- Morgenstern JP, Land H: Advanced mammalian gene transfer: high titre retroviral vectors with multiple drug-selection markers and complementary helper free packing cell line. *Nucleic Acids Res* 1990, 18:3587–3596.

Appendix 2

Fringe boundaries coincide with Notch-dependent patterning centers in mammals and alter Notch-dependent development in *Drosophila*

With permission, from Nature,
Nature Genetics, Vol. 16, pages 283-288, 1997

Fringe boundaries coincide with Notch-dependent patterning centres in mammals and alter Notch-dependent development in *Drosophila*

Brenda Cohen^{1,*}, Arash Bashirullah^{2,3,*}, Lina Dagnino¹, Christine Campbell¹, William W. Fisher², Ching Ching Leow^{1,4}, Elisabeth Whiting¹, David Ryan¹, Dawn Zinyk^{2,4}, Gabrielle Boulianne^{5,6,7}, Chi-chung Hui^{2,4,5}, Brenda Gallie^{1,4,5}, Robert A. Phillips^{1,4,5}, Howard D. Lipshitz^{2,3,4,5} & Sean E. Egan^{1,4,5}

In both vertebrate and invertebrate development, cells are often programmed to adopt fates distinct from their neighbors. Genetic analyses in *Drosophila melanogaster* have highlighted the importance of cell surface and secreted proteins in these cell fate decisions. Homologues of these proteins have been identified and shown to play similar roles in vertebrate development¹⁻⁵. Fringe, a novel signalling protein, has been shown to induce wing margin formation in *Drosophila*⁶. Fringe shares significant sequence homology and predicted secondary structure similarity with bacterial glycosyltransferases⁷. Thus, fringe may control wing development by altering glycosylation of cell surface and/or secreted molecules. Recently, two fringe genes were isolated from *Xenopus laevis*⁸. We report here the cloning and characterization of three murine fringe genes (*lunatic fringe*, *manic fringe* and *radical fringe*). We find in several tissues that fringe expression boundaries coincide with Notch-dependent patterning centres and with Notch-ligand expression boundaries. Ectopic expression of murine *manic fringe* or *radical fringe* in *Drosophila* results in phenotypes that resemble those seen in *Notch* mutants.

To identify mammalian genes related to fringe, we searched the public data bases for sequences with similarity to the *Drosophila* fringe protein. One such human sequence was identified in the expressed sequence tag data base. Degenerate PCR followed by cDNA library screening was used to clone three mouse fringe-related genes: *lunatic fringe*, *manic fringe* and *radical fringe*. Their predicted amino acid sequence reveals that in each case an N-terminal signal sequence is present to target these proteins to the secretory pathway (Fig. 1). The N-termini of the three mouse, two published *Xenopus* and single *Drosophila* fringe proteins differ in both length and sequence^{6,8}. In contrast, the C-terminal 270 amino acids of all fringe proteins are very highly conserved. D-Fringe contains seven cysteine residues that are thought to form disulfide bonds in the native protein⁶. All vertebrate fringe proteins contain six of these cysteines at identical positions, suggesting that they may form an essential scaffold for this protein family. The mammalian fringe proteins, like the *Drosophila* and *Xenopus* fringe proteins⁷, are highly related to glycosyltransferases. The *Drosophila* fringe, *Xenopus lunatic* and *radical fringe* and mouse *lunatic fringe* genes all encode proteins with a putative N-terminal 'pro region' followed by a basic motif⁶. In contrast, the predicted mouse manic and radical fringe proteins contain only a few amino acid residues between the leader sequence and the conserved C-terminal region, indicating that these two proteins may not require regulated proteolytic activation.

Northern blot analysis of day 7 to 17 mouse embryos indicated that the three fringe genes are expressed throughout this period; in addition, they are widely expressed in adult tissues. Expression of fringe gene occurs at developmentally important boundaries in mesodermal, neuroepithelial, epidermal and haematopoietic tissues (Fig. 2 and data not shown). *Lunatic fringe* is highly expressed during somitogenesis in two mesodermal stripes that generate boundaries at both the anterior and posterior margin of the forming somite (Fig. 2a). These two stripes move towards the posterior of the embryo as new somites are generated, suggesting that *lunatic fringe* expression boundaries may be involved in the segmentation of mesoderm into somites. In addition, *lunatic fringe* is expressed in the undifferentiated neuroblast layers of the neural tube, brain and otic vesicle during central nervous system development (Fig. 2a-c). *Lunatic fringe* is also expressed in the myotome, which contains undifferentiated myoblasts (Fig. 2b), and in the intervertebral mesenchyme. Throughout development, *lunatic fringe* is expressed in proliferating cells in the ventricular zones of the nervous system and in uncommitted neuroblasts in the retina. Expression is also observed in the basal cells of the skin and tongue epidermis; in the perichondrium, which contains proliferating chondroblasts; in the fetal heart; in haematopoietic cells in the fetal liver; in S-shaped bodies of the developing kidney; and in a subset of splenic lymphocytes. *Lunatic fringe* is expressed in the thymic cortex but not the thymic medulla. This *lunatic fringe* expression boundary coincides with the boundary between immature and mature thymocytes.

In contrast to *lunatic fringe*, *manic fringe* and *radical fringe* are usually expressed in cells that are undergoing or have completed terminal differentiation. Both of these genes are expressed in the marginal zones of the neural tube and brain throughout development (Fig. 2d for *radical fringe*), and both are expressed from day E11.5 to E13.5 in the dorsal root ganglia. These genes are also expressed in E12.5 fetal liver, and in the suprabasal epithelium of both tongue and skin. Strikingly, these genes are often expressed in cells directly juxtaposed with cells expressing *lunatic fringe*. The *manic fringe* gene is very highly expressed in megakaryocytes present in the adult spleen; these are the precursors of platelets.

In many of the developing tissues described above, the undifferentiated cells express high levels of *lunatic fringe*. *Manic* and *radical fringe* genes, on the other hand, are expressed in differentiated populations. To study this apparently conserved pattern at high resolution, we analysed two tissues in which stem cells and their differentiated progeny are physically separated. Sections through

¹Division of Immunology and Cancer Research, ²Division of Endocrinology, ³Program in Developmental Biology and ⁴Division of Neurology, The Hospital for Sick Children, 555 University Avenue, Toronto, Ontario M5G 1X8, Canada. ⁵Division of Biology, California Institute of Technology, Pasadena, California, USA. ⁶Department of Molecular and Medical Genetics, University of Toronto, Ontario, Canada. ⁷Department of Neurology, The Hospital for Sick Children, Toronto, Ontario, Canada. ⁸Department of Physiology, The University of Toronto, Toronto, Ontario, Canada. *B.C. & A.B. contributed equally to this work. Correspondence to S.E.E. at Division of Immunology and Cancer Research, The Hospital for Sick Children, 555 University Avenue, Toronto, Ontario M5G 1X8, Canada. e-mail: segan@sickkids.on.ca

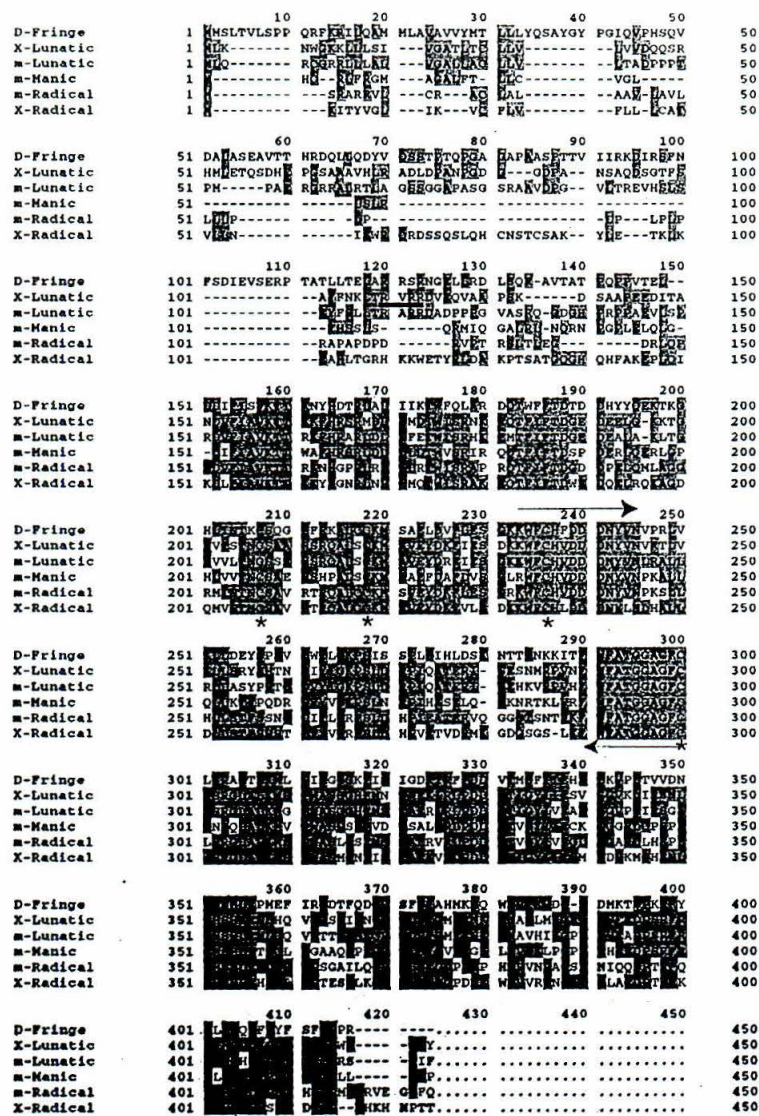


Fig. 1 Comparison of the predicted fringe amino acid sequences. The red bar indicates the predicted cleavage site for *Xenopus* and mouse lunatic fringe proteins. The blue arrows correspond to the amino acid sequences from which degenerate oligonucleotide primers were designed for RT-PCR cloning of the mammalian fringe gene family and red asterisks denote conserved cysteine residues. Identical residues are highlighted in yellow. Starting at residue 152 in the multiple sequence alignment, mouse and *Xenopus* lunatic fringe proteins are 77% identical; mouse and *Xenopus* radical fringe proteins are 59% identical; mouse lunatic, manic and radical fringe proteins are more than 50% identical to each other, and all vertebrate fringes are approximately 30% identical to D-fringe^{6,8}. Manic fringe does not contain a basic cleavage sequence and encodes only 29 amino acids from the start codon to the region where lunatic fringe is predicted to be cleaved. These 29 amino acids code for little more than the leader sequence; thus, manic fringe may be secreted in an active form that does not require proteolytic cleavage. The mouse radical fringe protein also lacks a tetrabasic cleavage site and contains a shorter N-terminus than the *Xenopus* radical fringe. From the start codon to the location of predicted cleavage in lunatic fringe, mouse radical fringe only has 44 amino acids, including the leader sequence. (*Xenopus* radical fringe has 71 amino acids in the corresponding region.) Mouse radical fringe may thus also not require regulated proteolytic activation.

During somitogenesis, Notch1 is required for proper segmentation of presomitic mesoderm into somites but not to form somite-like tissue⁹. This observation suggests that activation of Notch may block differentiation of mesoderm into somite tissue at the boundary between adjacent somites. Analysis of mouse *Delta-like gene 1* (*Dll1*, a Notch-ligand) expression in mesoderm undergoing somitogenesis in E8.5 embryos reveals that *Dll1* is highly expressed in presomitic mesoderm and further induced in the forming somite (Fig. 3a)¹⁰. Despite this extremely high level of *Dll1* expression in the forming somite, Notch1 activation is probably restricted to the inter-somite tissue⁹. *Lunatic fringe* is expressed at this stage in two bands that surround the forming somite (Fig. 3b). A mouse homologue of the *Drosophila* Notch-ligand and *Serrate*, *Jagged1*¹¹ is also weakly expressed in two bands that surround the forming somite (Fig. 3c). The thin domains of mesoderm, which fail to differentiate into somite tissue but form inter-somite tissue under the influence of Notch1, occur at the *Dll1/lunatic fringe* expression boundary on either side of the forming somite. *Dll1* and *Jagged1* are also expressed in complementary domains within the developing neural tube (Fig. 3d, f)^{11,12}. *Lunatic fringe* is expressed in domains within the neural tube which overlap the *Dll1* expression domains (Fig. 3e); therefore, *lunatic fringe* expression boundaries are coincident with *Dll1/Jagged1* expression boundaries in the neural tube. A similar situation is found in the developing retina (data not shown). The two cloned mammalian *Serrate* homologues are also differentially expressed in the epidermis¹³. Basal cells express *Jagged2*, whereas differentiated suprabasal cells express *Jagged1*. The *lunatic* versus *manic/radical fringe* expression boundary in

the neural tube in day 10.5 embryos reveal that *lunatic fringe* is expressed in the ventricular zone, which corresponds to the neuroblast population, but not in the marginal zone, which contains differentiated neurons (Fig. 2e). Adjacent sections probed with *manic* or *radical fringe* probes revealed a striking complementary expression profile for these two genes. As neurons are born, they turn off *lunatic fringe*, leave the ventricular zone and turn on both *manic* and *radical fringe* genes (Fig. 2f, g). Similarly, tongue epithelium is continuously generated through division of basally located stem cells that express *lunatic fringe* (Fig. 2h). As the cells differentiate, they move apically, turn off *lunatic fringe* and turn on both *manic* and *radical fringe* genes (Fig. 2i, j). Consequently, in neural tissue and in the epidermis, there is a boundary between stem cells, which express *lunatic fringe*, and their committed progeny, which express the *manic* and *radical fringe* genes.

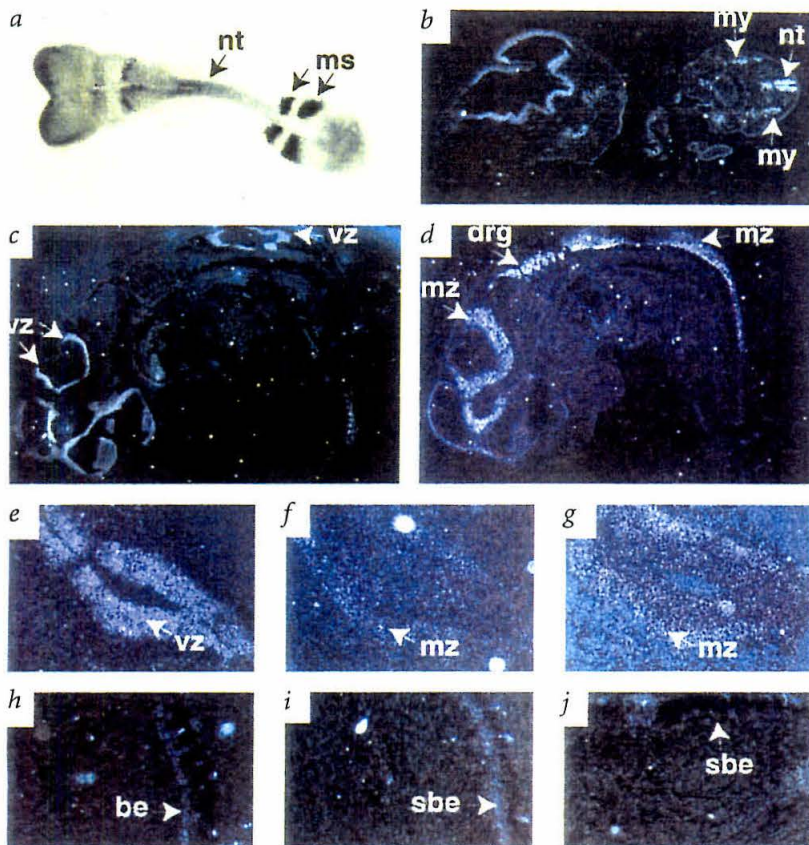


Fig. 2 Expression of mouse *fringe* genes in embryonic and selected adult tissues as assayed by RNA tissue *in situ* hybridization. (a, b, c, e, h) *Lunatic fringe*; (f, i) *manic fringe*; (d, g, j) *radical fringe*. (a) Stage E8.5; (b) E11.5; (c, d) E12.5; (e–g) E10.5; (h–j) adult. (a) shows a whole mount, while all others are dark-field views of tissue sections. (a–d) are views of entire embryos while (e–g) are neural tube and (h–j) are tongue epithelium. ms, mesoderm; my, myotome; nt, neural tube; drg, dorsal root ganglia; vz, ventricular zone; mz, marginal zone; be, basal epithelium; sbe, suprabasal epithelium.

skin (Fig. 2), therefore, corresponds to a *Jagged2–Jagged1* expression boundary. Thus, in mammalian tissues (somites, neural tube, retina and skin), as in *Drosophila*, a *fringe* expression boundary coincides with a Notch-dependent patterning center and with a Notch-ligand expression boundary.

In *Drosophila*, D-*fringe* is expressed in the dorsal but not ventral compartment of the developing wing disc. The D-*fringe* expression boundary produced in this way is essential for formation of the endogenous wing margin, and an ectopic D-*fringe* expression boundary is sufficient to induce an ectopic margin¹⁴. We assayed mammalian *manic* and *radical fringe* functions in transgenic *Drosophila*, since these do not possess N-terminal pro-regions and are probably synthesized in an active form. Spatially regulated expression was accomplished with the two component GAL4-upstream activator sequence (UAS) system¹⁵. Initially, we chose GAL4^{ptc} to drive expression in cells in which the *patched* gene is expressed. In the wing imaginal disc, *patched* is expressed in a stripe of cells on the anterior side of the AP compartment boundary^{14,16}. Ectopic expression of D-*fringe* by means of this driver leads to a loss of wing margin tissue at the AP boundary and an ectopic wing margin on the ventral surface of the wing^{6,14}. In contrast, ectopic expression of either *manic* or *radical fringe* causes the loss of endogenous margin tissue without the generation of an ectopic margin on the ventral surface (Fig. 4b, c).

The *Drosophila* hypomorphic *fringe* allele *frng*⁵² shows a weak wing vein-splitting or 'delta' phenotype but a normal wing margin in heterozygotes⁶. A heterozygous *frng*⁵² mutation enhanced wing defects produced by GAL4^{ptc}, UAS-*manic fringe* and GAL4^{ptc}, UAS-*radical*

fringe. Thus, both *manic fringe* and *radical fringe* interfere with essential functions of endogenous D-*fringe* at the dorsal-ventral (DV) compartment boundary. Crosses combining GAL4^{ptc}, UAS-*manic fringe* and GAL4^{ptc}, UAS-*radical fringe* are lethal, whereas increasing the expression of either of these mammalian *fringe* proteins through increasing GAL4 activity (at 29 °C), or by doubling the dose of either mammalian *fringe*, enhanced the wing phenotypes. *Manic* and *radical fringe*, therefore, may inhibit distinct functions of D-*fringe*, producing synthetic lethality when assayed together in *Drosophila*.

The GAL4^{C96} line expresses GAL4 at the dorso-ventral compartment boundary in the wing disc, which represents the future wing margin¹⁷. GAL4^{C96}-driven *manic fringe* produced a dramatic loss of margin tissue and reduction of wing size (Fig. 4d). In contrast, GAL4^{C96}-driven *radical fringe* had little effect, producing a small loss of margin tissue in only some of the flies (not shown). The GAL4^{C5} enhancer trap line expresses GAL4 in all cells that will give rise to the wing blade¹⁸. GAL4^{C5}-driven *manic fringe* produced a dramatic loss of margin and wing blade tissue (Fig. 4e). In contrast, GAL4^{C5}-driven *radical fringe* produced wings with small vein deltas or vein splitting but no loss of margin (Fig. 4f).

The effects of ectopic *manic fringe* and *radical fringe* expression could also be documented in tissues other than the wing, since GAL4^{ptc} drives expression in other imaginal discs. GAL4^{ptc}-driven *manic fringe* induces a dramatic reduction in size of the eye (Fig. 4h) and fused ocelli (data not shown). GAL4^{ptc}-driven *radical fringe*, on the other hand, had no effect on the eye (Fig. 4i) or ocellar development, but an extra pair of scutellar setae developed within the normal proneural region (data not shown). Loss of wing margin, vein splitting, extra macrochaetae, fused ocelli and reduction in eye size are phenotypes previously noted for mutants in Notch-mediated signalling^{19–27}. We tested whether reduction of *Notch* gene dosage (using *Df(1)N8/+* hemizygotes) affected GAL4^{ptc}, UAS-*manic* and GAL4^{ptc}, UAS-*radical fringe*-induced phenotypes. In each case, the phenotypes were dramatically enhanced (data not shown). A more direct assay of the effects of ectopic mammalian *fringe* expression on Notch-mediated signalling in *Drosophila* will require marker gene expression analysis (for instance, *wingless* at the dorso-ventral compartment boundary of imaginal wing discs).

Mammalian *fringe* expression boundaries coincide with tissue boundaries undergoing Notch-dependent patterning and also with

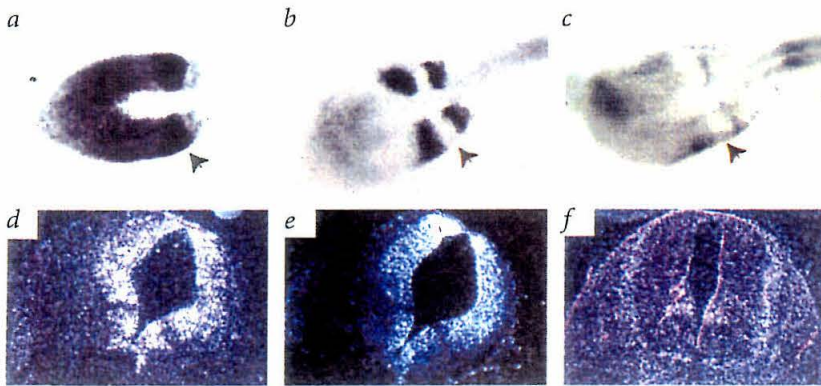


Fig. 3 Expression of mammalian Notch ligands and *lunatic fringe* during somitogenesis and neural tube patterning. (a,b,c) Whole-mount *in situ* hybridization with antisense probes to *Dll1*(a), *lunatic fringe*(b) and *Jagged1*(c) transcripts in E8.5 mouse embryonic posterior mesoderm. Arrowhead points to a forming somite. (d,e,f) Dark-field view of a tissue-section *in situ* hybridized with antisense probes to *Dll1*(d), *lunatic fringe*(e) and *Jagged1*(f) genes in E10.5 mouse embryonic neural tube.

Notch-ligand expression boundaries. Ectopic expression of *manic fringe* and *radical fringe* in *Drosophila* produces phenotypes similar to those caused by disruption of Notch-dependent development. We speculate that—directly or indirectly—the fringe proteins alter the sensitivity of Notch for its specific ligands. A direct test of this hypothesis will require biochemical assays that probe Notch activation by its ligands in the presence or absence of fringe proteins.

During somitogenesis, *lunatic fringe* is strongly expressed in two stripes that surround the forming somite. *Dll-1* is expressed at extremely high levels in the forming somite, where Notch1 is not expected to be activated¹⁰. Notch1 activation is required between the forming somites in order to facilitate segmentation⁹. We hypothesize that *Dll-1* can activate Notch1 only between the forming somites because this is where *Dll-1*-expressing cells abut *lunatic fringe*-expressing cells. *Lunatic fringe* may therefore facilitate activation of Notch1 by *Dll-1*. In the developing neural tube a *lunatic fringe* expression boundary coincides with a *Dll-1/Jagged1* expression boundary, suggesting that *lunatic fringe* may control devel-

opment at this boundary. *Lunatic fringe* is expressed in the thymic medulla but not in the cortex. Notch1-mediated signals are involved in lineage commitment of immature cortical thymocytes as they differentiate and move into the medulla²⁸. *Lunatic fringe* may therefore function together with Notch1 to control lineage commitment in the thymus. Finally, downregulation of *lunatic fringe* and upregulation of *manic* and/or *radical fringe* during differentiation may be required to regulate Notch activation at the boundary between stem cells and their progeny in many tissues. As discussed above, biochemical analyses will be needed to address the postulated role of mammalian fringe proteins in regulating boundary formation and lineage commitment in these developmental contexts.

Note added in proof: Molecular cloning of avian *fringe* genes and their analysis in limb-bud development have been reported^{29,30}. In addition, the role of *Dll-1* in somite patterning has been demonstrated through genetic analysis³¹. Results similar to those reported here by us have recently appeared³².

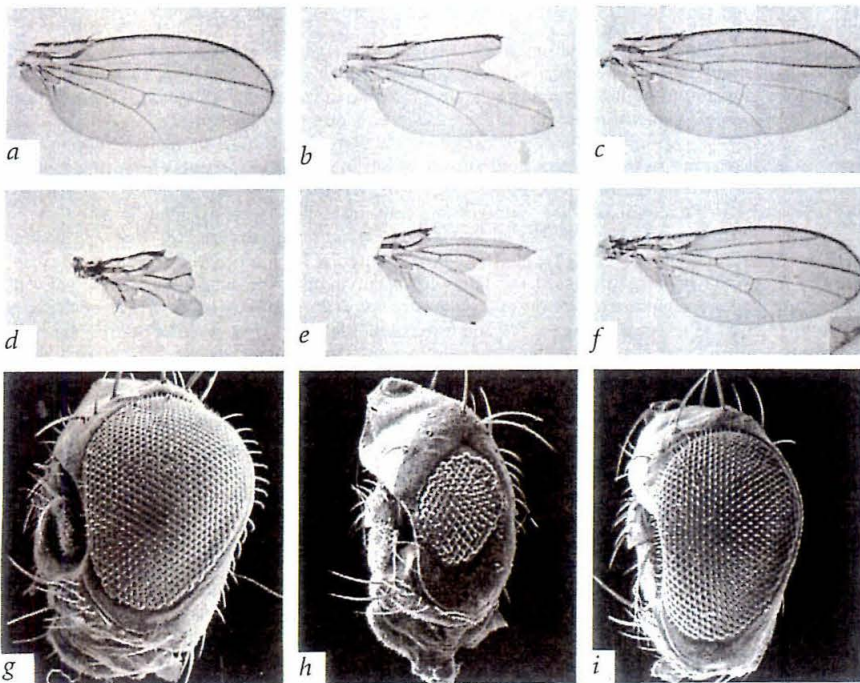


Fig. 4 Effects of ectopic expression of *manic* and *radical fringe* in *Drosophila*. a, wild-type wing; b, wing from a *GAL4^{P1/C}*, *UAS-manic fringe* fly; c, wing from a *GAL4^{P1/C}*, *UAS-radical fringe* fly; d, wing from a fly expressing *manic fringe* from the *GAL4^{C96}* driver; e, wing from a fly expressing *manic fringe* from the *GAL4^{C5}* driver; f, wing from fly expressing *radical fringe* from the *GAL4^{C5}* driver; g, eye from a wild-type fly; h, eye from a fly carrying *GAL4^{P1/C}*, *UAS-manic fringe*; i, eye from a fly carrying *GAL4^{P1/C}*, *UAS-radical fringe*.

Methods

RT-PCR. Mouse tissues were homogenized in TRIZOL (Gibco BRL), total RNA extracted and poly(A)⁺ RNA prepared with Oligotex (Qiagen). mRNA was heated to 95 °C for 5 min before cDNA synthesis, and reverse transcription was carried out at 37 °C for 1–2 h in x1 First Strand Buffer (Gibco BRL), 10 mM DTT, 1 mM dNTPs (Pharmacia), 10 U RNasin (Pharmacia), 0.5 µg pd(N)6 (Pharmacia) and 200 U of M-MLV reverse transcriptase. cDNA was then used in *Taq* polymerase PCR reactions containing 1X PCR Buffer (Perkin Elmer), 1 mM MgCl₂, 0.2 mM dNTPs, 0.01% gelatin and 1 mg of forward and reverse primers. Degenerate primers were as follows: Fringe upstream 5'-GCC GAA TTC TGG TT(T/C) TG(T/C) CA(T/C) (G/T)TN GA(C/T) GA(C/T) GA(C/T) AA(C/T) TA(C/T)GT (codes for amino acids WFCH(V/F)DDDNYV with 5' EcoRI site); Fringe downstream 5'-GCC TCT AGA CA (G/A)AA NCC NGC NCC NCC NGT NGC (G/A)AA CCA (G/A)AA (codes for anti-sense of amino acids FWFATGGAGFC with 5' *Xba*I site). PCR reaction conditions were as follows: initial denaturation at 96 °C for 7 min, followed by 2 cycles of 94 °C for 50 s, 50 °C for 2 min, 72 °C for 2 min, 35 cycles of 94 °C for 50 s, 55 °C for 2 min, 72 °C for 1.5 min and a final incubation of 72 °C for 10 min. PCR products (expected size 216 bp, based on the human EST) were run out on 3% NuSieve agarose (Mandel) gels, purified with Qiaex II (Qiagen), digested with *Eco*RI and *Xba*I and subcloned into Bluescript (Stratagene) for dideoxy sequencing with Sequenase v2.0 (US Biochemicals). DNA and amino acid sequences were analysed with MacDNASIS software (Hitachi), and searches for related sequences were done through the BLAST network service provided by the National Center for Biotechnology Information.

Isolation of murine *fringe* cDNA clones. Approximately 1×10⁶ plaques of a mouse embryonic day 14 cDNA library (Stratagene) were transferred and ultraviolet light cross-linked to uncharged nylon membranes (Qiabran, Qiagen), and screened with a mixture of ³²P-labelled inserts from PCR clones of *lunatic*, *manic* and *radical fringe*. Hybridization was performed at 48 °C for 24 h in 1M NaCl, 1% SDS, 10% dextran sulphate, 50 mM Tris pH 7.5, 1X Denhardt's and 100 mg/ml denatured salmon sperm DNA. Filters were washed twice with 2X SSC, 0.5% SDS, once with 1X SSC, 0.5% SDS, and once with 1X SSC, 0.5% SDS. All washes were at 48 °C for 30 min, and filters were exposed to Kodak BioMax film for 48 h. Twenty-two positively hybridizing plaques were identified and purified, and cycle sequencing was performed on 11 excised clones with an ABI Biotechnology Automatic DNA sequencer. Of these 11 clones, 8 were *radical*, 1 was *manic* and 2 were *lunatic fringe*. The 5' ends of *lunatic* and *manic fringe* were cloned by 5' RACE with 5'-AmplifINDER™ Race Kit (Clontech) according to the manufacturer's specifications. The 3'-specific primer used for RACE PCR synthesis of *lunatic fringe* was 5'-ATC AGT GAA GAT GAA CGT CAT CTC CTT, and the 3'-specific primer used for RACE PCR synthesis of *manic fringe* was 5'-CTG CAG AAC AGT TGG TGA.

Tissue section *in situ* hybridization. *In situ* hybridization experiments were performed with 8 µm paraffin or frozen sections from developmentally staged C.B.-17 embryos. Midday on the day of appearance of vaginal plugs was considered 0.5 dpc to time pregnancies. For paraffin sections, embryos were fixed overnight in 4% paraformaldehyde, dehydrated in ethanol and embedded in paraffin. For cryosections, embryos were protected by embedding in OCT compound (Miles) before freezing in liquid N₂. Pretreatments of frozen sections included fixing in 4% paraformaldehyde for 1 h, followed by proteinase K digestion (20 mg/ml, 7.5 min, 25 °C) and acetylation (0.1 M triethanolamine pH 8.0, 0.25% acetic anhydride, 10 min, 25 °C). Subsequently, the sections were dehydrated with ethanol and air-dried before addition of hybridization solution.

Riboprobes were synthesized with T7 RNA polymerase (Pharmacia, Boehringer Mannheim), T3 RNA polymerase (Pharmacia) and SP6 RNA polymerase (Pharmacia) according to the protocol of the manufacturer. pBK-*radical*δKpnl (clone 16) was used to synthesize sense (T3) and antisense (T7) probes of 709 bp, which span from nt 418 of *radical fringe* to 118 nt downstream of coding sequence. A probe for *lunatic fringe* was generated by PCR with the use of the following primers: 5'-GAATTC CTG CTG TTC GAG ACC TGG ATC (contains EcoRI site) and 5'-AGATCT ACC AGG ATT GTA GAA GAT CGC (contains BglII site) and pBK-*lunatic* (clone 24) as template. The 756-bp PCR product, which spans nt 273 to nt 1030 of the *lunatic* coding sequence, was subcloned into pGemT (Promega)

and sense and antisense riboprobes synthesized with SP6 and T7 polymerase, respectively. pBK-*manic* (clone 30) was digested with EcoRI and a 426-bp EcoRI fragment from 3' untranslated region of *manic fringe* (begins 284 bp downstream of last coding nt) was subcloned into phosphatase-treated EcoRI-digested pBluescript vector (Stratagene). Sense and antisense *manic* riboprobes were synthesized from this plasmid using T3 and T7 polymerases respectively. A probe for mouse *Jagged1* was generated with the following primers: 5'-TCC AGC TGA CAG AGG TTT CC and 5'-GAC CAG AAT GGC AAC AAA ACC TGC. The 937-bp PCR product, which covers nt 641–1578 of the rat sequence, was designed from a search for stretches of DNA identity between rat and chicken *Serrate-1*, which was predicted to be identical in mouse *Serrate-1*. This PCR product was subcloned into pGemT (Promega), and antisense riboprobes were generated by transcription with T7 RNA polymerase. A 777-bp *Scal*/*Pst*I fragment of mouse *Delta-like1* spanning nt 669–1446 was subcloned in pBK (Stratagene), and antisense riboprobes were generated with T3 RNA polymerase.

Pre-treatment of paraffin sections and hybridization to [³³P]UTP-labelled sense and antisense probes (15,000–40,000 cpm/ml) were conducted as described³³, with the following modifications. The hybridization and washing steps omitted use of DTT. After RNase treatment, the sections were washed sequentially with 2× SSC, 1× SSC and 0.5× SSC at 37 °C, 10 min each, and with 0.1×SSC at 65 °C for 30 min. Exposure of slides to emulsion was allowed to proceed for 1–3 weeks; after development, the tissues were stained lightly with hematoxylin and eosin.

Whole-mount *in situ* hybridization. Embryos were dissected into PBS and extra-embryonic tissues removed. Embryos were fixed overnight at 4 °C with 4% paraformaldehyde (PFA) in PBS, rinsed once with cold PBT (PBS with 0.1% Tween-20) and dehydrated through an ascending methanol series (25%, 50%, 75%) in PBT and then stored in 100% methanol at –20 °C until further use. Antisense riboprobes were synthesized from the same DNA templates as described above for sections with a digoxigenin RNA labelling kit (Boehringer Mannheim). Embryos were rehydrated through a descending methanol series rinsed twice in PBT, and then bleached for 1 h at RT in 6% hydrogen peroxide in PBT. After three rinses with PBT, embryos were permeabilized with 10 µg/ml proteinase K (5 min for E9.5 embryo and 2 min for E8.5 embryo), rinsed twice with PBT and then fixed with glutaraldehyde 0.2%/PFA 4%/PBT for 20 min at RT. After fixation, embryos were washed four times with PBT, washed once with hybridization buffer (50% formamide, 5× SSC [pH 4.5], 50 µg/ml yeast tRNA, 1% SDS, 50 µg/ml heparin), and incubated with 1.5 ml of fresh hybridization buffer for 1 h at 70 °C. Digoxigenin-labeled riboprobe (1.5 mg) was added directly and embryos were incubated overnight at 70 °C.

After hybridization, embryos were washed twice for 30 min at 70 °C with solution 1 (50% formamide, 5× SSC [pH 4.5], 1% SDS), washed once for 10 min at 70 °C with 50/50 solution 1/solution 2 (0.5 M NaCl, 0.01 M Tris [pH 7.5], 0.1% Tween-20), rinsed three times with solution 2 at RT, once with solution 3 at RT (50% formamide, 2× SSC [pH 4.5]) and twice for 30 min at 65 °C with solution 3. Embryos were then rinsed three times at RT with TBS-TL (137 mM NaCl, 2.7 mM KCl, 25 mM Tris [pH 7.5] plus 2 mM levamisole and 0.1% Tween, 20) and incubated for 1 h at RT with TBS-TL containing 10% heat-inactivated (65 °C for 30 min) goat serum to prevent non-specific binding of antibody. Anti-digoxigenin Fab alkaline phosphatase conjugate (1/5000, Boehringer Mannheim) was pre-absorbed in TBS-TL with 1% heat-inactivated goat serum and approximately 3 mg heat-inactivated embryo powder per ml antibody. After an overnight incubation at 4 °C with the pre-absorbed antibody, embryos were rinsed three times with TBS-TL, washed four times for 1 h with TBS-TL at RT and then left overnight at 4 °C in fresh TBS-TL. The buffer was exchanged by washing three times for 10 min with NTMT (0.1 M NaCl, 0.1 M Tris [pH 9.5], 0.05 M MgCl₂, 0.1% Tween-20, 2 mM levamisole), and the antibody detection reaction was performed by incubating embryos with detection solution (NTMT with 0.25 mg/ml nitroblue tetrazolium and 0.13 mg/ml 5-bromo-4-chloro-3-indolylphosphate p-toluidinium). Detection reactions were complete within 15 min–1 h, and then embryos were washed twice in PBT. Colour was intensified by dehydration/rehydration through ascending and descending methanol/PBT rinses. Embryos were then cleared through 50% and 80% glycerol in CMFET (137 mM NaCl, 3 mM KCl, 8 mM Na₂HPO₄, 1.5 mM KH₂PO₄, 0.7 mM EDTA, 0.1% EDTA, 0.1% Tween-20), and whole embryos were photographed under transmitted light with a Leica MZ12 microscope with Kodak Tungsten 160 ASA film.

Ectopic expression in *Drosophila*. An EcoRI fragment containing the entire *radical fringe* open reading frame was purified from pBK-phagemid vector (clone 89) and ligated with phosphatase-treated EcoRI digested transformation vector pUAST¹⁵. The 5' end of *manic fringe* was PCR-modified to contain Kozak consensus sequence (5' GAT CTA CCA ATG G), and an Apal site was introduced by PCR at nt 304–309 to allow ligation with pBK-phagemid vector *manic fringe* cDNA (clone 8). The entire *manic fringe* cDNA was then subcloned as a BglII fragment into phosphatase-treated BglII-digested transformation vector pUAST¹⁵. The recombinant plasmids, pUAST-*radical fringe* and pUAST-*manic fringe*, with the open reading frames in the correct orientation relative to the promoter, were used to transform *Drosophila* by standard procedures³⁴. For analysis of ectopic expression, transgenic flies carrying pUAST-*manic* and pUAST-*radical* were crossed to GAL4 enhancer trap lines. The GAL4 drivers used were GAL4^{AP16}, GAL4^{C5}, which is expressed throughout the wing disc pouch¹⁸, and GAL4^{C96}, which is expressed only along the D/V boundary¹⁷. These crosses were repeated with several independent transgenic lines for pUAST-*manic* and pUAST-*radical*. Progeny of such crosses were scored for defects. Wings were dissected from adult flies, mounted in GMM³⁵ and photographed with a Zeiss MC63 camera control system mounted on a Zeiss Axioskop microscope. Pictures of adult fly eyes were obtained by scanning electron microscopy by standard procedures³⁶.

Acknowledgements

We thank K. Irvine, T. Vogt, E. Laufer and R. Fleming for exchange of information and H.X. Cheng, along with ACGT and the Centres of Excellence sequencing facility, for DNA sequencing. We are also indebted to K. Irvine, H. Krause and the Bloomington stock center for *Drosophila* stocks. Finally, we thank S. Cohen, W. Fu, A. Karaiskakis, T. Yager, J. Rossant, M. Crickower, D. Van der Kooy, E. Zacksenhaus, H. Schachter, members of our labs, C. Kintner, Yi Rao and many other colleagues either for advice, help, information or encouragement. C.C. is a research fellow of the National Cancer Institute of Canada. This work was supported by grants to S.E.E. from the Medical Research Council of Canada, to H.D.L. from the National Science Foundation (USA) and the Medical Research Council of Canada, to R.A.P. from The National Cancer Institute of Canada with funds from the Canadian Cancer Society, to B.G. from the National Cancer Institute of Canada with funds from the Terry Fox Run, to C.C.H. from the National Cancer Institute of Canada with funds from the Terry Fox Run and to G.B. from the Medical Research Council of Canada.

Received 28 February; accepted 28 May 1997.

- Parr, B.A. & McMahon, A.P. Wnt genes and vertebrate development. *Curr. Opin. Genet. Dev.* **4**, 523–528 (1994).
- Ingham, P.W. Signaling by hedgehog-family proteins in *Drosophila* and vertebrate development. *Curr. Opin. Genet. Dev.* **5**, 492–498 (1995).
- Hogan, B.L.M. Bone morphogenetic proteins: multifunctional regulators of vertebrate development. *Genes Dev.* **10**, 1580–1594 (1996).
- Lardelli, M., Williams, R. & Lendahl, U. Notch-related genes in animal development. *Int. J. Dev. Biol.* **39**, 769–780 (1995).
- Kopan, R. & Turner, D.L. The Notch pathway: democracy and aristocracy in the selection of cell fate. *Curr. Opin. Neurobiol.* **6**, 594–601 (1996).
- Irvine, K.D. & Wieschaus, E. Fringe, a boundary-specific molecule, mediates interactions between dorsal and ventral cells during *Drosophila* wing development. *Cell* **79**, 595–606 (1994).
- Yuan, Y.P., Schultz, J., Mlodzik, M. & Bork, P. Secreted Fringe-like signaling molecules may be glycosyltransferases. *Cell* **88**, 9–11 (1997).
- Wu, J.Y., Wen, L., Zhang, W.-J. & Rao, Y. The secreted product of *Xenopus* gene *lunatic fringe*, a vertebrate signaling molecule. *Science* **273**, 355–358 (1996).
- Conlon, R.A., Reaume, A.G. & Rossant, J. Notch1 is required for the coordinate segmentation of somites. *Development* **121**, 1533–1545 (1995).
- Bettenhausen, B., Hrabce de Angelis, M., Simon, D., Guenet, J.-L. & Gossler, A. Transient and restricted expression during mouse embryogenesis of Dll1, a murine gene closely related to *Drosophila* Delta. *Development* **121**, 2407–2418 (1995).
- Lindsell, C.E., Shawber, C.J., Boulter, J. & Weinmaster, G. Jagged: a mammalian ligand that activates Notch1. *Cell* **80**, 909–917 (1995).
- Myat, A., Henrique, D., Ish-Horowitz, D. & Lewis, J. A chick homologue of Serrate and its relationship with Notch and Delta homologues during central neurogenesis. *Dev. Biol.* **174**, 233–247 (1996).
- Shawber, C., Boulter, J., Lindsell, C.E. & Weinmaster, G. Jagged2: A serrate-like gene expressed during rat embryogenesis. *Dev. Biol.* **180**, 370–376 (1996).
- Kim, J., Irvine, K.D. & Carroll, S.B. Cell recognition, signal induction, and symmetrical gene activation at the dorsal-ventral boundary of the developing *Drosophila* wing. *Cell* **82**, 795–802 (1995).
- Brand, A.H. & Perrimon, N. Targeted gene expression as a means of altering cell fates and generating dominant phenotypes. *Development* **118**, 401–415 (1993).
- Hinz, U., Giebel, B. & Campos-Ortega, J.A. The basic-helix-loop-helix domain of *Drosophila* lethal of scute protein is sufficient for proneural function and activates neurogenic genes. *Cell* **76**, 77–87 (1994).
- Gustafson, K. & Boulianne, G.L. Distinct expression patterns detected within individual tissues by the GAL4 enhancer trap technique. *Genome* **39**, 174–182 (1996).
- Yeh, E., Gustafson, K. & Boulianne, G.L. Green fluorescent protein as a vital marker and reporter of gene expression in *Drosophila*. *Proc. Natl. Acad. Sci. USA* **92**, 7036–7040 (1995).
- Fleming, R.J., Scottgate, T.N., Diederich, R.J. & Artavanis-Tsakonas, S. The gene *Serrate* encodes a putative EGF-like transmembrane protein essential for proper ectodermal development in *Drosophila melanogaster*. *Genes Dev.* **4**, 2188–2201 (1990).
- Thomas, U., Speicher, S.A. & Knust, E. The *Drosophila* gene *Serrate* encodes an EGF-like transmembrane protein with a complex expression pattern in embryos and wing discs. *Development* **111**, 749–761 (1991).
- Speicher, S.A., Thomas, U., Hinz, U. & Knust, E. The *Serrate* locus of *Drosophila* and its role in morphogenesis of the wing imaginal discs: control of cell proliferation. *Development* **120**, 535–544 (1994).
- Artavanis-Tsakonas, S., Matsuno, K. & Fortini, M.E. Notch signaling. *Science* **268**, 225–232 (1995).
- Vassin, H., Bremer, K.A., Knust, E. & Campos-Ortega, J.A. The neurogenic gene *Delta* of *Drosophila melanogaster* is expressed in neurogenic territories and encodes a putative transmembrane protein with EGF-like repeats. *EMBO J.* **6**, 3431–3440 (1987).
- Kopczynski, C.C., Alton, A.K., Fehcht, K., Kooh, P.J. & Muskavitch, M.A.T. *Delta*, a *Drosophila* neurogenic gene, is transcriptionally complex and encodes a protein related to blood coagulation factors and epidermal growth factor of vertebrates. *Genes Dev.* **2**, 1723–1735 (1988).
- Parks, A.L. & Muskavitch, M.A.T. *Delta* function is required for bristle organ determination and morphogenesis in *Drosophila*. *Dev. Biol.* **157**, 484–496 (1993).
- Parody, T.R. & Muskavitch, M.A.T. The pleiotropic function of *Delta* during postembryonic development of *Drosophila melanogaster*. *Genetics* **135**, 527–539 (1993).
- Muskavitch, M.A.T. *Delta*-Notch signaling and *Drosophila* cell fate choice. *Dev. Biol.* **166**, 415–430 (1994).
- Robey, E. et al. An activated form of Notch influences the choice between CD4 and CD8 T cell lineages. *Cell* **87**, 483–492 (1996).
- Rodriguez-Esteban, C. et al. *Radical fringe* positions the apical ectodermal ridge at the dorsoventral boundary of the vertebrate limb. *Nature* **386**, 360–366 (1997).
- Laufer, E. et al. Expression of *Radical fringe* in limb-bud ectoderm regulates apical ectodermal ridge formation. *Nature* **386**, 366–373 (1997).
- de Angelis, M.H., McIntyre II, J. & Gossler, A. Maintenance of somite borders in mice requires the *Delta* homologue *Dll1*. *Nature* **386**, 717–721 (1997).
- Johnston, S.H. et al. A family of mammalian fringe genes implicated in boundary determination and the Notch pathway. *Development* **124**, 2245–2254 (1997).
- Hui, C.-C., Slusarski, D., Platt, K.A., Holmgren, R. & Joyner, A.L. Expression of three mouse homologs of the *Drosophila* segment polarity gene *cubitus interruptus*, *Gli*, *Gli-2*, and *Gli-3*, in ectoderm- and mesoderm-derived tissues suggests multiple roles during postimplantation development. *Dev. Biol.* **162**, 402–413 (1994).
- Spradling, A.C. P-element-mediated transformation in *Drosophila*: A practical approach (ed. Roberts, D.B.) 175–197 (IRL Press, Oxford, 1986).
- Lawrence, P.A., Johnston, P. & Morata, G. Methods of marking cells in *Drosophila*: A Practical Approach. (ed. Roberts, D.B.) 229–242 (IRL Press, Oxford, 1986).
- Tomlinson, A. & Ready, D.F. Cell fate in the *Drosophila* ommatidium. *Dev. Biol.* **123**, 264–275 (1987).